Cover Page

Universiteit Leiden

Leiden University Repository

The handle http://hdl.handle.net/1887/37233 holds various files of this Leiden University dissertation

Author: Tummers, Bart
Title: Human papillomavirus targets crossroads in immune signaling
Issue Date: 2016-01-21

Human papillomavirus targets crossroads in immune signaling

Bart Tummers

Human papillomavirus targets crossroads in immune signaling

Author: Bart Tummers
Lay out: Mariska Offerman (Mikka Art) and Gildeprint, Enschede
Cover lay out: Bart Tummers, adapted from DragonArtz - DragonArtz.net.
Thesis printing: Gildeprint Drukkerijen, Enschede

ISBN nummer: 978-94-6233-193-8

Copyright © by 2015 B. Tummers. All rights reserved. No part of this thesis may be reproduced in any form or by any means without permission of the author.

Human papillomavirus targets crossroads in immune signaling

Proefschrift

ter verkrijging van de graad van Doctor aan de Universiteit Leiden,
op gezag van Rector Magnificus prof.mr. C.J.J.M. Stolker,
volgens besluit van het College voor Promoties
te verdedigen op

donderdag 21 januari 2016 klokke 16:15 uur

door

Bart Tummers
geboren te IJsselstein in 1984

Promotor	Prof. Dr. S.H. van der Burg	
Co-promotor	Dr. J.M. Boer	
Leden promotiecommissie	Prof. Dr. T.H.M. Ottenhoff	LUMC
	Prof. Dr. T.D. de Gruijl	VUMC, Amsterdam
	Prof. Dr. E. Wiertz	UMCU, Utrecht

The studies described in this thesis were performed in the laboratory of Prof. Dr. S.H. van der Burg at the Department of Clinical Oncology, Leiden University Medical Center (LUMC), Leiden, The Netherlands, in collaboration with the laboratory of Prof. Dr. C. Meyers at the Department of Microbiology and Immunology, The Pennsylvania State University College of Medicine, Hershey, Pennsylvania, United States of America. This work was supported by the Netherlands Organization for Health Research (NWO/ZonMw) TOP grant 91209012.

Learn from yesterday,
Live for today,
Hope for tomorrow.
The important thing is not to stop questioning.

Albert Einstein (1879 - 1955)

Voor pap en mam

Chapter 1 General introduction *09*
Scope of the thesis

Chapter 2 Human papillomavirus (HPV) upregulates the cellular deubiquitinase UCHL1 to suppress the keratinocyte's innate immune response *33*

Chapter 3 CD40-mediated amplification of local immunity by epithelial cells in impaired by HPV *71*

Chapter 4 The interferon-related developmental regulator 1 (IFRD1) is used by Human papillomavirus (HPV) to suppress NFκB activation *99*

Chapter 5 Human papillomavirus (HPV) downregulates the expression of IFITM1 to resist the anti-proliferative effects of IFNγ and TNFα *139*

Chapter 6 General discussion *161*

Chapter 7 Samenvatting in het Nederlands *175*

Addendum Frequently used abbreviations *183*
Curriculum Vitae
Publications
Acknowledgements

1

General introduction

Adapted from:

Human papillomavirus targets crossroads in immune signaling

Bart Tummers, Sjoerd H. van der Burg.

Viruses. 2015 May 21;7(5):2485-506

INTRODUCTION

1.1 Human papillomaviruses

Human papillomaviruses (HPV) are small, non-enveloped viruses belonging to the *Papillomaviridae* family. The icosahedral virion encapsulates a double-stranded episomal DNA genome of 7 – 8 kb, comprising an early open reading frame (ORF), containing 6 non-structural early genes (E6, E7, E1, E2, E4 and E5), and a late ORF, containing 2 late genes (L2 and L1) that encode the capsid proteins. A non-coding long control region (LCR), between the L1 and E6 genes, contains regulatory elements that control replication and viral gene expression [1]. Over 180 HPV types have currently been identified. They are divided into genera α, β, γ, μ and ν, based on the nucleotide sequence of the L1 gene [2].

1.2 Clinical implications

HPV is widespread within all human populations and transmitted via the skin, including the genitalia. Diseases associated with HPV infection range from warts to cancers [3]. HPV types of the α genus (~40) infect cutaneous and mucosal epithelia. Based on their oncogenic potential, mucosal HPVs are classified as low-risk, associated with benign warts or epithelial lesions, or high-risk, that can cause oropharyngeal and anogenital malignancies, including cancers of the cervix, vulva, vagina, penis and anus. HPV types of the other genera infect cutaneous epithelium and are associated with non-melanoma skin cancer (β genus) or cutaneous papillomas and warts. Most HPV infections resolve spontaneously within one (70%) to two (90%) years [4], and in only <1% of cases malignancies develop. Still, HPV causes ~530,000 new cancer cases and ~275,000 deaths each year [5]. High-risk HPV (hrHPV) types are responsible for ~5% of all human cancers and 33% of all tumors induced by viruses. They are detected in 99.7% of cervical cancer cases, the second most common cancer in women, accounting for 20% of all cancer-associated deaths in women worldwide per year [6, 7]. HPV types 16, 18, 31, 33, 35, 39, 45, 51, 52, 56, 59, 69, 73 and 82 have been detected in cervical carcinomas, but HPV16 and 18 are by far the most prevalent types responsible for ~50% and ~20% of all cases, respectively [8, 9].

1.3 The viral life cycle

HPVs exclusively infect keratinocytes (KCs) of the basal layer of the epidermis and mucosal epithelia, which they reach via micro-wounds and abrasions. Binding of the L1 protein of HPV to heparan sulfate proteoglycans at the surface of KCs induces endocytosis of the virion. Subsequently, the capsid disassembles following acidification of the endosome and then the viral episome, still associated with L2, travels via the Golgi apparatus and ER to the nucleus [10] where low levels of viral early proteins are produced that reside mainly in the nucleus [11]. E1 and E2 initiate episome replication and, together with the host DNA replication machinery, maintain a low episome copy-number of 50 – 100 per cell [12]. Furthermore, E6 and E7 are produced to prevent cell growth arrest and apoptosis and delay differentiation, by inactivating p53 and the retinoblastoma protein (pRB). This induces a proliferative, non-differentiating state of the infected KC, resulting in lateral cell division. As the infected KC differentiates and migrates through the suprabasal layers of the epithelium, the expression of all viral genes is induced to enhance viral episome replication, which reaches high copy-numbers of hundreds to thousands per cell. In the higher layers of the epithelium the production of the late proteins L1 and L2, together forming the viral capsid, is induced and virion assembly takes place. With the rupture and shedding of the matured KC the viral particles are released [13].

1.4 Malignant transformation

Sometimes, for yet unknown reasons, hrHPV genomes can spontaneously integrate into the host genome. When this happens, the E6 and E7 oncogenes are fully integrated whereas the E2 gene is not. Abrogation of E2 expression releases the tight regulation of E6 and E7 expression. The newly transformed cells stably express E6, which binds to p53 and recruits the E3 ligase E6AP to target p53 for proteasomal degradation, as well as E7, which recruits the E3 ligase cullin 2 to target pRb for proteasomal degradation. The loss of these tumor suppressors results in uncontrollable cell growth, host genome mutations and inhibition of apoptosis, ultimately leading to cancer formation [1, 13, 14].

2. HPV immune evasion strategies

High-risk HPV infections can last up to two years despite viral activity in keratinocytes, indicating that hrHPV has developed mechanisms to effectively evade or suppress the hosts innate and/or adaptive immune response. Indeed, several studies on the spontaneous immune response to HPV have shown that HPV-specific cellular immunity develops quite late during persistent HPV infections and often is of dubious quality in people with progressive infections [15].

Viral persistence may be linked to the life cycle of HPV since HPV does not cause viremia, cell death, or cell lysis, and the life-cycle takes place within the boundary of the *lamina basalis*, away from dermal immune cells. Thus, spontaneous contact between the immune system and the virus is minimal and inflammatory responses are not readily elicited. Langerhans cells residing within the epidermis can sense viral presence, but HPV counteracts their recruitment by interfering with the production of immune attractants. After the infection is established, the virus produces only low quantities of viral proteins that mainly reside in the nucleus of the cells. Besides these passive mechanisms to evade the immune system, hrHPV also actively interferes with innate and adaptive immune mechanisms.

2.1 Viral recognition by keratinocytes

Keratinocytes are well equipped to sense pathogens. Basal KCs express pattern-recognition receptors (PRRs), such as Toll-like receptors (TLRs), NOD-like receptors (NLRs), and RNA helicases, to recognize pathogen-associated molecular patterns (PAMPs) on viruses and microbes. PRR ligation leads to activation of inflammatory and proliferative signaling cascades and subsequent production of pro-inflammatory cytokines that can induce innate and adaptive immune responses. KCs express TLR 1, 2, 3, 5 and 6 on the cell-surface and the nucleic acid-sensing TLR3 in endosomes. TLR7 and TLR8 are not expressed, but TLR7 expression can be induced upon TLR3 ligation [16]. The expression of TLR4 and TLR9 in basal KCs is still under debate, but TLR9 expression can be induced after terminal differentiation [17]. Cytosolically, KCs express the RNA helicases retinoic acid-inducible gene I (RIG-I; DDX58) and melanoma differentiation-associated protein 5 (MDA5; IFIH1) [18], and the dsDNA sensors gamma-interferon-inducible 16 (IFI16) and absent in melanoma 2 (AIM2) [19].

Although the vesicle-mediated entry mechanism used by HPV may hide the virus from recognition by cytoplasmic DNA sensors, KCs can produce type I interferon (IFN) and pro-inflammatory cytokines upon viral entry and, therefore, do recognize HPV [17]. Indeed, the episome contains CpG motifs that can be recognized by TLR9 [20] and the viral capsid itself is a potential PAMP. Whether HPV interferes with the expression of TLRs, RIG-I or MDA5 in HPV episome-containing KCs is still under debate [17, 18, 21], and while *TLR9* expression and function was shown to be abolished in KCs that overexpressed HPV16 E6 and E7 [20], by an E7-induced recruitment of a NFκB1, ERα and HDAC1 inhibitory complex to the TLR9 promotor [22], others concluded that E6 nor E7 influenced TLR9 expression or function [23]. The DNA sensor AIM2 is strongly expressed in HPV16-infected skin lesions, whereas IFI16 expression is not elevated [19]. Hence, it is not yet clear if HPV affects the expression of virus sensory molecules on KCs.

2.2 HPV influences innate immune signaling

Keratinocytes produce type I IFNs and pro-inflammatory cytokines upon PRR ligation through signaling via interferon regulatory factor (IRF) and nuclear factor of kappa-light-chain-enhancer of activated B cells (NFκB) activating pathways. Type I IFNs (mainly IFNα (13 subtypes) and IFNβ, but also IFNε, IFNτ, IFNκ, IFNω, IFNδ and IFNζ) stimulate cells to express genes inducing an anti-viral state. They can also stimulate dendritic cells and as such act as a bridge between innate and adaptive immunity [24-26]. Pro-inflammatory cytokines are chemoattractants for immune cells and regulate cell migration, activation, polarization and proliferation. Several genome-wide transcription studies reported that hrHPV types 16, 18 and 31 influence – mainly reduce – basal, TLR3-induced cytokine expression, and type I IFN-induced interferon-stimulated gene (ISG) expression [18, 27-29], indicating that hrHPV affects PRR- and type I IFN-induced signaling pathways.

2.2.1 The effect of HPV on the IRF signaling pathway

All TLRs, except TLR3, convey their signals via the adapter molecule MyD88. This induces the IRAK complex (consisting of IRAK1, 2 and 4) to recruit TRAF3, which stimulates IKKα to phosphorylate IRF7. TLR3 and 4 signal via

TRIF, cytosolic RNA sensors via MAVS, and cytosolic DNA sensors signal via the adaptor molecule STING to activate TRAF3, which then induces the TBK1-IKKε complex to phosphorylate IRF3. Phosphorylated IRF3 and IRF7 homo-dimerize and translocate to the nucleus where production of type I IFNs is initiated. Furthermore, PRR ligation can result in IRF1 activation (Figure 1).

HrHPV influences type I IFN production by interfering at several points in the signaling cascade. Its E2 proteins reduce the expression of *STING* and *IFNκ* [30], the latter of which its expression is also reduced by E6 [21, 31]. HPV16, but not HPV18, E6 protein binds to IRF3 and, thereby, may prevent its transcriptional activity [32]. E7 blocks *IFNβ* transcription by binding to IRF1 and recruiting histone deacetylases (HDACs) to the *IFNβ* promotor site [33, 34]. In contrast, E5 enhances *IFNβ* and *IRF1* expression [35].

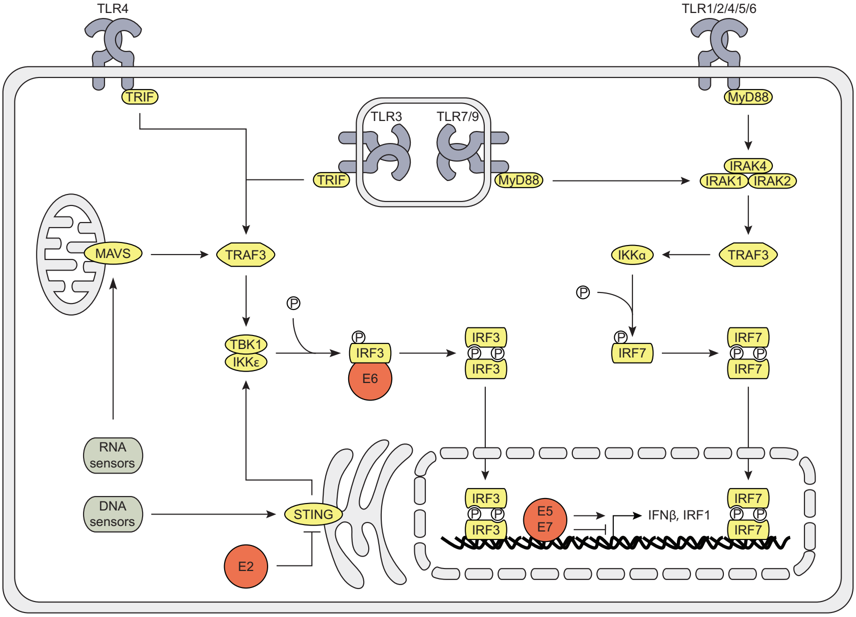
TLR4
TLR1/2/4/5/6
TRIF
MyD88
TLR3
TLR7/9
TRIF
MyD88
IRAK4
IRAK1
IRAK2
MAVS
TRAF3
IKKα
TRAF3
Ⓟ
Ⓟ
TBK1
IKKε
Ⓟ
IRF3
E6
IRF3
Ⓟ Ⓟ
IRF3
Ⓟ
IRF7
IRF7
Ⓟ Ⓟ
IRF7
RNA sensors
DNA sensors
STING
E2
IRF3
Ⓟ Ⓟ
IRF3
E5
E7
IFNβ, IRF1
IRF7
Ⓟ Ⓟ
IRF7

Figure 1: The effects of hrHPV on IRF signaling
Schematic representation of the effects of hrHPV on IRF signaling. All TLRs, except TLR3, activate IRF7 via signaling through MyD88, the IRAK complex, TRAF3 and IKKα. TLR3 and 4 signal via TRIF, cytosolic RNA sensors through MAVS and cytosolic DNA sensors via STING activate IRF3 through TRAF3, TBK1 and IKKε. Activated IRFs dimerize, translocate to the nucleus and initiate gene transcription. HPV utilizes its encoded E proteins (red) to interfere with these signaling pathways.

2.2.2 The effects of HPV on IFNAR signaling

The PRR-induced type I IFNs IFNα and IFNβ are secreted and can induce IFN-stimulated gene (ISG) expression in the infected cell itself but also in their uninfected neighbors. IFNα and IFNβ bind to the heterodimeric transmembrane IFNα/β receptor (IFNAR), composed of the IFNAR1 and IFNAR2 subunits. The IFNAR activates the receptor-associated protein tyrosine kinases Janus kinase 1 (JAK1) and tyrosine kinase 2 (TYK2), which recruit and phosphorylate STAT1 and STAT2, causing them to hetero-dimerize, bind IRF9, thereby forming the IFN-stimulated gene factor 3 (ISGF3) complex, and translocate to the nucleus. ISGF3 binds to IFN-stimulated response elements (ISREs) on the DNA and activates ISG transcription. IFNAR ligation can also lead to STAT1 homo-dimerization. STAT1 homo-dimers translocate to the nucleus and bind to γ-activated sequences (GAS) on the DNA, thereby activating ISG transcription more associated with IFNγ signaling (Figure 2) [25, 36].

HrHPV also interferes with IFNAR signaling. HPV18 E6 can bind to TYK2 in order to hamper phosphorylation of STAT1 and STAT2 [37]. E6, and to a lesser extend E7, of the hrHPV types 16 and 31 were shown to impair STAT1 transcription and translation, and binding of STAT1 to the ISRE [27, 29, 38]. However, although hrHPV represses STAT1 protein levels, the IFNβ-induced STAT1 signal cascade is not affected by hrHPV, as phosphorylation of STAT1 still occurs [38]. Expression of STAT2 and IRF9 are not affected, but E7 can interact with cytosolic IRF9, preventing IRF9 to translocate to the nucleus with as a consequence impairment of ISGF3 complex formation [39, 40].

2.2.3 The effect of HPV on the NFκB signaling pathway

PRRs also induce cytokine production through signaling via TRIF, MAVS, STING and the IRAK complex, which leads to the K63-linked poly-ubiquitination of TRAF6. The TAB1-TAB2-TAK1 complex and the IKK complex (consisting of NEMO, IKKα and IKKβ) bind to the poly-ubiquitin chain on TRAF6, resulting in the phosphorylation of IKKβ by TAK1. Activated IKKβ then phosphorylates IκBα, leading to the SCF-βTrCP-mediated K48-linked poly-ubiquitination of IκBα and its subsequent degradation. This releases the NFκB1 complex (consisting of RelA and p50) and allows it to translocate to the nucleus where it is further modified to induce DNA binding and transcriptional activation (Figure 3) [26, 41].

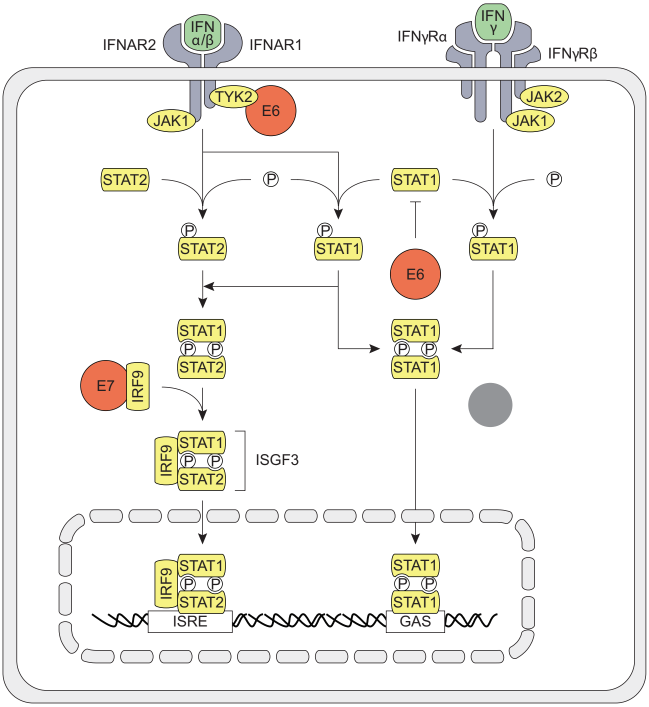
IFNAR2
IFN α/β
IFNAR1
IFNγRα
IFN γ
IFNγRβ
TYK2
E6
JAK1
JAK2
JAK1
STAT2
P
STAT1
P
P
STAT2
P
STAT1
E6
P
STAT1
STAT1
P P
STAT2
STAT1
P P
STAT1
E7
IRF9
IRF9
STAT1
P P
STAT2
ISGF3
IRF9
STAT1
P P
STAT2
ISRE
STAT1
P P
STAT1
GAS

Figure 2: The effects of hrHPV on IFNAR and IFNγR signaling

Schematic representation of the effects of hrHPV on IFNAR and IFNγR signaling. Type I IFN binding to the IFNAR leads to signaling via JAK1 and TYK2 to activate STAT1 and STAT2. STAT1 and STAT2 heterodimerize and recruit IRF9, forming the ISGF3 complex, which translocates to the nucleus, binds to ISREs and initiates ISG transcription. Activated STAT1 can also homodimerize, translocate to the nucleus, bind to GAS and initiate ISG transcription. Type II IFN binding to the IFNγR results in the activation of JAK1 and JAK2 and recruitment and phosphorylation of STAT1, which homo-dimerizes, translocates to the nucleus, binds to GAS on the DNA and initiates ISG transcription. HPV proteins (red) interfere with both IFNAR and IFNγR signaling by decreasing STAT1 levels, and hampering TYK2 and IRF9.

By the use of several different model systems hrHPV or its individual proteins have been shown to affect the PRR-induced signaling cascade that leads to NFκB nuclear translocation and to impair the function of NFκB within the nucleus. HrHPV upregulates the NFκB family members RelA, c-Rel, and the precursor proteins p105 and p100, which are processed into p50 and p52, respectively, and sequesters these proteins in the cytoplasm [29, 42-45]. The last NFκB family member, RelB, is not reported to be regulated by HPV.

Within the nucleus, E6 reduces NFκB RelA-dependent transcriptional activity [46], by binding to the C/H1, C/H3 and C terminal domains of CBP/p300 [47, 48], thereby competing with RelA and SRC1, which bind the C/H1 and C terminal domain of CBP/p300, respectively [49]. P/CAF can still bind to the C/H3 domain of CBP/p300 in presence of E6, but P/CAF cannot acetylate NFκB since E7 binds to, and thereby blocks, the HAT domain of P/CAF [49]. E7 blocks NFκB DNA binding activity [34] and competes with E2 for binding the C/H1 domain of p300/CBP, thereby hampering E2 transactivation [50]. In contrast, E2 binds to p300/CBP [51, 52] and increases NFκB signaling by enhancing RelA expression and transcriptional activation upon TNFα treatment [44].

2.2.4 The effect on the inflammasome pathway

It is not clear whether the inflammasome pathway is important in the protection against HPV. However, recently it was reported that the production of IL1β, a cytokine that is secreted upon cleavage of pro-IL1β by inflammasome-activated caspase1, is impaired. HPV E6 binds to E6-AP and p53 and this complex induces the inflammasome-independent proteasome-mediated degradation of pro-IL1β and as such hampers IL1β formation [53], indicating that hrHPV may suppress immunity by interference with post-translational processes.

2.3 HPV suppresses the action of KCs to secondary immune signals

Cells of the adaptive immune system, in particular T cells, are activated by antigen-presenting cells (APCs) in the lymph nodes and migrate to infected sites. They produce cytokines and express ligands that can activate signaling cascades in the KC involved in survival and pro-inflammatory cytokine production, leading to killing of KCs and in parallel the reinforcement of adaptive immunity. Despite the infiltration of adaptive immune effector cells the persistence of hrHPV-infected sites suggests that hrHPV has evolved mechanisms to resist this attack. Especially CD4$^+$ T helper 1 (Th1) cells are important in controlling hrHPV infections. However, even vaccines that boost viral Th1 immunity during chronic infection are only partially successful [54]. Th1 cells produce IFNγ and TNFα, and express CD40L, which induce cytokine production and proliferative changes in KCs.

2.3.1 The effect of HPV on the TNFα-activated NFκB signaling pathway

TNFα is the ligand for both the TNFα receptor 1 (TNFR1) and TNFR2. TNFR1 activates canonical NFκB1 by recruiting and activating TRADD, leading to the formation of a complex consisting of RIP1,

TRAF2 or 5, and cIAP1 or 2. cIAP1/2 is ubiquitinated with a K63-linked poly-ubiquitin chain to which the LUBAC complex (consisting of Sharpin, HOIP and HOIL1) binds. RIP1 is ubiquitinated with both K63-linked and linear poly-ubiquitin chains. The TAB1-TAB2-TAK1 complex binds to the K63-linked poly-ubiquitin chain and phosphorylates the IKK complex that binds to the linear poly-ubiquitin chain of RIP1, leading to NFκB1 release through IKKβ-induced SCF-βTrCP-mediated degradation of IκBα. TNFR2 activates the non-canonical NFκB2 pathway by recruiting TRAF2/5, cIAP1/2 and TRAF3, resulting in TRAF3 degradation. This abrogates TRAF3-induced NIK degradation, causing NIK to accumulate and activate IKKα. IKKα phosphorylates the p100 NFκB precursor protein of the NFκB2 complex, which further consists of RelB. This induces SCF-βTrCP to ubiquitinate p100 with a K48-linked poly-ubiquitin chain, leading to the proteosomal processing of p100 into p52, and the subsequent nuclear translocation of the p52-RelB dimer (Figure 3).

HPV interferes with these cascades in a similar way as it attenuates PRR-induced NFκB. Additionally, E6 binds to the C terminus of TNFR1 [55], and the N terminus of the death effector domains (DEDs) of FADD, which accelerates the degradation of FADD [56], thereby hampering the induction of apoptosis. E6 does not bind to the TRADD adaptor molecule [56]. Furthermore, E7 binds to the IKK complex and attenuates TNFα-induced kinase activity of IKKα and IKKβ, which hampers IκBα phosphorylation and degradation, and subsequent NFκB nuclear translocation [46]. In contrast to E6 and E7, E2 stimulates TNFα-induced, but not IL1-induced, NFκB signaling [44, 57], by directly interacting

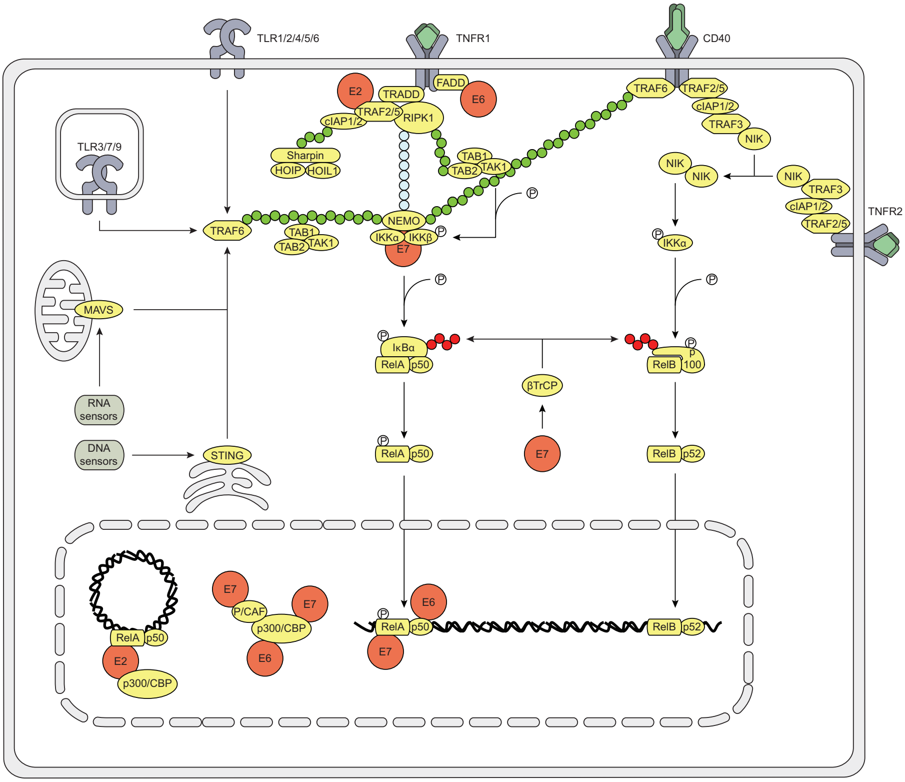
TLR1/2/4/5/6
TNFR1
CD40
E2
TRADD
FADD
E6
TRAF2/5
RIPK1
cIAP1/2
Sharpin
HOIP
HOIL1
TAB1
TAB2
TAK1
TRAF6
TRAF2/5
cIAP1/2
TRAF3
NIK
TLR3/7/9
NIK
NIK
NIK
TRAF3
cIAP1/2
TRAF2/5
TNFR2
TRAF6
TAB1
TAB2
TAK1
NEMO
IKKα
IKKβ
Ⓟ
E7
Ⓟ
IKKα
MAVS
Ⓟ
Ⓟ
Ⓟ
IκBα
RelA
p50
Ⓟ
p100
RelB
βTrCP
RNA sensors
DNA sensors
STING
Ⓟ
RelA
p50
E7
RelB
p52
E7
P/CAF
E7
p300/CBP
E6
RelA
p50
E2
p300/CBP
E6
Ⓟ
RelA
p50
E7
RelB
p52

Figure 3: The effects of hrHPV on NFκB signaling
Schematic representation of the effects of hrHPV on NFκB signaling. The canonical NFκB1 pathway is activated by PRRs and CD40 through TRAF6 and TNFR1 through RIP1. Poly-ubiquitination of TRAF6 and RIP1 recruits the TAB1-TAB2-TAK1 and IKK complexes resulting in the phosphorylation of IKKβ by TAK1. IKKβ phosphorylates IκBα, which is then ubiquitinated by SCF-βTrCP and subsequently degraded, and thereby releases the NFκB1 complex to translocate to the nucleus. CD40 and TNFR2 initiate non-canonical NFκB2 signaling by recruitment of TRAF2/5, cIAP1/2 and TRAF3 to the respective receptor, leading to TRAF3 degradation. This causes NIK to accumulate and activate IKKα to phosphorylate p100. This induces SCF-βTrCP to ubiquitinate p100, leading to the proteosomal processing of p100 into p52, and the subsequent nuclear translocation of NFκB2. In the nucleus NFκB binds to the DNA and is aided by coactivators to initiate gene transcription. HPV utilizes its encoded E proteins (red) to interfere with NFκB1 signaling at multiple positions in the pathway. Green circles indicate K63-linked poly-ubiquitin chains, red circles indicate K48-linked poly-ubiquitin chains, and blue circles indicate linear poly-ubiquitin chains.

with TRAF5 and TRAF6, but not TRAF2, thereby stimulating K63-linked ubiquitination of TRAF5 [57].

2.3.2 The effects of HPV on IFNγR signaling

Ligation of the IFNγR with type II IFN results in the activation of JAK1 and JAK2 and recruitment and phosphorylation of STAT1, which homo-dimerizes, translocates to the nucleus, binds to GAS on the DNA and initiates ISG transcription (Figure 2). The effects of hrHPV on the IFNγ-signaling pathway might be explained by the repressed STAT1 expression and protein levels in HPV infected cells, albeit that STAT1 phosphorylation still is intact [38].

2.4 HrHPV influences MHC surface expression and peptide presentation

The attack of virus-infected cells by T cells is a highly effective and specific mechanism to prevent the production and spread of virus particles. T cells recognize cells when viral protein-derived peptides are presented in the context of MHC molecules. Literature shows that primary KCs constitute excellent targets for antigen-specific cytotoxic T lymphocytes (CTLs) if their cognate peptide is presented on the KCs cell surface [58]. The overexpression of E5 [59] or E7 [60], however, makes cells more resistant to CTL-mediated lysis. E5 and E7 both reduce MHC-I surface expression, but act on different levels (Figure 4). E7 reduces MHC-I gene expression by physically associating with a putative RXRbeta binding motif (GGTCA) of the proximal promoter of MHC-I genes and recruiting HDAC1, 2 and 8 to this promoter site, leading to repressed chromatin activation. Indeed, E7 knock-down in Caski cells released HDAC1 and 2 from the MHC class-I promoter, and increased histone acetylation and MHC-I expression [60-64]. Furthermore, E7 represses the LMP2 and TAP1 promotors [61, 62], two important proteins involved in peptide production and transportation, respectively. E7 also reduces IRF1 expression by suppression of IFNγ-induced STAT1-Tyr701 phosphorylation, repressing IFNγ-mediated upregulation of MHC-I expression via the JAK1/JAK2/STAT1/IRF-1 signal transduction pathway [65, 66]. E5 does not influence MHC-I synthesis, but reduces MHC-I surface expression [65] by retaining MHC-I in the Golgi complex via interaction of di-leucine motifs (LL1 and LL3) localized in the N-terminal helical transmembrane (TM1) region of the protein [67]. This E5 – MHC-I interaction is not haplotype specific, suggesting that E5 can hamper

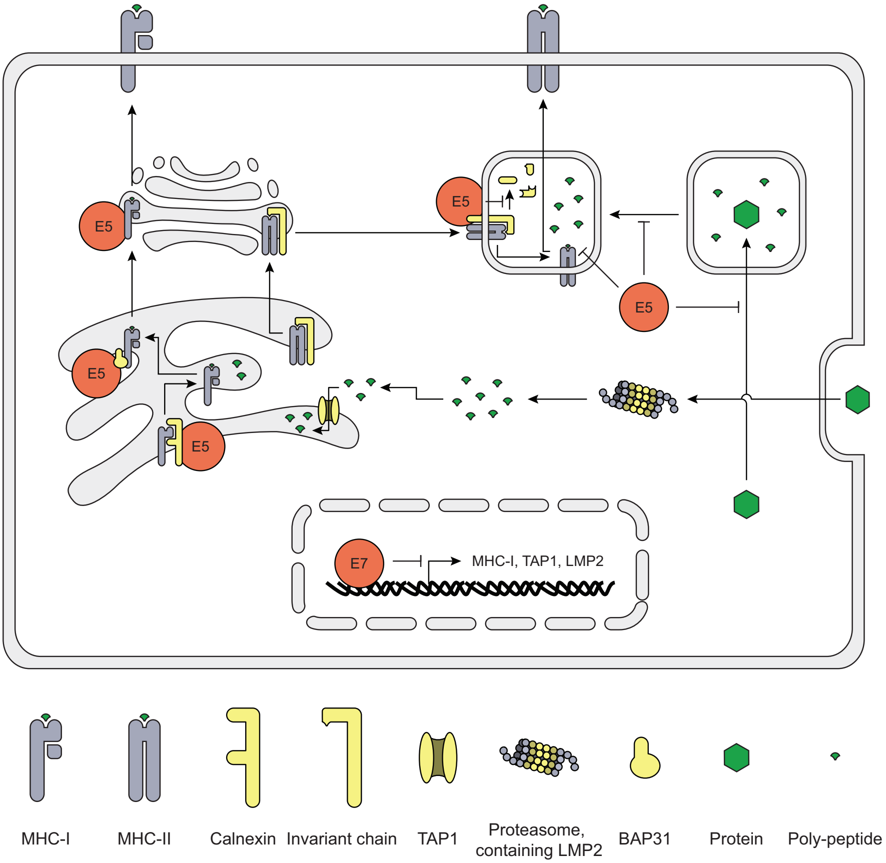
E5
E5
E5
E5
E5
E5
E7
MHC-I, TAP1, LMP2
MHC-I
MHC-II
Calnexin
Invariant chain
TAP1
Proteasome, containing LMP2
BAP31
Protein
Poly-peptide

Figure 4: The effects of hrHPV on antigen presentation
Schematic representation of the effects of hrHPV on antigen presentation. The proteasome processes proteins into peptides, which are transported into the ER via TAP1. Aided by several chaperone proteins, MHC-I is folded and loaded with peptide after which it exits the ER to travel via the Golgi apparatus to the plasma membrane were the peptides are presented to T cells. HPV proteins (red) attenuate gene expression of critical components of this pathway as well as actively retains MHC-I in the ER and Golgi apparatus. MHC-II forms in the ER and complexes with the invariant chain. The complex travels via the ER and Golgi apparatus to lysosomes where the invariant chain is degraded and MHC-II is loaded with processed peptides from endocytosed proteins. Loaded MHC-II then travels to the plasma membrane to present the peptides. Upon IFNγ stimulation, HPV E5 (red) blocks invariant chain degradation and peptide loading, as well as inhibits endosome acidification and maturation.

all MHC-I-dependent antigen presentation [68]. Moreover, binding of the TM1 domain of E5 to the ER chaperone Calnexin retains MHC-I in the ER [69], and down-regulates surface expression of CD1d, a sentinel protein in bridging innate and adaptive immunity [70]. Furthermore, via its C-terminus E5 can bind the B-cell-associated protein 31 (BAP31) [71], a protein involved in the exit of peptide-loaded MHC-I from the ER [72]. Interestingly, E5 selectively downregulates the surface expression of HLA-A and -B, but not that of HLA-C and HLA-E [65]. Under normal conditions expression of HLA class II is not affected but upon IFNγ stimulation E5 does abrogate MHC-II surface expression and blocks peptide-loading of MHC-II and invariant chain degradation [73], by inhibiting endosome acidification [74] or perturbing trafficking from early to late endocytic structures [75].

SCOPE OF THIS THESIS

In this thesis we examined how hrHPV interferes with innate and adaptive immune signaling in keratinocytes. It is clear that hrHPV invests heavily in 1) preventing infected cells to adapt an anti-viral state, 2) suppressing the production of cytokines that can induce the attraction of adaptive immune cells which may control HPV infection, and 3) perturbating the expression of HLA class I and II molecules making the infected cells less visible to the adaptive immune system. Until now, studies focused specifically on the effects of hrHPVs' early proteins. In the present studies, we show that hrHPV also exploits cellular proteins to intervene with innate and adaptive immune signaling. We used a cell culture system that resembles the natural infection of KCs with hrHPV as close as possible. Primary basal layer KCs of foreskin, vaginal and cervical origin stably expressing full HPV16 or HPV18 episomes following electroporation were studied. These HPV-positive KCs mimic HPV infection *in vivo* as they undergo the entire differentiation-dependent HPV life cycle, documented by episome amplification, late gene expression and virus production, when cultured in organotypic raft cultures [76-78]. These raft cultures produce infectious authentic HPV virions, which we used to infect basal primary KCs.

In **chapter 2**, the impact of hrHPV presence in KCs on the production of type I IFNs and pro-inflammatory cytokines after PRR ligation was assessed. HrHPV presence attenuated pro-inflammatory cytokine production, hampered RelA and IRF3 phosphorylation, and decreased NEMO protein levels. HrHPV upregulated the expression of UCHL1, which impaired IRF3 phosphorylation by removing K63-linked polyubiquitin chains from TRAF3, thereby impairing TBK1 binding to TRAF3. Furthermore, UCHL1 hampered RelA phosphorylation by affecting TRAF6 ubiquitination and inducing degradation of NEMO.

Chapter 3 focused on the reaction of keratinocytes to CD40 ligation and the impact of hrHPV herein. Keratinocytes reacted very coordinately to CD40 ligation, predominantly expressing genes involved in leukocyte migration, cell-to-cell signaling and interaction, as well as cell death and survival. HrHPV presence did not affect the gene expression profile of CD40 stimulated KCs, but attenuated the extent of the response, resulting in the impairment of the attraction of PBMCs.

In **chapter 4**, the impact of hrHPV presence in KCs on pro-inflammatory cytokine production after IFNγR and TNFR ligation was studied. Pro-inflammatory cytokine production induced by IFNγ, TNFα or their combination was impaired when hrHPV was present in the KCs. HrHPV attenuated RelA acetylation by upregulating the expression of IFRD1 in an EGFR-dependent way. The effects of hrHPV on the cytokine expression in KCs could partially be overcome by treatment with the EGFR antibody cetuximab and the HDAC1/3-specific inhibitor entinostat. Notably, these treatments also enhanced Poly(I:C)-induced cytokine expression.

In **chapter 5**, the impact of hrHPV on the effects of IFNγ, TNFα and their combination on the proliferation of keratinocytes was studied, as these cytokines were shown to have growth inhibitory effects on KCs. HrHPV rendered KCs resistant to the growth inhibitory effects of these cytokines by counteracting the IFNγ-induced arrest in cell proliferation via downregulation of the anti-proliferative gene *IFITM1*.

Finally, **chapter 6** presents a general discussion and the conclusions of the findings of this thesis.

REFERENCES

1. zur *Hausen H. P*apillomaviruses and cancer: from basic studies to clinical application. *Nat Rev Cancer* 2002,2:342-350.
2. de Villiers EM, Fauquet C, Broker TR, Bernard HU, zur Hausen H. Classification of papillomaviruses. *Virology* 2004,324:17-27.
3. Cubie HA. Diseases associated with human papillomavirus infection. *Virology* 2013,445:21-34.
4. Veldhuijzen NJ, Snijders PJ, Reiss P, Meijer CJ, van de Wijgert JH. Factors affecting transmission of mucosal human papillomavirus. *Lancet Infect Dis* 2010,10:862-874.
5. Arbyn M, Anttila A, Jordan J, Ronco G, Schenck U, Segnan N*, et al.* European Guidelines for Quality Assurance in Cervical Cancer Screening. Second edition--summary document. *Ann Oncol* 2010,21:448-458.
6. Pisani P, Bray F, Parkin DM. Estimates of the world-wide prevalence of cancer for 25 sites in the adult population. *Int J Cancer* 2002,97:72-81.
7. Walboomers JM, Jacobs MV, Manos MM, Bosch FX, Kummer JA, Shah KV*, et al.* Human papillomavirus is a necessary cause of invasive cervical cancer worldwide. *J Pathol* 1999,189:12-19.
8. Munoz N, Bosch FX, de Sanjose S, Herrero R, Castellsague X, Shah KV*, et al.* Epidemiologic classification of human papillomavirus types associated with cervical cancer. *N Engl J Med* 2003,348:518-527.
9. Smith JS, Lindsay L, Hoots B, Keys J, Franceschi S, Winer R*, et al.* Human papillomavirus type distribution in invasive cervical cancer and high-grade cervical lesions: a meta-analysis update. *Int J Cancer* 2007,121:621-632.
10. Sapp M, Bienkowska-Haba M. Viral entry mechanisms: human papillomavirus and a long journey from extracellular matrix to the nucleus. *FEBS J* 2009,276:7206-7216.
11. Doorbar J. The papillomavirus life cycle. *J Clin Virol* 2005,32 Suppl 1:S7-15.
12. Bedell MA, Hudson JB, Golub TR, Turyk ME, Hosken M, Wilbanks GD*, et al.* Amplification of human papillomavirus genomes in vitro is dependent on epithelial differentiation. *J Virol* 1991,65:2254-2260.
13. Doorbar J. Molecular biology of human papillomavirus infection and cervical cancer. *Clin Sci (Lond)* 2006,110:525-541.
14. Lou Z, Wang S. E3 ubiquitin ligases and human papillomavirus-induced carcinogenesis. *J Int Med Res* 2014,42:247-260.
15. van der Burg SH, Melief CJ. Therapeutic vaccination against human papilloma virus induced

malignancies. *Curr Opin Immunol* 2011,23:252-257.

16. Nestle FO, Di Meglio P, Qin JZ, Nickoloff BJ. Skin immune sentinels in health and disease. *Nat Rev Immunol* 2009,9:679-691.

17. Karim R, Tummers B, Meyers C, Biryukov JL, Alam S, Backendorf C*, et al.* Human papillomavirus (HPV) upregulates the cellular deubiquitinase UCHL1 to suppress the keratinocyte's innate immune response. *PLoS Pathog* 2013,9:e1003384.

18. Karim R, Meyers C, Backendorf C, Ludigs K, Offringa R, van Ommen GJ*, et al.* Human papillomavirus deregulates the response of a cellular network comprising of chemotactic and proinflammatory genes. *PLoS One* 2011,6:e17848.

19. Reinholz M, Kawakami Y, Salzer S, Kreuter A, Dombrowski Y, Koglin S*, et al.* HPV16 activates the AIM2 inflammasome in keratinocytes. *Arch Dermatol Res* 2013,305:723-732.

20. Hasan UA, Bates E, Takeshita F, Biliato A, Accardi R, Bouvard V*, et al.* TLR9 expression and function is abolished by the cervical cancer-associated human papillomavirus type 16. *J Immunol* 2007,178:3186-3197.

21. Reiser J, Hurst J, Voges M, Krauss P, Munch P, Iftner T*, et al.* High-risk human papillomaviruses repress constitutive kappa interferon transcription via E6 to prevent pathogen recognition receptor and antiviral-gene expression. *J Virol* 2011,85:11372-11380.

22. Hasan UA, Zannetti C, Parroche P, Goutagny N, Malfroy M, Roblot G*, et al.* The human papillomavirus type 16 E7 oncoprotein induces a transcriptional repressor complex on the Toll-like receptor 9 promoter. *J Exp Med* 2013,210:1369-1387.

23. Andersen JM, Al-Khairy D, Ingalls RR. Innate immunity at the mucosal surface: role of toll-like receptor 3 and toll-like receptor 9 in cervical epithelial cell responses to microbial pathogens. *Biol Reprod* 2006,74:824-831.

24. Le Bon A, Tough DF. Links between innate and adaptive immunity via type I interferon. *Curr Opin Immunol* 2002,14:432-436.

25. McNab F, Mayer-Barber K, Sher A, Wack A, O'Garra A. Type I interferons in infectious disease. *Nat Rev Immunol* 2015,15:87-103.

26. O'Neill LA, Golenbock D, Bowie AG. The history of Toll-like receptors - redefining innate immunity. *Nat Rev Immunol* 2013,13:453-460.

27. Chang YE, Laimins LA. Microarray analysis identifies interferon-inducible genes and Stat-1 as major transcriptional targets of human papillomavirus type 31. *J Virol* 2000,74:4174-4182.

28. Karstensen B, Poppelreuther S, Bonin M, Walter M, Iftner T, Stubenrauch F. Gene expression profiles reveal an upregulation of E2F and downregulation of interferon targets by HPV18 but no changes between keratinocytes with integrated or episomal viral genomes. *Virology* 2006,353:200-209.

29. Nees M, Geoghegan JM, Hyman T, Frank S, Miller L, Woodworth CD. Papillomavirus type

16 oncogenes downregulate expression of interferon-responsive genes and upregulate proliferation-associated and NF-kappaB-responsive genes in cervical keratinocytes. *J Virol* 2001,75:4283-4296.

30. Sunthamala N, Thierry F, Teissier S, Pientong C, Kongyingyoes B, Tangsiriwatthana T*, et al.* E2 proteins of high risk human papillomaviruses down-modulate STING and IFN-kappa transcription in keratinocytes. *PLoS One* 2014,9:e91473.

31. Rincon-Orozco B, Halec G, Rosenberger S, Muschik D, Nindl I, Bachmann A*, et al.* Epigenetic silencing of interferon-kappa in human papillomavirus type 16-positive cells. *Cancer Res* 2009,69:8718-8725.

32. Ronco LV, Karpova AY, Vidal M, Howley PM. Human papillomavirus 16 E6 oncoprotein binds to interferon regulatory factor-3 and inhibits its transcriptional activity. *Genes Dev* 1998,12:2061-2072.

33. Park JS, Kim EJ, Kwon HJ, Hwang ES, Namkoong SE, Um SJ. Inactivation of interferon regulatory factor-1 tumor suppressor protein by HPV E7 oncoprotein. Implication for the E7-mediated immune evasion mechanism in cervical carcinogenesis. *J Biol Chem* 2000,275:6764-6769.

34. Perea SE, Massimi P, Banks L. Human papillomavirus type 16 E7 impairs the activation of the interferon regulatory factor-1. *Int J Mol Med* 2000,5:661-666.

35. Muto V, Stellacci E, Lamberti AG, Perrotti E, Carrabba A, Matera G*, et al.* Human papillomavirus type 16 E5 protein induces expression of beta interferon through interferon regulatory factor 1 in human keratinocytes. *J Virol* 2011,85:5070-5080.

36. Ivashkiv LB, Donlin LT. Regulation of type I interferon responses. *Nat Rev Immunol* 2014,14:36-49.

37. Li S, Labrecque S, Gauzzi MC, Cuddihy AR, Wong AH, Pellegrini S*, et al.* The human papilloma virus (HPV)-18 E6 oncoprotein physically associates with Tyk2 and impairs Jak-STAT activation by interferon-alpha. *Oncogene* 1999,18:5727-5737.

38. Hong S, Mehta KP, Laimins LA. Suppression of STAT-1 expression by human papillomaviruses is necessary for differentiation-dependent genome amplification and plasmid maintenance. *J Virol* 2011,85:9486-9494.

39. Barnard P, McMillan NA. The human papillomavirus E7 oncoprotein abrogates signaling mediated by interferon-alpha. *Virology* 1999,259:305-313.

40. Barnard P, Payne E, McMillan NA. The human papillomavirus E7 protein is able to inhibit the antiviral and anti-growth functions of interferon-alpha. *Virology* 2000,277:411-419.

41. Oeckinghaus A, Hayden MS, Ghosh S. Crosstalk in NF-kappaB signaling pathways. *Nat Immunol* 2011,12:695-708.

42. Havard L, Delvenne P, Frare P, Boniver J, Giannini SL. Differential production of cytokines and activation of NF-kappaB in HPV-transformed keratinocytes. *Virology* 2002,298:271-285.

43. Havard L, Rahmouni S, Boniver J, Delvenne P. High levels of p105 (NFKB1) and p100 (NFKB2) proteins in HPV16-transformed keratinocytes: role of E6 and E7 oncoproteins. *Virology* 2005,331:357-366.

44. Prabhavathy D, Prabhakar BN, Karunagaran D. HPV16 E2-mediated potentiation of NF-kappaB activation induced by TNF-alpha involves parallel activation of STAT3 with a reduction in E2-induced apoptosis. *Mol Cell Biochem* 2014,394:77-90.

45. Vancurova I, Wu R, Miskolci V, Sun S. Increased p50/p50 NF-kappaB activation in human papillomavirus type 6- or type 11-induced laryngeal papilloma tissue. *J Virol* 2002,76:1533-1536.

46. Spitkovsky D, Hehner SP, Hofmann TG, Moller A, Schmitz ML. The human papillomavirus oncoprotein E7 attenuates NF-kappa B activation by targeting the Ikappa B kinase complex. *J Biol Chem* 2002,277:25576-25582.

47. Patel D, Huang SM, Baglia LA, McCance DJ. The E6 protein of human papillomavirus type 16 binds to and inhibits co-activation by CBP and p300. *EMBO J* 1999,18:5061-5072.

48. Zimmermann H, Degenkolbe R, Bernard HU, O’Connor MJ. The human papillomavirus type 16 E6 oncoprotein can down-regulate p53 activity by targeting the transcriptional coactivator CBP/p300. *J Virol* 1999,73:6209-6219.

49. Huang SM, McCance DJ. Down regulation of the interleukin-8 promoter by human papillomavirus type 16 E6 and E7 through effects on CREB binding protein/p300 and P/CAF. *J Virol* 2002,76:8710-8721.

50. Bernat A, Avvakumov N, Mymryk JS, Banks L. Interaction between the HPV E7 oncoprotein and the transcriptional coactivator p300. *Oncogene* 2003,22:7871-7881.

51. Lee D, Lee B, Kim J, Kim DW, Choe J. cAMP response element-binding protein-binding protein binds to human papillomavirus E2 protein and activates E2-dependent transcription. *J Biol Chem* 2000,275:7045-7051.

52. Marcello A, Massimi P, Banks L, Giacca M. Adeno-associated virus type 2 rep protein inhibits human papillomavirus type 16 E2 recruitment of the transcriptional coactivator p300. *J Virol* 2000,74:9090-9098.

53. Niebler M, Qian X, Hofler D, Kogosov V, Kaewprag J, Kaufmann AM*, et al.* Post-translational control of IL-1beta via the human papillomavirus type 16 E6 oncoprotein: a novel mechanism of innate immune escape mediated by the E3-ubiquitin ligase E6-AP and p53. *PLoS Pathog* 2013,9:e1003536.

54. van der Burg SH, Arens R, Melief CJ. Immunotherapy for persistent viral infections and associated disease. *Trends Immunol* 2011,32:97-103.

55. Filippova M, Song H, Connolly JL, Dermody TS, Duerksen-Hughes PJ. The human

papillomavirus 16 E6 protein binds to tumor necrosis factor (TNF) R1 and protects cells from TNF-induced apoptosis. *J Biol Chem* 2002,277:21730-21739.

56. Filippova M, Parkhurst L, Duerksen-Hughes PJ. The human papillomavirus 16 E6 protein binds to Fas-associated death domain and protects cells from Fas-triggered apoptosis. *J Biol Chem* 2004,279:25729-25744.

57. Boulabiar M, Boubaker S, Favre M, Demeret C. Keratinocyte sensitization to tumour necrosis factor-induced nuclear factor kappa B activation by the E2 regulatory protein of human papillomaviruses. *J Gen Virol* 2011,92:2422-2427.

58. Zhou F, Frazer IH, Leggatt GR. Keratinocytes efficiently process endogenous antigens for cytotoxic T-cell mediated lysis. *Exp Dermatol* 2009,18:1053-1059.

59. Campo MS, Graham SV, Cortese MS, Ashrafi GH, Araibi EH, Dornan ES*, et al.* HPV-16 E5 down-regulates expression of surface HLA class I and reduces recognition by CD8 T cells. *Virology* 2010,407:137-142.

60. Zhou F, Leggatt GR, Frazer IH. Human papillomavirus 16 E7 protein inhibits interferon-gamma-mediated enhancement of keratinocyte antigen processing and T-cell lysis. *FEBS J* 2011,278:955-963.

61. Georgopoulos NT, Proffitt JL, Blair GE. Transcriptional regulation of the major histocompatibility complex (MHC) class I heavy chain, TAP1 and LMP2 genes by the human papillomavirus (HPV) type 6b, 16 and 18 E7 oncoproteins. *Oncogene* 2000,19:4930-4935.

62. Heller C, Weisser T, Mueller-Schickert A, Rufer E, Hoh A, Leonhardt RM*, et al.* Identification of key amino acid residues that determine the ability of high risk HPV16-E7 to dysregulate major histocompatibility complex class I expression. *J Biol Chem* 2011,286:10983-10997.

63. Li H, Ou X, Xiong J, Wang T. HPV16E7 mediates HADC chromatin repression and downregulation of MHC class I genes in HPV16 tumorigenic cells through interaction with an MHC class I promoter. *Biochem Biophys Res Commun* 2006,349:1315-1321.

64. Li H, Zhan T, Li C, Liu M, Wang QK. Repression of MHC class I transcription by HPV16E7 through interaction with a putative RXRbeta motif and NF-kappaB cytoplasmic sequestration. *Biochem Biophys Res Commun* 2009,388:383-388.

65. Ashrafi GH, Haghshenas MR, Marchetti B, O'Brien PM, Campo MS. E5 protein of human papillomavirus type 16 selectively downregulates surface HLA class I. *Int J Cancer* 2005,113:276-283.

66. Zhou F, Chen J, Zhao KN. Human papillomavirus 16-encoded E7 protein inhibits IFN-gamma-mediated MHC class I antigen presentation and CTL-induced lysis by blocking IRF-1 expression in mouse keratinocytes. *J Gen Virol* 2013,94:2504-2514.

67. Cortese MS, Ashrafi GH, Campo MS. All 4 di-leucine motifs in the first hydrophobic domain of the E5 oncoprotein of human papillomavirus type 16 are essential for surface MHC class

I downregulation activity and E5 endomembrane localization. *Int J Cancer* 2010,126:1675-1682.

68. Ashrafi GH, Haghshenas M, Marchetti B, Campo MS. E5 protein of human papillomavirus 16 downregulates HLA class I and interacts with the heavy chain via its first hydrophobic domain. *Int J Cancer* 2006,119:2105-2112.

69. Gruener M, Bravo IG, Momburg F, Alonso A, Tomakidi P. The E5 protein of the human papillomavirus type 16 down-regulates HLA-I surface expression in calnexin-expressing but not in calnexin-deficient cells. *Virol J* 2007,4:116.

70. Miura S, Kawana K, Schust DJ, Fujii T, Yokoyama T, Iwasawa Y*, et al.* CD1d, a sentinel molecule bridging innate and adaptive immunity, is downregulated by the human papillomavirus (HPV) E5 protein: a possible mechanism for immune evasion by HPV. *J Virol* 2010,84:11614-11623.

71. Regan JA, Laimins LA. Bap31 is a novel target of the human papillomavirus E5 protein. *J Virol* 2008,82:10042-10051.

72. Abe F, Van Prooyen N, Ladasky JJ, Edidin M. Interaction of Bap31 and MHC class I molecules and their traffic out of the endoplasmic reticulum. *J Immunol* 2009,182:4776-4783.

73. Zhang B, Li P, Wang E, Brahmi Z, Dunn KW, Blum JS*, et al.* The E5 protein of human papillomavirus type 16 perturbs MHC class II antigen maturation in human foreskin keratinocytes treated with interferon-gamma. *Virology* 2003,310:100-108.

74. Straight SW, Herman B, McCance DJ. The E5 oncoprotein of human papillomavirus type 16 inhibits the acidification of endosomes in human keratinocytes. *J Virol* 1995,69:3185-3192.

75. Thomsen P, van Deurs B, Norrild B, Kayser L. The HPV16 E5 oncogene inhibits endocytic trafficking. *Oncogene* 2000,19:6023-6032.

76. Conway MJ, Alam S, Ryndock EJ, Cruz L, Christensen ND, Roden RB*, et al.* Tissue-spanning redox gradient-dependent assembly of native human papillomavirus type 16 virions. *J Virol* 2009,83:10515-10526.

77. McLaughlin-Drubin ME, Christensen ND, Meyers C. Propagation, infection, and neutralization of authentic HPV16 virus. *Virology* 2004,322:213-219.

78. Meyers C, Mayer TJ, Ozbun MA. Synthesis of infectious human papillomavirus type 18 in differentiating epithelium transfected with viral DNA. *J Virol* 1997,71:7381-7386.

2

Human papillomavirus (HPV) upregulates the cellular deubiquitinase UCHL1 to suppress the keratinocyte's innate immune response

Karim R#, Tummers B#, Meyers C, Biryukov JL, Alam S, Backendorf C,
Jha V, Offringa R, van Ommen GJ, Melief CJ, Guardavaccaro D,
Boer JM, van der Burg SH.

PLoS Pathog. 2013;9(5):e1003384.

# These authors contributed equally

ABSTRACT

Persistent infection of basal keratinocytes with high-risk human papillomavirus (hrHPV) may cause cancer. Keratinocytes are equipped with different pattern recognition receptors (PRRs) but hrHPV has developed ways to dampen their signals resulting in minimal inflammation and evasion of host immunity for sustained periods of time. To understand the mechanisms underlying hrHPV's capacity to evade immunity, we studied PRR signaling in non, newly, and persistently hrHPV-infected keratinocytes. We found that active infection with hrHPV hampered the relay of signals downstream of the PRRs to the nucleus, thereby affecting the production of type-I interferon and pro-inflammatory cytokines and chemokines. This suppression was shown to depend on hrHPV-induced expression of the cellular protein ubiquitin carboxyl-terminal hydrolase L1 (UCHL1) in keratinocytes. UCHL1 accomplished this by inhibiting tumor necrosis factor receptor-associated factor 3 (TRAF3) K63 poly-ubiquitination which lead to lower levels of TRAF3 bound to TANK-binding kinase 1 and a reduced phosphorylation of interferon regulatory factor 3. Furthermore, UCHL1 mediated the degradation of the NF-κB essential modulator with as result the suppression of p65 phosphorylation and canonical NF-κB signaling. We conclude that hrHPV exploits the cellular protein UCHL1 to evade host innate immunity by suppressing PRR-induced keratinocyte-mediated production of interferons, cytokines and chemokines, which normally results in the attraction and activation of an adaptive immune response. This identifies UCHL1 as a negative regulator of PRR-induced immune responses and consequently its virus-increased expression as a strategy for hrHPV to persist.

AUTHOR SUMMARY

A persistent infection with high-risk human papillomavirus (hrHPV) may cause cancer. Whereas keratinocytes – the cells infected by hrHPV – are equipped with different receptors allowing them to recognize invading pathogens and to activate the immune system, hrHPV has developed ways to evade the host's immune response for sustained periods of time. We showed that hrHPV accomplishes this by interfering with the signaling of the pathogen receptors, thereby hampering the production of cytokines that are known to attract and activate the immune system. HrHPV accomplishes this by upregulating the expression of a cellular protein called ubiquitin carboxyl-terminal hydrolase L1 (UCHL1). This protein suppresses the activation of signals downstream of the pathogen receptor leading to reduced transcription factor activation and downstream gene expression, in particular that of type I interferon and pro-inflammatory cytokines. This lowers the attraction of immune cells and thereby the chance of hrHPV-infected cells to be recognized and eliminated and as such enables hrHPV to persist.

INTRODUCTION

Human papillomaviruses (HPVs) are absolutely species-specific small double-stranded DNA viruses. Persistent infections with a number of HPVs, predominantly types 16 and 18, can induce cancers of the anogenitalia as well as of the head and neck region. These so-called high-risk HPVs (hrHPVs) are widespread within all human populations where they are commonly transmitted by sexual contact [1]. The undifferentiated keratinocytes of the squamous epithelia are the primary target for hrHPV [2] where it establishes an infection that can last for up to 2 years, indicating that hrHPV has evolved mechanisms to effectively evade the innate and adaptive immune mechanisms protecting the majority of immunocompetent hosts [3,4].

Viruses and microbes contain pathogen-associated molecular patterns that are recognized by the host’s pattern recognition receptors (PRRs), comprising the Toll-like receptors (TLRs), nucleotide oligomerization domain-like receptors and retinoic acid-inducible gene I (RIG-I)-like receptors (RLRs) [5]. While all of these receptors activate signaling cascades that lead to activation of NF-κB via the canonical route, only RLRs and some TLRs activate interferon regulatory factors (IRFs) which induce the production of type I interferons (IFN) and other effector molecules [6]. The signals from the PRR to the cell nucleus are coordinated via ubiquitination, including that of the different tumor-necrosis factor receptor-associated factors (TRAFs) and the NF-κB essential modulator (NEMO). Poly-ubiquitination of TRAF and NEMO allows downstream signaling whereas disassembly of the formed poly-ubiquitin chains by deubiquitinating enzymes provides a mechanism for downregulating immune responses [6,7].

Keratinocytes (KCs) express TLRs 1-3, TLR5, TLR6, TLR10, RIG-I, protein kinase R (PKR), and MDA5 independent of their differentiation status and gain the expression of TLR9 upon full differentiation indicating that these cells may respond to pathogenic challenges [8,9,10]. Thus, KCs should be able to sense the presence of hrHPV genomic DNA directly via TLR9 or indirectly via RIG-I [5,11,12]. The expression levels of these PRR were not altered in hrHPV+ KCs [10]. However, via genome-wide expression profiling of keratinocytes activated through TLR3, PKR, RIG-I and MDA-5 we found that the presence of hrHPV dampens a network of genes encoding chemotactic, pro-inflammatory and antimicrobial cytokines suggesting that HPV’s immune evasion strategy may rely on countering PRR-mediated cell signaling [10].

To understand the mechanisms underlying hrHPV's capacity to dampen PRR signaling we utilized a system that resembles the natural infection with HPV as closely as possible. It comprises the use of primary KCs that stably maintain the hrHPV genome as episomes following transfection. These hrHPV+ KCs grow at similar rates as non-transfected KC and have been shown to mimic HPV infection *in vivo* as they undergo the entire differentiation-dependent HPV life cycle documented by genome amplification, late gene expression, and virus production, upon culture of hrHPV+ KCs in organotypic raft cultures [13,14,15]. In addition, we used non-infected primary KC cultures and primary KCs newly infected with authentic HPV16 virions. These primary KCs were compared with respect to PRR signaling under different conditions and resulted in the identification of the cellular enzyme ubiquitin carboxyl-terminal hydrolase L1 (*UCHL1*) that was specifically upregulated by hrHPV in primary keratinocytes to dampen innate immunity. UCHL1 acted on the PRR-signaling pathway adaptor molecules TRAF3 and NEMO and its inhibition restored PRR-induced production of IFNβ and pro-inflammatory and chemotactic cytokines.

RESULTS

High risk HPV is associated with a decreased induction of type I IFN and pro-inflammatory cytokines following stimulation of keratinocytes via different pattern-recognition receptors.

Undifferentiated uninfected primary KCs and hrHPV+ KCs were tested for their capacity to respond to triggers of innate immunity by incubation with Pam3CSK4 (TLR1/2), poly(I:C) (TLR3, RIG-I, PKR and MDA-5)[9], lipopolysaccharide (LPS, TLR4), flagellin (TLR5), R848 (TLR7/8), or CpG (TLR9). The supernatant of non-infected keratinocytes contained higher levels of MIP3α and IL-8 but not MIP1α than hrHPV+ KCs at the basal level. Activation with poly(I:C) induced the production of high amounts of MIP3α, IL-8 and MIP1α in KCs but not in hrHPV+ KCs. Flagellin especially triggered the production of MIP3a by KCs but not in hrHPV+ KCs, although IL-8 was still produced (Figure 1A). The function of TLR9, expressed only at high protein levels in differentiated keratinocytes as measured by immunohistochemistry [10] and by RT-qPCR (Figure 1B), was tested by the capacity of CpG oligodeoxynucleotides (CpG ODN) to trigger the expression of mRNAs of pro-inflammatory cytokines and chemokines. Because suspension in methyl cellulose – to differentiate keratinocytes – does not allow the harvest of supernatant, secreted protein levels could not be measured. However, the experiments clearly showed that CpG ODN-stimulation resulted in the gene expression of *IFNB1* (*IFNβ*), *IL-8* and *CCL20* (*MIP3α*) in differentiated KCs but not in undifferentiated KC cultures (Figure 1C). As a control, KCs were also stimulated with poly(I:C) as TLR3, RIG-I and MDA-5 expression is independent of KC differentiation [10] and this resulted in the induction of pro-inflammatory cytokine expression in both undifferentiated and differentiated KCs (Figure S1). In contrast to differentiated uninfected KCs, the hrHPV+ KCs that expressed TLR9 after differentiation, failed to induce the expression of *IFNβ, IL-8 and MIP3α* upon incubation with CpG (Figure 1C), indicating that PRR-signaling can be suppressed in undifferentiated and differentiated hrHPV+ KCs.

As the basal KCs are the target for hrHPV and TLR9 is not functionally expressed in basal KCs and hrHPV+ KCs displayed an impaired production of cytokines in response to poly(I:C), subsequent studies were performed in the context of poly(I:C) stimulation. In addition to the secretion of cytokines, also

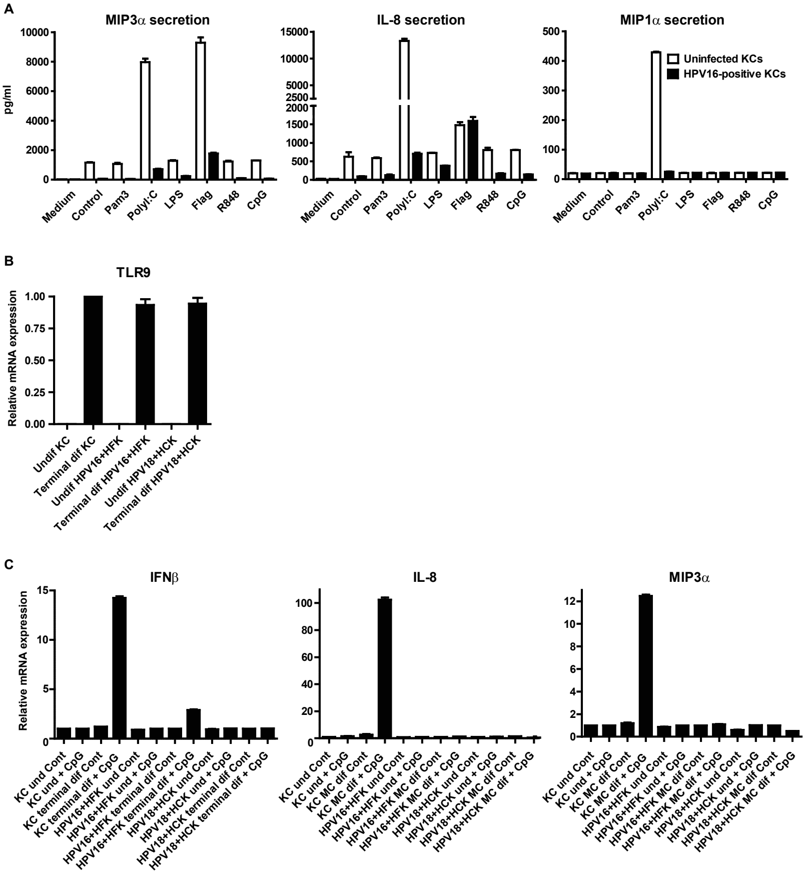

Figure 1: The presence of high risk human papillomavirus interferes with pattern recognition receptor (PRR) signaling of keratinocytes.

(A) Cytokine production of non-differentiated uninfected or HPV16+ keratinocytes after stimulation with different indicated PRR stimuli as measured by ELISA.

(B) TLR9 expression as measured by qRT-PCR on total RNA samples from undifferentiated (und) and terminally differentiated (terminal dif) uninfected KCs, and HPV16 and HPV18 positive KC cultures.

(C) IFNβ, IL-8 and MIP3α expression levels in unstimulated or CpG ODN-stimulated uninfected KCs, and two different HPV (16 or 18) positive KC cultures as examined by qRT-PCR. KCs were either left undifferentiated (und) or terminally differentiated (terminal dif) after which they were stimulated with CpG (10 µg/ml) for 7 hours. (B – C) Gene expression was normalized using GAPDH mRNA expression levels.

the gene expression levels of *MIP3α*, *CCL5* (*RANTES*) and *IFNβ* in hrHPV+ KCs were lower when compared to uninfected KCs upon 3 or 24 hours of poly(I:C) stimulation (Figure 2A).

The production of pro-inflammatory cytokines and chemokines upon activation of the NF-κB pathway requires the phosphorylation and nuclear translocation of the subunit p65 [6]. The levels of phosphorylated p65 were lower in poly(I:C) stimulated hrHPV+ KCs than in non-infected KCs (Figure 2B), suggesting that the functional impairment of PRR signaling occurs upstream of this molecule. The IKK complex is a key component of the poly(I:C)-induced NF-κB pathway, with NEMO (IKKγ) functioning as a scaffold. The degradation of NEMO may form a mechanism for viruses to avoid innate immune signaling [16,17]. Therefore, the effect of hrHPV on the protein levels of NEMO was analyzed. Following treatment of non-infected KCs and hrHPV+ KCs with cycloheximide (CHX) – to prevent new protein synthesis – it became clear that NEMO degradation was enhanced in hrHPV+ KCs (Figure 2C and Figure S2), thereby explaining the decreased phosphorylation of p65 observed.

The production of type I IFN (*e.g.* IFNb) requires the activation of cytosolic IRF3 by phosphorylation and subsequent translocation to the nucleus. Analysis of poly(I:C) stimulated KCs and hrHPV+ KCs suggested that also the levels of phosphorylated IFR3 levels were decreased in HPV+ KCs (Figure 2D).

The high risk HPV viral transcript is needed to impair PRR signaling.

To confirm that the impairment in the production of IFNb and pro-inflammatory cytokines did not simply reflect biological differences between the different primary KCs used but indeed was caused by hrHPV, we infected primary keratinocytes with infectious HPV16 virions (Figure 3A) for 24 hours and then stimulated the non-infected and newly infected KCs with poly(I:C) for another 24 hours after which the levels of *IFNb, RANTES* and *MIP3a* transcripts were measured (Figure 3B). After 24 hours of infection there was a small but discernible increase in the levels of these genes indicating that the keratinocytes initially react to the presence of the virus. However, the levels already dropped at 48 hours post-infection indicating that the virus rapidly exerted its PRR-signaling inhibitory effects. In addition, at the same time point these newly hrHPV-infected keratinocytes displayed a hampered activation

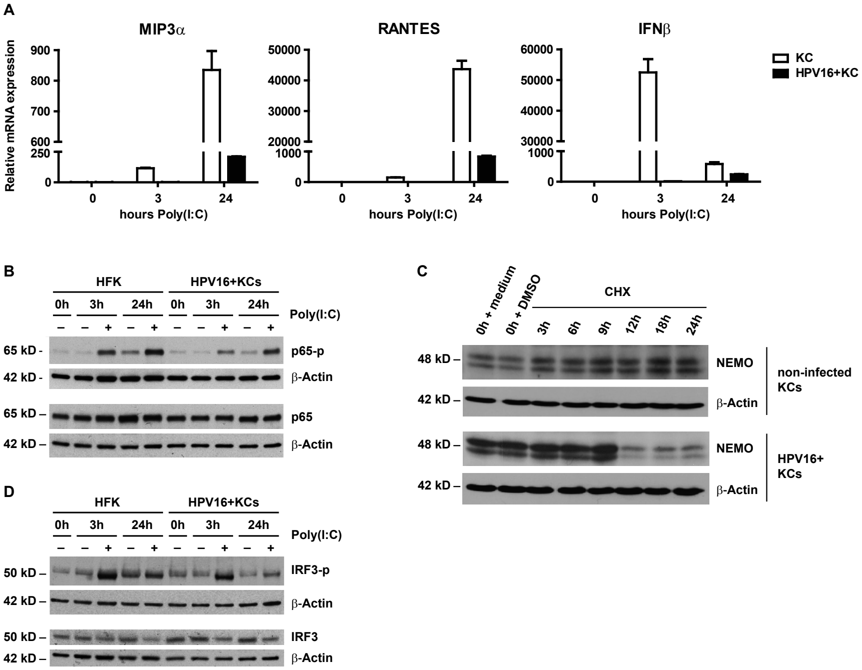

Figure 2: Canonical NF-κB signaling is impaired upstream of the transcription factor p65.

(A) Poly(I:C) induced cytokine expression in HPV16+ KCs compared to non-infected KCs. MIP3a, RANTES and IFNβ expression was measured by qRT-PCR. Gene expression was normalized using GAPDH mRNA levels and standardized against 0h of stimulation with poly(I:C).
(B) Poly(I:C) stimulated phosphorylation levels of p65 in HPV16+ KCs compared to non-infected KCs. Total p65 levels and p65 phosphorylation status were determined in whole cell extracts by western blotting. β-actin served as loading control.
(C) NEMO degradation in HPV16+ KCs compared to non-infected KCs. Monolayer cultures were treated with 100 μM cycloheximide (CHX) and harvested after 0, 3, 6, 9, 12, 18 and 24 hours. Whole cell extracts were analyzed by western blotting using antibodies against NEMO and β-actin (control for protein degradation).
(D) Poly(I:C) stimulation-induced phosphorylation levels of IRF3 in hrHPV+ KCs compared to KCs. Total IRF3 levels and IRF3 phosphorylation status were determined in whole cell extracts by western blotting. β-actin served as loading control.

of *IFNb, RANTES* and *MIP3a* following 24 hours of stimulation with poly(I:C) (Figure 3B). Moreover, we repressed the polycistronic viral mRNA transcript [18,19] in hrHPV+ KCs by the use of siRNA targeting HPV16 *E2* as this allows the destruction of the whole RNA chain. Indeed the suppression of HPV early gene E2 expression translated into an overall decrease in viral early gene expression (Figure 3C) and an increase in the transcription of *IFNb, RANTES* and *MIP3a* following poly(I:C) stimulation (Figure 3D).

Together these data demonstrate that the innate immune response to viral and bacterial-derived PRR stimuli of both undifferentiated and differentiated hrHPV+ keratinocytes is suppressed by HPV at a point downstream of the PRR receptors but upstream of the transcription factors that relay the PRR signals to the nucleus.

The ubiquitin-modifying enzyme UCHL1 is over-expressed in hrHPV-positive keratinocytes and responsible for suppressing the production of type I IFN as well as pro-inflammatory and chemotactic cytokines.

Our data suggest that hrHPV+ keratinocytes manifest a generalized inability to respond to stimulation through interference at, or downstream of the cytosolic part of the PRR signaling pathways. We therefore re-analyzed the genome-wide expression profiles (Gene Expression Omnibus accession number GSE21260) of several different uninfected KC cultures and hrHPV+ KC cultures reported previously [10] by Ingenuity Pathways Analysis (IPA) and found a highly significant enrichment of genes belonging to the protein ubiquitination pathway (Table S1; $p=6.69 \times 10^{-5}$). In this pathway, the gene for the enzyme ubiquitin carboxyl-terminal hydrolase L1 (*UCHL1)* was the most upregulated gene in hrHPV+ KCs compared to uninfected KCs (Figure 4A and B). The upregulation of *UCHL1* in hrHPV+ KCs was confirmed by RT-qPCR in both foreskin and vaginal epithelial hrHPV+ KC cultures and expression was not influenced by poly(I:C) activation (Figure 4C). Furthermore, UCHL1 upregulation at the protein level was tested and shown for three different hrHPV+ KCs by western blotting (Figure 4D). Moreover, expression of *UCHL1* was upregulated 2 days post-infection of HPV16 in primary keratinocytes when compared to mock-infected primary keratinocytes (Figure 4E), whereas knock-down of the polycistronic viral mRNA transcript in hrHPV+ KCs by siRNA for HPV16 E2 resulted in a decreased *UCHL1* expression (Figure 4F). Thus, the

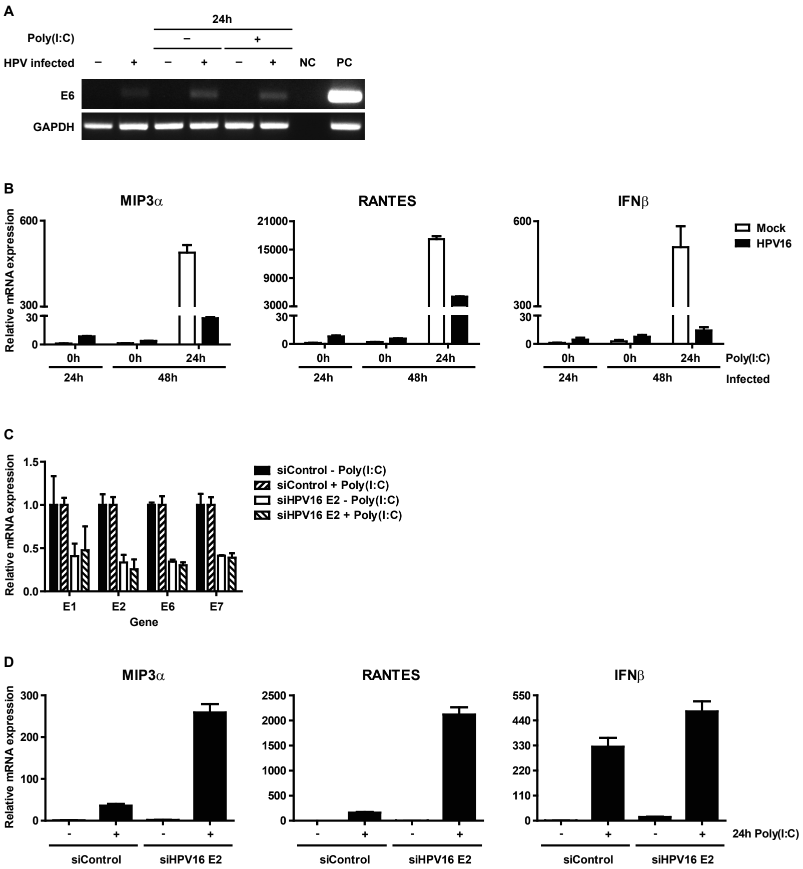

Figure 3. Expression of human papillomaviral transcripts are required to impair cytokine expression of poly(I:C) stimulated keratinocytes.
(A, B) Cytokine expression at the initial stage of HPV16 infection. Primary basal layer human foreskin keratinocytes were infected with native HPV16. (A) Viral early gene E6 expression was analyzed 1 and 2 (24h poly(I:C)) days after infection by PCR. NC: negative control, PC: positive control, HPV16+ KCs. (B) MIP3a, RANTES and IFNβ expression was measured by qRT-PCR. Gene expression was normalized against GAPDH mRNA levels and standardized against the 0h poly(I:C) stimulated non-infected cells. Similar results were observed in two independent experiments.
(C, D) Poly(I:C)-induced cytokine expression in HPV+ KCs transfected with control siRNA (siControl) or siRNA targeting HPV16 E2 (siHPV16 E2). E1, E2, E6, E7 (C) as well as MIP3a, RANTES, and IFNβ (D) expression was analyzed by qRT-PCR. Gene expression was normalized against GAPDH mRNA levels and standardized against no poly(I:C) siControl. For all three genes the response to poly(I:C) was significantly higher when HPV16 E2 was suppressed (p<0.001, one-way ANOVA).

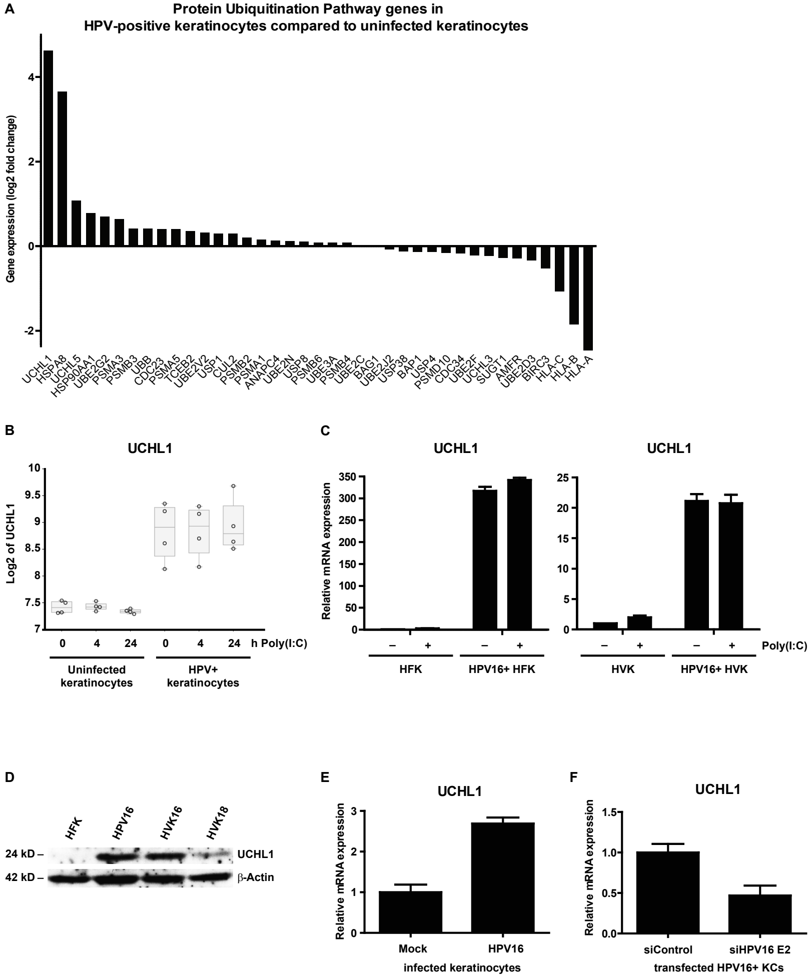

Figure 4. HPV induces expression of UCHL1 in keratinocytes.
(A) Summary of all differentially expressed genes within the Protein Ubiquitination Pathway. Differentially expressed genes between four uninfected KC and four hrHPV+ KC cultures with adjusted p-value ≤ 0.05 identified 24 hours after poly(I:C) stimulation by microarray analysis (log2 ratios) are shown.
(B) UCHL1 microarray gene expression values (log2 intensities) after 0, 4, and 24 hours of poly(I:C) stimulation in four primary KCs and four hrHPV+ KCs (circles). The box represents the 25th and 75th percentiles, the median is indicated with a horizontal line within the box, and the whiskers represent the minimum and maximum.
(C) UCHL1 expression in HPV16+ human foreskin keratinocytes (HFK; left panel) and HPV16+ human vaginal keratinocytes (HVK; right panel) when compared to uninfected KCs. KCs were either left unstimulated or stimulated with poly(I:C) for 24 hrs. UCHL1 expression was normalized

against GAPDH.

(D) UCHL1 protein levels in HPV16+ human foreskin keratinocytes (HPV16) and HPV16+ or HPV18+ human vaginal keratinocytes (HVK16 or HVK18, respectively) when compared to non-infected KCs (HFK) as detected by western blotting (WB) in whole cell extracts. β-actin served as loading control.

(E) UCHL1 expression at the initial stage of HPV16 infection. Primary basal layer human foreskin keratinocytes were infected with native HPV16 (HPV16 infected keratinocytes) or not (Mock). UCHL1 mRNA expression was analyzed by qRT-PCR 2 days after infection. Gene expression was normalized against GAPDH mRNA levels and standardized against the non-infected cells. Similar results were observed in two independent experiments.

(F) UCHL1 expression in HPV+ KCs transfected with control siRNA (siControl) or siRNA targeting HPV16 E2 (siHPV16 E2). UCHL1 expression was analyzed by qRT-PCR. Gene expression was normalized against GAPDH mRNA levels and standardized against siControl. Similar results were observed in more than 3 independent experiments.

cellular deubiquitinase UCHL1 is upregulated by hrHPV.

Although UCHL1 had not been associated with the inhibition of PRR signaling, its enhanced expression in hrHPV+ KCs fits well with the general role of deubiquitinases in controlling PRR signaling [6]. To test whether hrHPV-induced UCHL1 inhibits PRR signaling, we used lentiviral vectors expressing short-hairpin RNA (shRNA) against *UCHL1* and this resulted in a downregulated expression of *UCHL1* transcripts and protein levels in hrHPV+ KCs (Figure 5A and B). Upon stimulation with poly(I:C), hrHPV+ KCs expressing shRNA against *UCHL1* (shUCHL1) but not hrHPV+ KCs expressing a control shRNA (shControl) restored poly(I:C)-mediated induction of type I interferon and proinflammatory cytokines (Figure 5C). Similar results were obtained using transiently transfected RNA interference (RNAi) oligos targeting *UCHL1* but not with control RNAi oligos (Figure S3). An increase in the expression levels of *IL8* and *MIP3a* was detected in hrHPV+ KCs in which *UCHL1* was downregulated. Gene expression increased to the same levels found in *UCHL1*-non silenced hrHPV+ KCs cells stimulated with poly(I:C) (Supplemental Figure 3). This suggests that downregulation of *UCHL1* increases the gene expression of *IL-8* and *MIP3a* in hrHPV+ KCs. Conversely, transfection of uninfected KCs to overexpress *UCHL1* resulted in a decreased expression of *MIP3a, RANTES* and *IFNb* upon poly(I:C) stimulation (Figure 5D and E). Based on control experiments in which KCs were transfected with green fluorescent protein expressing plasmids, the transfection efficiency of keratinocytes was 30-40% (not shown), indicating that in a large part of the keratinocytes the activation of cytokine-encoding genes is not impaired and explaining the expression levels of these cytokine-encoding genes that are still detected.

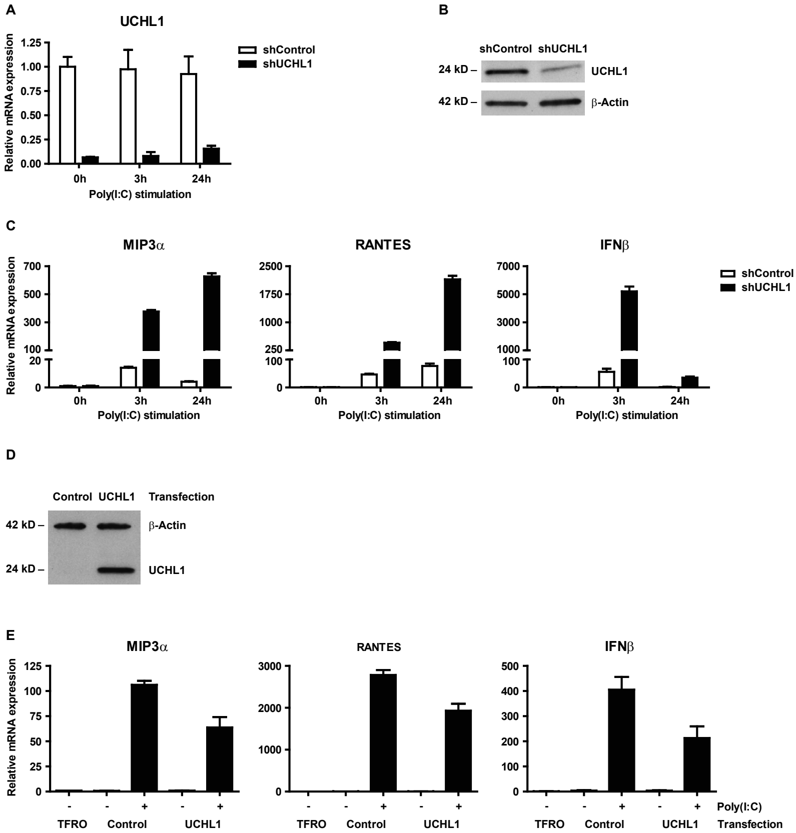

Figure 5. UCHL1 is responsible for suppressing poly(I:C) mediated gene activation of IFN-I and proinflammatory cytokines in hrHPV-infected KC.

(A – C) UCHL1 knock-down effect of poly(I:C) mediated gene expression of IFN-I and proinflammatory cytokines. HPV16+ keratinocytes were transduced with lentiviral vectors expressing shRNA against control mRNA (TurboGFP; shControl) or targeting mRNA of UCHL1 (shUCHL1). Cells were either left unstimulated, or were stimulated with poly(I:C) for 3 or 24 hrs. (A) UCHL1 mRNA expression was analyzed by qRT-PCR and (B) UCHL1 protein levels were analyzed by western blotting in whole cell extracts, β-actin served as loading control. (C) MIP3α, RANTES and IFNβ mRNA expression was analyzed by qRT-PCR. Gene expression was normalized against GAPDH mRNA levels and standardized against 0h of stimulation with poly(I:C).

(D, E) UCHL1 overexpression effect on the activation of poly(I:C) mediated gene expression of IFNβ and proinflammatory cytokines. Uninfected keratinocytes were transfected with a vector harboring the UCHL1 gene, an empty control or only received the transfection agent (TFRO). Cells were either left unstimulated, or were stimulated with poly(I:C) for 24 hrs. (D) UCHL1 protein levels were upregulated in the UCHL1-transfected cells as detected by western blotting in whole

cell extracts, β-actin served as loading control. (E) MIP3α and RANTES mRNA expression was analyzed by qRT-PCR. Gene expression was normalized against GAPDH mRNA levels and standardized against the TFRO at 0h of stimulation with poly(I:C).

All together, these data clearly demonstrate that UCHL1 can downregulate the PRR-mediated activation of both the type I IFN and proinflammatory cytokine and chemokine pathways.

Knock down of UCHL1 increases the phosphorylation of IRF3 and NFκB p65 and alleviates NEMO degradation.

We then asked whether the restoration of PRR signaling, as indicated by an increased induction of type I interferon and proinflammatory cytokines by the knock down of UCHL1 in hrHPV+ KCs would also be reflected in the levels of phosphorylated p65 (p65-p) and IRF3 (IRF3-p) upon poly(I:C) stimulation. Therefore, the p65-p and IRF3-p levels were analyzed in whole cell extracts of HPV16+ KCs stably expressing shRNA against *UCHL1* or control shRNA and following 3h or 24h of stimulation with poly(I:C). Knock down of UCHL1 in hrHPV+ KCs resulted in increased p65 phosphorylation at 3 and 24 hours after poly(I:C) stimulation (Figure 6A) coinciding with enhanced cyto- and chemokine production (Figure 5C). In addition, analysis of hrHPV+ KCs treated with cycloheximide revealed that NEMO degradation was alleviated when UCHL1 was knocked down by shUCHL1 as compared to the shControl hrHPV+ KCs (Figure 6B). Furthermore, higher levels of phosphorylated IRF3 were detected in hrHPV+ KCs in which *UCHL1* was knocked down as compared to hrHPV+ KCs expressing the shControl after 3 hours of poly(I:C) stimulation (Figure 6C).

UCHL1 alters the poly-ubiquitination of TRAF3 and NEMO.

TRAF3 ubiquitination is critical for type I IFN production and is a likely target for ubiquitin-modifying enzymes such as UCHL1. As the biochemical experiments to understand the nature of this interaction would require substantial amounts of primary KCs, which can only grow for a few passages thereby restricting their use in biochemical studies, we switched to the HEK293T cell system that is widely used for these purposes. To investigate the interaction between UCHL1 and TRAF3 we overexpressed UCHL1 and Flag-tagged TRAF3 in HEK293T cells. After FLAG immunoprecipitation, we

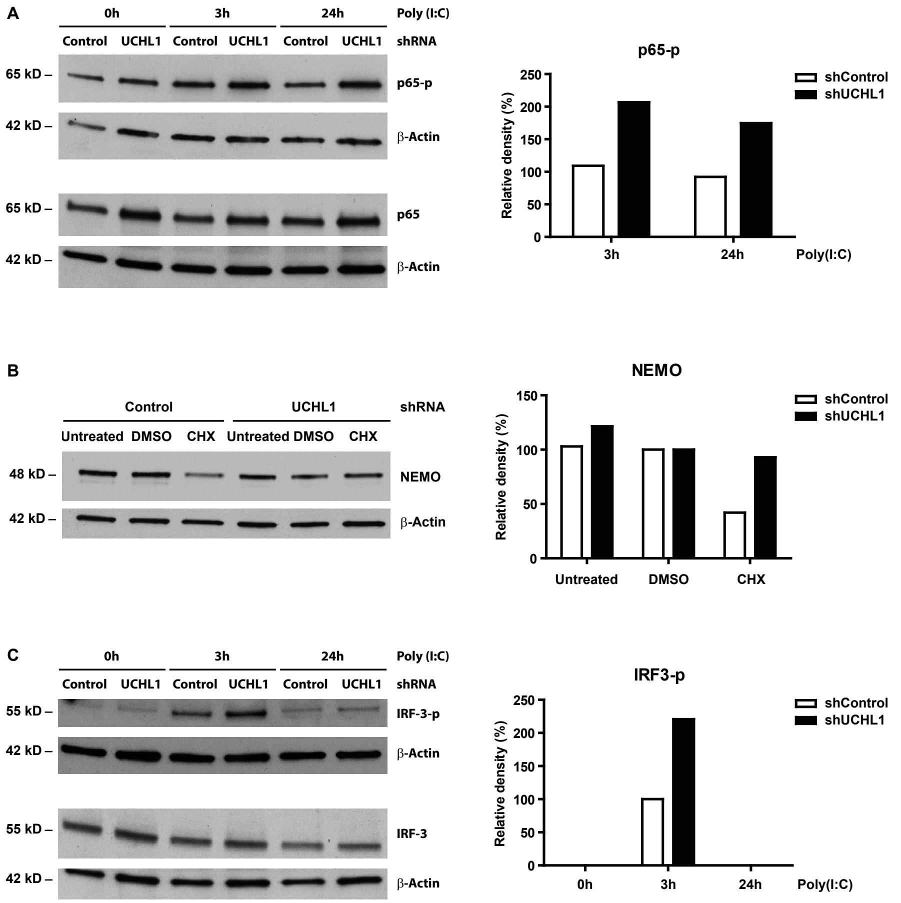

Figure 6. UCHL1 reduces phosphorylation levels of IRF3 and p65 and degrades NEMO in hrHPV-positive KC.

(A) UCHL1 knock down effect on poly(I:C) stimulated p65 phosphorylation in HPV16+ keratinocytes. Monolayer cultures of shControl or shUCHL1-expressing HPV16+ KCs were stimulated for 0, 3 or 24 hours with Poly(I:C). Whole cell extracts were analyzed by western blotting for p65, p65-p and β-Actin (as loading control). The relative expression of p65-p was quantified by measuring its density and by normalizing it to that of β-Actin. The expression levels of p65-p in the 0h Poly(I:C) cells were set to 100% for both shControl and shUCHL1 cells. The p65-p levels in the 3h and 24h Poly(I:C) cells were calculated against the levels measured at 0h Poly(I:C) (right panel).

(B) NEMO protein levels after knock down of UCHL1 in HPV16+ KCs. Monolayer cultures of shControl or shUCHL1-expressing HPV16+ KCs were treated with 100 µM cycloheximide (CHX) for 16 hours. Whole cell extracts were analyzed by western blot using antibodies against NEMO and β-Actin (control for protein content). The relative expression of NEMO was quantified by

measuring its density and by normalizing it to that of β-Actin. The expression of NEMO in the DMSO control was set to 100% (right panel).
(C) UCHL1 knock down effect on poly(I:C) stimulated IRF3 phosphorylation in HPV16+ keratinocytes. Similar to A, however cell extracts were analyzed by western blotting using antibodies against IRF3, IRF3-p and β-Actin (as loading control). The relative expression of IRF3-p was quantified by measuring its density and by normalizing it to that of β-Actin. The expression of IRF3-p in the 3h Poly(I:C) control cells (no knock down of UCHL1) was set to 100% (right panel).

confirmed that UCHL1 co-immunoprecipitated with TRAF3 (Figure 7A). TRAFs are activated by oligomerization and auto-ubiquitination, a process that resultsin lysine 63 (K63)-linked poly-ubiquination of TRAF, and this event can be induced by either their overexpression or by receptor activation. In contrast K48-linked poly-ubiquitination results in proteasome-mediated degradation of ubiquitinated TRAFs [6]. To test whether UCHL1 modified TRAF3 ubiquitination status, Flag-tagged TRAF3 and haemagglutinin A (HA)-tagged ubiquitin were overexpressed in control or UCHL1 overexpressing HEK293T cells. Poly-ubiquitination of TRAF3 was clearly visible by immunoblot analysis but strongly reduced when UCHL1 was also overexpressed (Figure 7B, Figure S4). No reduction in poly-ubiquitination was detected when as a control the growth regulated ubiquitin-specific protease 8 (USP8), which similar to UCHL1 displays carboxyl-terminal hydrolase activity, was overexpressed (Figure 7B). The UCHL1-associated decreased detection of poly-ubiquitinated TRAF3 was not the result of increased TRAF3 degradation as blocking the proteasomal degradation pathway by the inhibitor MG132 did not result in a reappearance of poly-ubiquitinated TRAF3 (Figure 7C). Instead, experiments in which HA-tagged ubiquitin mutants 'K63 Only' and 'K48 Only' (where all lysine residues, except at position K63 and K48, respectively, were mutated to arginine) showed that UCHL1 removed K63-linked poly-ubiquitins but not K48-linked poly-ubiquitins (Figure 7D), consistent with the known deubiquitinating capacity of UCHL1 [20]. K63-linked ubiquitination is required for TRAF3 to bind its partner TBK1 to activate the downstream type I IFN-signaling pathway. As expected, UCHL1-mediated deubiquitination of TRAF3 resulted in less TRAF3 bound to TBK1 in UCHL1 overexpressing cells when compared to control cells (Figure 7E). These data clearly show that UCHL1 binds and deubiquitinates TRAF3 resulting in a decreased TRAF3-TBK1 complex formation.

Poly-ubiquitination of TRAF6 and its downstream partner NEMO is critical for the PRR-induced activation of proinflammatory cytokine genes [6]. Since the overexpression of UCHL1 clearly affected proinflammatory cytokine

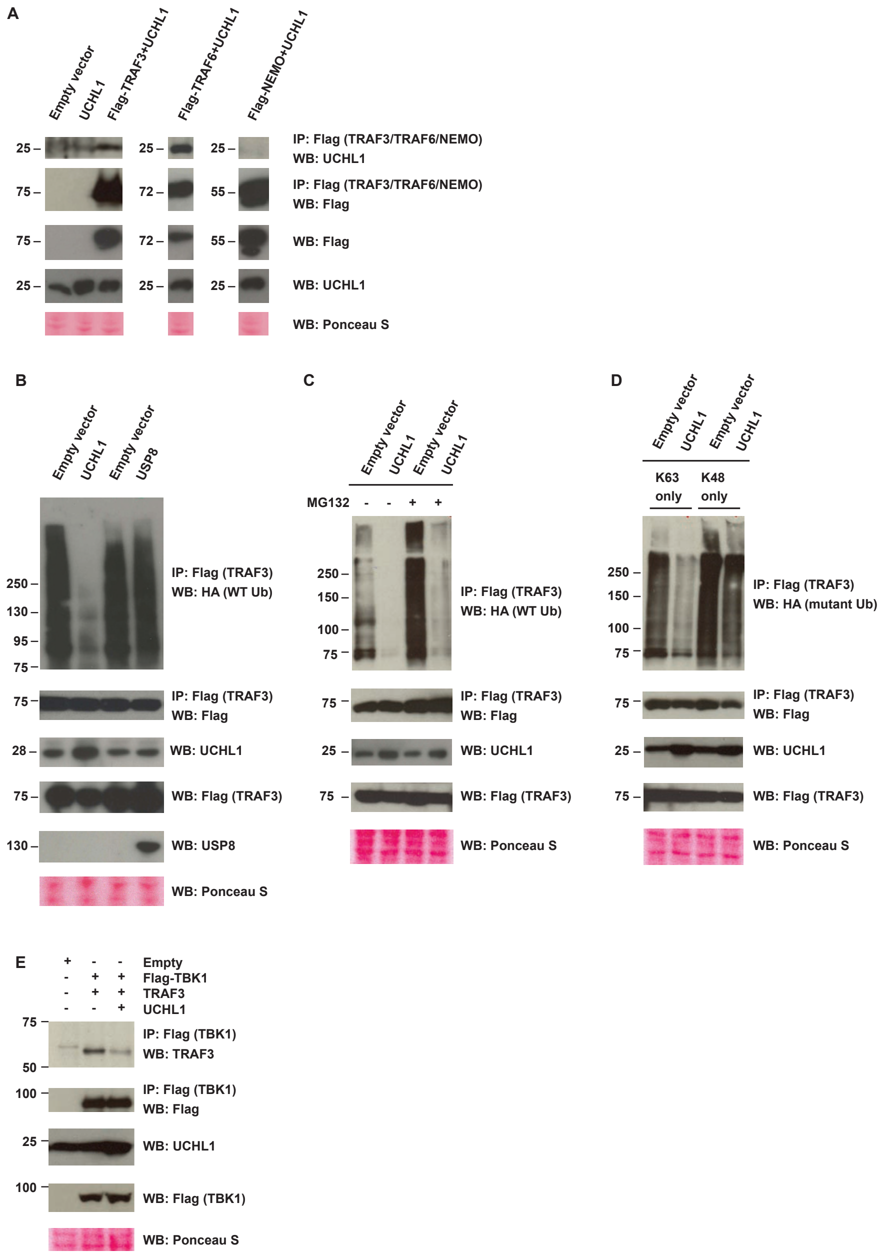
A
Empty vector
UCHL1
Flag-TRAF3+UCHL1
Flag-TRAF6+UCHL1
Flag-NEMO+UCHL1
25 –
75 –
72 –
55 –
IP: Flag (TRAF3/TRAF6/NEMO)
WB: UCHL1
IP: Flag (TRAF3/TRAF6/NEMO)
WB: Flag
WB: Flag
WB: UCHL1
WB: Ponceau S
B
Empty vector
UCHL1
Empty vector
USP8
250 –
130 –
95 –
75 –
28 –
IP: Flag (TRAF3)
WB: HA (WT Ub)
IP: Flag (TRAF3)
WB: Flag
WB: UCHL1
WB: Flag (TRAF3)
WB: USP8
WB: Ponceau S
C
Empty vector
UCHL1
Empty vector
UCHL1
MG132 - - + +
250 –
150 –
100 –
75 –
25 –
IP: Flag (TRAF3)
WB: HA (WT Ub)
IP: Flag (TRAF3)
WB: Flag
WB: UCHL1
WB: Flag (TRAF3)
WB: Ponceau S
D
Empty vector
UCHL1
Empty vector
UCHL1
K63 only
K48 only
250 –
150 –
100 –
75 –
25 –
IP: Flag (TRAF3)
WB: HA (mutant Ub)
IP: Flag (TRAF3)
WB: Flag
WB: UCHL1
WB: Flag (TRAF3)
WB: Ponceau S
E
+ - - Empty
- + + Flag-TBK1
- + + TRAF3
- - + UCHL1
75 –
50 –
100 –
25 –
IP: Flag (TBK1)
WB: TRAF3
IP: Flag (TBK1)
WB: Flag
WB: UCHL1
WB: Flag (TBK1)
WB: Ponceau S

Figure 7. Interaction of UCHL1 with the PRR downstream signaling molecule TRAF3. *(A) UCHL1 directly interacts with TRAF3 and TRAF6 but not NEMO. HEK293T cells were co-transfected as indicated and the respective TRAF3, TRAF6 or NEMO proteins were immunoprecipitated using Flag antibody, and co-precipitating UCHL1 was detected by WB. As a control a WB analysis for Flag was performed indicating that both TRAF3 and NEMO were present. The bottom three panels show a WB analysis of Flag and UCHL1 of non- immunoprecipitated lysate and a Ponceau S stained loading control for WB.*
(B) UCHL1, but not the control ubiquitin-specific protease 8 (USP8) mediates deubiquitination of TRAF3. HEK293T cells were co-transfected with Flag-TRAF3, HA-tagged wild-type ubiquitin (WT-Ub), and with either empty vector, WT UCHL1 or USP8. TRAF3 was immunoprecipitated with Flag antibody and WB was done with HA or Flag antibodies (top panels). The bottom four panels show a WB analysis of Flag, UCHL1, and USP8 of non- immunoprecipitated lysate and a Ponceau S stained loading control for WB.
(C) Deubiquitination but not degradation of TRAF3 by UCHL1. HEK293T cells were co-transfected with Flag-TRAF3, HA-tagged wild-type ubiquitin (WT-Ub), and with either empty vector or WT UCHL1. Cells were left untreated or treated with proteasome blocker MG132. TRAF3 was immunoprecipitated with Flag antibody and WB was done with HA or Flag antibodies (top two panels).
(D) UCHL1 mainly removes K63-linked poly-ubiquitin chains of TRAF3. HEK293T cells expressing Flag-TRAF3, HA-tagged mutant ubiquitin either K63 Only or K48 Only, and WT UCHL1 were immunoprecipitated with Flag antibody and analyzed by HA or Flag antibodies (top two panels).
(E) UCHL1 lowers TRAF3-TBK1 complex formation. HEK293T cells were co-transfected and TBK1 was immunoprecipitated using Flag antibody, and co-precipitating TRAF3 or TBK1 was detected by WB (top two panels).

synthesis (Figure 5) the interaction of UCHL1 with TRAF6 and NEMO was tested. Co-expression and immunoprecipitation experiments in HEK293T cells showed that UCHL1 bound to TRAF6 but not to NEMO (Figure 7A). In contrast to what we observed for TRAF3, UCHL1 displayed a modest effect on the poly-ubiquitination of TRAF6 (Figure 8A). However, poly-ubiquitination of NEMO was reduced in UCHL1 overexpressing cells (Figure 8B, Figure S4) but not in USP8 overexpressing cells (Figure 8D). Inhibition of proteasome function by MG132 suggested that the reduced poly-ubiquitination of NEMO was the result of enhanced degradation of NEMO in cells overexpressing UCHL1 (Figure 8C, compare lanes 2 and 4), albeit that the total protein levels of NEMO in these transfected cells remained unaffected. This is not unexpected as also in the endogenous setting (Figures 2 & 6) the degradation of NEMO could only be visualized when the hrHPV+ KCs where pretreated with cycloheximide to prevent new protein synthesis.

Collectively, these data support the notion that UCHL1 can suppress the PRR-signaling pathways necessary for type I IFN and pro-inflammatory cytokine production by the removal of the activating K63 ubiquitins from TRAF3 and the forced degradation of NEMO.

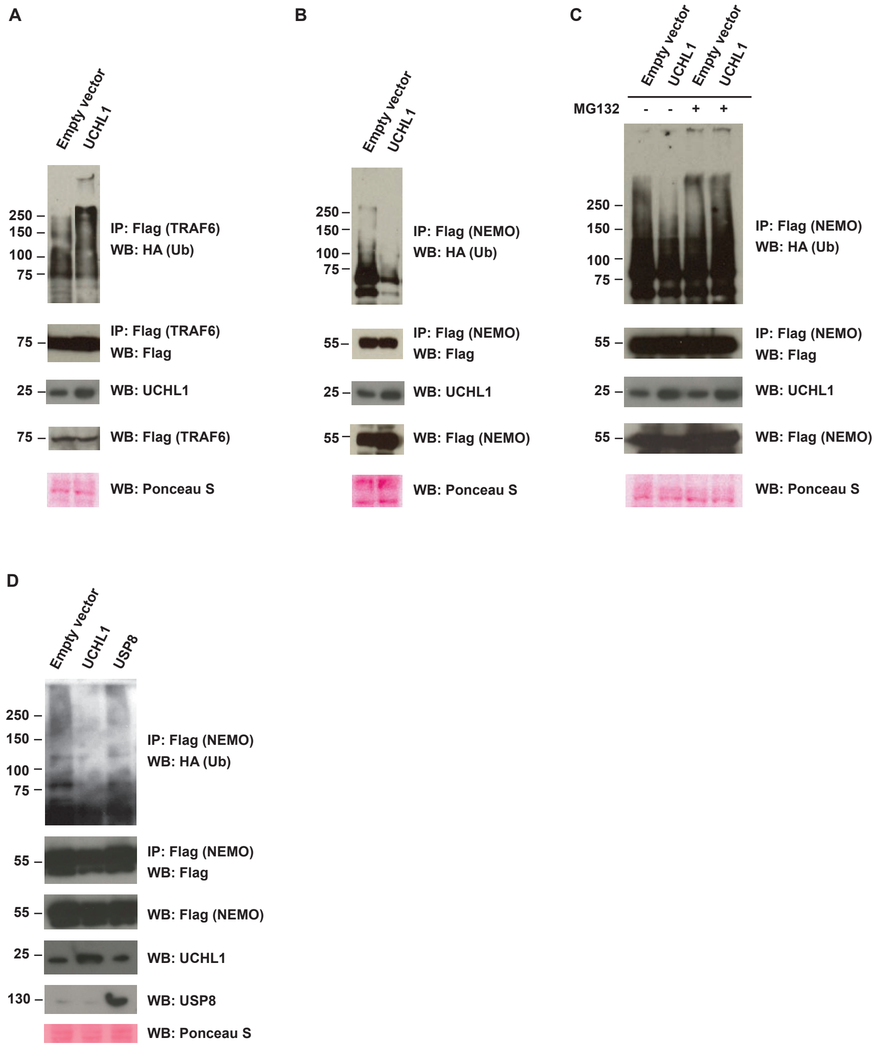
A
Empty vector
UCHL1
250
150
100
75
IP: Flag (TRAF6)
WB: HA (Ub)
75
IP: Flag (TRAF6)
WB: Flag
25
WB: UCHL1
75
WB: Flag (TRAF6)
WB: Ponceau S
B
Empty vector
UCHL1
250
150
100
75
IP: Flag (NEMO)
WB: HA (Ub)
55
IP: Flag (NEMO)
WB: Flag
25
WB: UCHL1
55
WB: Flag (NEMO)
WB: Ponceau S
C
Empty vector
UCHL1
Empty vector
UCHL1
MG132
-
-
+
+
250
150
100
75
IP: Flag (NEMO)
WB: HA (Ub)
55
IP: Flag (NEMO)
WB: Flag
25
WB: UCHL1
55
WB: Flag (NEMO)
WB: Ponceau S
D
Empty vector
UCHL1
USP8
250
150
100
75
IP: Flag (NEMO)
WB: HA (Ub)
55
IP: Flag (NEMO)
WB: Flag
55
WB: Flag (NEMO)
25
WB: UCHL1
130
WB: USP8
WB: Ponceau S

Figure 8. Interaction of UCHL1 with the PRR downstream signaling molecules TRAF6 and NEMO.

(A) UCHL1 overexpression results in a modest poly-ubiquitination of TRAF6. HEK293T cells were co-transfected with Flag-TRAF6, HA-tagged WT-Ub, and with either empty vector or WT UCHL1. TRAF6 was immunoprecipitated with Flag antibody and western Blotting (WB) was done with HA or Flag antibodies (top two panels). The bottom three panels show a WB analysis of UCHL1 and Flag of non-immunoprecipitated lysate and a Ponceau S stained loading control for WB.

(B) The effect of UCHL1 on NEMO. HEK293T cells were co-transfected with Flag-NEMO, HA-tagged WT-Ub, and with either empty vector or WT UCHL1. NEMO was immunoprecipitated with Flag antibody and WB was done with HA or Flag antibodies (top two panels).

(C) The overexpression of UCHL1 mediates the degradation of NEMO. HEK293T cells were co-transfected with Flag-NEMO, HA-tagged WT-Ub, and with either empty vector or WT UCHL1. Cells were left untreated or were treated with MG132, NEMO was immunoprecipitated with Flag antibody and WB was done with HA or Flag antibodies (top two panels).

(D) USP8 does not deubiquitinate NEMO. HEK293T cells were co-transfected with Flag-NEMO, HA-tagged wild-type ubiquitin (WT-Ub) and UCHL1 or USP8. NEMO was immunoprecipitated with Flag antibody and WB was done with HA antibodies (top panel). The bottom four panels show a WB analysis of Flag, UCHL1, and USP8 of non-immunoprecipitated lysate and a Ponceau S stained loading control for WB.

DISCUSSION

We have employed a unique model for hrHPV infection to examine the potential mechanisms underlying the capacity of hrHPV to evade host immunity by suppression of the innate immune response [10]. We utilized primary KC cultures that were newly infected with HPV16 virions or primary KCs stably maintaining the episomal hrHPV genome to show that despite the expression of multiple PRRs the production of IFNβ and pro-inflammatory cytokines and chemokines is suppressed by hrHPV as a consequence of reduced PRR signaling. We provided firm evidence that this suppression depends on the hrHPV-induced upregulation of the cellular ubiquitin-modifying enzyme UCHL1 in infected primary KCs.

Finally, classical biochemical studies in HEK293T cells [11,21,22] performed to understand how UCHL1 mechanistically could suppress the production of type I interferons and pro-inflammatory cytokines revealed that UCHL1 regulated the ubiquitination of the PRR-signaling pathway adaptor molecules TRAF3 and NEMO. UCHL1 removes activating K63-linked ubiquitin molecules from TRAF3 resulting in a lower amount of the downstream signaling complex TRAF3-TBK-1 to suppress the type I IFN pathway. This puts UCHL1 within the family of other deubiquinating enzymes that regulate the PRR pathways by selectively cleaving lysine-63 (K63)-linked ubiquitin chains from TRAFs (e.g. DUBA, OTUB1, OTUB2, A20) [21,22,23,24,25,26]. Furthermore, we showed that UCHL1 bound to TRAF6 and mediated the enhanced degradation of NEMO as a mechanism to suppress the proinflammatory cytokine NF-κB pathway. Notably, the ubiquitin-modifying enzyme A20, a known negative regulator of the TLR pathway, has two ubiquitin-editing domains allowing it to remove and to add ubiquitin chains (22, 26). UCHL1 has also been reported to have these two opposing functions (20). The ligase activity of UCHL1 may explain the ubiquitination of TRAF6 observed in our study. Although UCHL1 did not bind to NEMO, it is known that other deubiquitinating enzymes (*e.g.* CYLD, A20) bind to TRAFs in order to dock on the IKK complex and to associate with NEMO [21,27]. TRAF6-dependent poly-ubiquitination of NEMO is well known [28]. It is highly likely that UCH-L1 acts in a similar fashion and this would fit with TRAF6-NEMO interaction and our observations that NEMO is degraded.

Our data on the suppression of NF-κB signaling via the degradation of NEMO by UCHL1 fits well with earlier observations concerning the overexpression of UCHL1 in vascular cells. Here UCHL1 attenuated TNF-a induced NF-κB signaling and this was associated with stabilization of IκBa and a decrease in its basal ubiquitination [29]. The activation of NF-κB signaling requires IκBa to become degraded following an interaction with the IκB kinase complex (IKK) which comprises NEMO. Hence, the degradation of NEMO may explain previous observations on UCHL1-associated stabilization of IκBa.

UCHL1 is not found to be central in the network of genes affected by hrHPV, suggesting that it is not part of the cellular genes affected in order to assist in HPV genome replication and viral protein production [10]. This indicates that UCHL1 is not directly involved in viral propagation but rather recruited by hrHPV to suppress keratinocyte-mediated production of cytokines and chemokines that would result in the attraction and activation of an adaptive immune response, thereby enabling the virus to persist and propagate.

Many viruses utilize multifunctional viral proteins in order to evade NF-κB- and IRF-mediated immune responses, to favor viral replication and/or to modulate cellular apoptosis and growth pathways [30]. The group of pox viruses have evolved to inhibit NF-κB-signaling by targeting one or more of the many different molecules of this signaling cascade [31]. The vaccinia virus B14 protein is known to inhibit NF-κB signaling by a variety of toll-like receptor agonists at the level of the IKK complex, of which NEMO is a member [32]. The vaccinia virus A64R protein inhibits TRIF-TRAF3-IRF signaling [33]. The pathogenic NY-1 hantavirus Gn protein inhibits TRAF3 signaling by blocking the formation of TBK1-TRAF3 complexes [34] whereas the LMP1 protein of Epstein-Barr virus directly binds to TRAF3 [35]. Furthermore, foot-and-mouth disease virus 3c protease cleaves NEMO [16] and cytomegalovirus M54 protein induces the proteasome-independent degradation of NEMO [17]. In contrast, human papillomaviruses, with a rather limited coding capacity in their genomes, rely for many aspects of their life cycle on the utilization of cellular proteins [36] and this includes the recruitment of different cellular E3 ligases to mediate degradation of cellular proteins through the ubiquitin-proteasomal pathway [37]. UCHL1 is one of the most abundant proteins in the mammalian nervous system and is involved in regulating synaptic transmission at the neuromuscular junctions [38]. Aberrant expression is related to Parkinson's disease [20] and is also implicated in oncogenesis [39]. In hrHPV+ keratinocytes UCHL1 is expressed and redirected to adopt a new function that is to serve as a negative regulator of the PRR-signaling pathway. As such it mimics the ubiquitin-modifying enzyme A20 which is the natural negative regulator of the TLR pathway [22,26,40]. UCHL1 interferes with the adaptor molecules TRAF3, TRAF6 and NEMO which all function at junctions for the immune stimulating signals from different PRR and type I IFNR to activate NF-κB- and IRF-mediated immune responses. Therefore, the utilization of UCHL1 represents a truly effective use of a cellular protein as it may suppress the immunostimulatory signals initiated through recognition of HPV genomic DNA by TLR9 [5] and RIG-I [11,12] as well as those obtained via the cell surface receptors for type I IFN [41].

The high expression of UCHL1 in primary keratinocytes carrying infectious hrHPV [13,14] is generally lost after transformation of these keratinocytes to tumor cells. Although transformed keratinocytes expressing un-physiologically high levels of *E6* and *E7* via retroviral transduction still may express *UCHL1*, only a minority of spontaneously HPV-transformed cervical carcinoma's and none of the well known HPV-induced cancer cell lines overexpress UCHL1 [42], indicating that under normal conditions *UCHL1* overexpression in HPV transformed cells is not a common event. The expression of the hrHPV oncoproteins E6 and E7 is required to maintain the transformed state of keratinocytes [2,43] suggesting that it is not E6 or E7, but one or more of the other viral proteins responsible for upregulation of UCHL1 (currently under investigation). Previous studies on the innate immune response to hrHPV relied on the overexpression of hrHPV E6 and/or E7 proteins, showing that the viral DNA-sensing TLR9 was altered [8] and that overexpressed HPV E6 or E7 could bind to IRF3 [44] and/or the co-activator CPB [45]. Furthermore, overexpressed hrHPV E6 and/or E7 attenuated IκB kinase signaling [46], and interfered with the nuclear translocation of the interferon-stimulated gene factor 3 (ISGF3) transcription complex [47]. The fact that these studies were performed with only HPV E6- and E7 transfected or transformed cells may explain why the central role of UCHL1 in dampening immunity towards hrHPV+ keratinocytes was not discovered before. In addition, the loss of UCHL1 mediated suppression of the NF-κB pathway in hrHPV E6/E7-induced cancer cells fits well with the notion that solid tumors require the NF-κB-mediated expression of proteins that promote survival, proliferation, invasion and metastasis [48] which is acquired through the E6-mediated deactivation of CYLD [49], a negative regulator of TRAF2 and TRAF6-mediated activation of NF-κB [21,24].

All together, our data implicate UCHL1 as a negative regulator of the PRR pathways helping hrHPV to evade host immunity and allowing it to persist in keratinocytes.

METHODS

Cell culture.

Primary cultures of human epithelial keratinocytes were established from foreskin [50] and vaginal tissues and grown in serum-free medium (Defined KSFM, Invitrogen, Breda, The Netherlands). Keratinocyte lines stably maintaining the full episomal HPV genome following electroporation were grown in monolayer culture using E medium in the presence of mitomycin C treated J2 3T3 feeder cells [13,14] for two passages and were then adapted to Defined K-SFM for one passage before experimentation. None of the cell cultures were used after passage 15 and the non-transformed state of the cells used was confirmed by the expression of both *E1* and *E2* so that the cells used truly represent the preneoplastic state in which the HPV genomes remained episomal and were capable of the complete viral life cycle. Keratinocytes were terminally differentiated by placing them into serum-free medium containing 1.75% methyl cellulose and 1.8 mM Ca^{2+} for 24 hours [50]. Cells were harvested by washing out the methyl cellulose three times. HEK293T cells were cultured in Dulbecco's modified Eagle's medium supplemented with 10% fetal bovine serum, 2mM l-glutamine and 1% penicillin-streptomycin (Gibco-BRL, Invitrogen). Transient transfections were performed using calcium phosphate or Lipofectamine 2000 (Invitrogen).

HPV16 infection of non-infected keratinocytes.

Primary basal layer human foreskin keratinocytes were seeded at $7.5x10^4$ cells per well of a 24-wells plate in K-SFM and then allowed to attach for 48 hours. Cells received fresh medium (Mock infected) or medium containing native HPV16 isolated from raft cultures at a MOI 100 for 24 hours. Cells were stimulated with or without 25 ug/ml poly(I:C) in K-SFM for 0 or 24 hours and harvested at the indicated time-points.

Plasmid construction.

Full length human cDNA clones for UCHL1, TRAF3, TRAF6 and TBK1 were obtained from Open Biosystems (Surrey, UK). The cDNA clones were PCR amplified and subcloned either into pcDNA3.1 expression vector or into Flag-tagged pcDNA3.1 vector. Full-length Flag-NEMO construct was kindly provided by Dr. C. Sasakawa, University of Tokyo, Japan [51]. HA-tagged wild-type and mutant ubiquitin constructs were kindly provided by Dr. A. Iavarone, Columbia University, USA.

RNA expression analyses.

Total RNA was isolated using TRIzol (Invitrogen) according to manufacturer's instructions. RNA was purified using RNeasy Mini Protocol (Qiagen, Venlo, The Netherlands). Total RNA (0.2 µg) was reverse transcribed using SuperScript III reverse transcriptase (Invitrogen) and oligo dT primers (Promega, Madison, USA). TaqMan PCR was performed using TaqMan Universal PCR Master Mix and pre-designed, pre-optimized primers and probe mix for IL-8, MIP-1α, MIP-3α, RANTES, IL-1β, IFNβ, UCHL1 and GAPDH (Applied Biosystems, Foster City, USA). Threshold cycle numbers (Ct) were determined using the 7900HT Fast Real-Time PCR System (Applied Biosystems) and the relative quantities of mRNA per sample were calculated using the ΔΔCt method as described by the manufacturer using GAPDH as the calibrator gene.

Stimulation of cells with TLR ligands and ELISA.

$5x10^5$ cells were plated in 1 ml in each well of 24-well flat bottom plate. Cells were left unstimulated or stimulated with Pam3CSK4 (5 µg/ml), Poly(I:C) (25 µg/ml), LPS (3.33 µg/ml), flagellin (150 ng/ml), R848 (1 µg/ml), CpG (1 µM) or TNFα (50 ng/ml) for 24 hours. Flagellin was a kind gift from Jean-Claude Sirard (Institut Pasteur, Lille, France). TLR ligands were purchased from Invivogen (San Diego, USA). The supernatants were harvested and IL-8, MIP-3α, and MIP-1α concentrations were determined using corresponding Quantikine ELISA kits (R&D Systems, Oxon, UK).

RNAi and shRNA.

Non-targeting RNAi oligos (ON-TARGETplus Non-targeting Pool, catalogue D-001810-10-20) and oligos targeting UCHL1 (ON-TARGETplus SMARTpool, catalogue L-004309-00) were purchased from Dharmacon (Chicago, IL). Cells were transfected with RNAi using N-TER Nanoparticle siRNA Transfection System (Sigma-Aldrich, St. Louis, MO) according to manufacturer’s instructions. 24 hours after transfection, cells were stimulated with poly(I:C) (25 µg/ml) for another 24 hours and experiments were performed.

The shRNA’s used were obtained from the MISSION TRC-library of Sigma-Aldrich (Zwijndrecht, The Netherlands). The MISSION shRNA clones are sequence-verified shRNA lentiviral plasmids (pLKO.1-puro) provided as frozen bacterial glycerol stocks (Luria Broth, carbenicillin at 100 µg/ml and 10% glycerol) in Escherichia coli for propagation and downstream purification of the shRNA clones. pLKO.1 contains the puromycin selection marker for transient or stable transfection. The construct against UCHL1 (NM_004181) was TRCN0000011079 (LV079): CCGGCAGTTCTGAAACAGTTTCTTTCTCGAGAAAGAAACTGTTTCAGAACTGTTTTT and the control was: SHC004 (MISSION TRC2-pLKO puro TurboGFP shRNA Control vector): CCGGCGTGATCTTCACCGACAAGATCTCGAGATCTT GTCGGTGAAGATCACGTTTTT.

HPV16+ KCs were seeded 7.5x104 cells per well to a 12-wells plate in K-SFM and were allowed to attach over night. Medium was replaced by infection medium (K-SFM + 30% virus supernatant; MOI=5), containing either the lentivirus LV079 in IMDM 5% FCS or as control SHC004. HPV16+ KCs were infected over night after which infection medium was replaced by K-SFM containing 1000 ng/ml puromycin for 48 hours to select for successfully infected HPV16+ KCs. Then the medium was replaced by K-SFM without puromycin and cells were grown for 24 hours. To stimulate the PRR pathways lentivirus-infected HPV16+ KCs were given K-SFM containing either no poly(I:C) (two wells) or 25 ug/ml poly(I:C) and were cultured for 21 hours. Then one of the two non-stimulated wells received 25 ug/ml poly(I:C) and all cells were cultured for another 3 hours. Cells were harvested and total RNA was isolated.

Silencer Select siRNA against HPV16 E2 (AACACUACACCCAUAGUACAUtt) was designed using siRNA Target Finder software (Ambion, Invitrogen). Blast search revealed that the designed E2 siRNA does not match with the known human transcriptome. E2 and Negative control #2 (NC2) siRNA (sequence not provided by manufacturer) were purchased from Ambion. HPV16+ KCs were transfected with 50 nM siRNA E2 or NC2 using Lipofectamine 2000 (Invitrogen) according to the manufacturer's instructions. 48 hours post-transfection cells received K-SFM containing no Poly(I:C) or 25 ug/ml Poly(I:C) and were cultured for 24 hours after which target gene expression was assayed by qRT-PCR.

Western blot analysis and immunoprecipitation.

For Western blotting, polypeptides were resolved by SDS–polyacrylamide gel electrophoresis (SDS–PAGE) and transferred to a PVDF membrane (Bio-Rad, Veenendaal, The Netherlands). Immunodetection was achieved with anti-Flag (1:2000, Sigma-Aldrich), anti-HA (1:1000, Covance), anti-TRAF3, anti-TRAF6 (both 1:500, Santa Cruz, CA), anti-ubiquitin lysine 48-specific (1:1000, Millipore, Amsterdam, The Netherlands), anti-poly-ubiquitin lysine 63 specific (1:1000, Millipore), anti-TBK1 (1:400, Santa Cruz), anti-NEMO (FL-419, Santa Cruz), anti-UCHL1 (1:1000 Millipore, 1:100 Abcam or 1:1000 Santa Cruz), anti-USP8 (#8728, Cell Signaling Technology, Danvers, MA, USA), anti-phospho-p65 (Ser538; 1:1000, #3033 Cell Signaling Technology) and anti-phospho-IRF3 (Ser396; 1:2000, #4947, Cell Signaling Technology) or β-actin (1:10,000, Sigma-Aldrich) antibodies. The proteins were visualized by a chemoluminescence reagent (Thermo Scientific, Etten-Leur, The Netherlands). X-Ray films were scanned using a GS-800 calibrated densitometer and Quantity One software (Bio-Rad, Veenendaal, The Netherlands) to quantify the intensity of the bands as a measure of the amount of protein of interest in the blot. The relative amount was determined by calculating the ratio of each protein over that of the density measured for the household protein β-Actin.

For immunoprecipitation, cells were collected after 48h and then lysed in NP40 buffer supplemented with a complete protease inhibitor cocktail (Roche, Almere, The Netherlands). After pre-clearing with protein A/G agarose beads for 1h at 4°C, whole-cell lysates were used for immunoprecipitation with either mouse or rabbit anti-Flag antibodies (Sigma-Aldrich), or rabbit anti-TRAF3 or rabbit anti-TRAF6. One to two µg of the antibody was added to 1 ml of cell lysate, which was incubated at 4°C for 2-3h. After addition of protein A/G agarose beads, the incubation was continued for 1h. Immunoprecipitates were extensively washed with lysis buffer and eluted with SDS loading buffer and boiled for 5 min. For immunoprecipitation under denaturing conditions, proteins were extracted using regular immunoprecipitation buffer plus 1% SDS and heated at 95^0C for 5 min. The samples were diluted (10-fold) in regular immunoprecipitation buffer before immunoprecipitation.

REFERENCES

1. *zur Hausen H (2002) Papillomaviruses and cancer: from basic studies to clinical application. Nat Rev Cancer 2: 342-350.*
2. *Doorbar J (2006) Molecular biology of human papillomavirus infection and cervical cancer. Clin Sci (Lond) 110: 525-541.*
3. *Frazer IH (2009) Interaction of human papillomaviruses with the host immune system: a well evolved relationship. Virology 384: 410-414.*
4. *Richardson H, Kelsall G, Tellier P, Voyer H, Abrahamowicz M, et al. (2003) The natural history of type-specific human papillomavirus infections in female university students. Cancer Epidemiol Biomarkers Prev 12: 485-490.*
5. *Takeuchi O, Akira S (2009) Innate immunity to virus infection. Immunol Rev 227: 75-86.*
6. *Bhoj VG, Chen ZJ (2009) Ubiquitylation in innate and adaptive immunity. Nature 458: 430-437.*
7. *Zhao T, Yang L, Sun Q, Arguello M, Ballard DW, et al. (2007) The NEMO adaptor bridges the nuclear factor-kappaB and interferon regulatory factor signaling pathways. Nat Immunol 8: 592-600.*
8. *Hasan UA, Bates E, Takeshita F, Biliato A, Accardi R, et al. (2007) TLR9 expression and function is abolished by the cervical cancer-associated human papillomavirus type 16. J Immunol 178: 3186-3197.*
9. *Kalali BN, Kollisch G, Mages J, Muller T, Bauer S, et al. (2008) Double-stranded RNA induces an antiviral defense status in epidermal keratinocytes through TLR3-, PKR-, and MDA5/RIG-I-mediated differential signaling. J Immunol 181: 2694-2704.*
10. *Karim R, Meyers C, Backendorf C, Ludigs K, Offringa R, et al. (2011) Human Papillomavirus Deregulates the Response of a Cellular Network Comprising of Chemotactic and Proinflammatory Genes. Plos One 6:e17848.*
11. *Ablasser A, Bauernfeind F, Hartmann G, Latz E, Fitzgerald KA, et al. (2009) RIG-I-dependent sensing of poly(dA:dT) through the induction of an RNA polymerase III-transcribed RNA intermediate. Nat Immunol 10: 1065-1072.*
12. *Chiu YH, Macmillan JB, Chen ZJ (2009) RNA polymerase III detects cytosolic DNA and induces type I interferons through the RIG-I pathway. Cell 138: 576-591.*
13. *Meyers C, Mayer TJ, Ozbun MA (1997) Synthesis of infectious human papillomavirus type 18 in differentiating epithelium transfected with viral DNA. J Virol 71: 7381-7386.*
14. *McLaughlin-Drubin ME, Christensen ND, Meyers C (2004) Propagation, infection, and neutralization of authentic HPV16 virus. Virology 322: 213-219.*

15. *Conway MJ, Alam S, Ryndock EJ, Cruz L, Christensen ND, et al. (2009) Tissue-spanning redox gradient-dependent assembly of native human papillomavirus type 16 virions. J Virol 83: 10515-10526.*
16. *Wang D, Fang L, Li K, Zhong H, Fan J, et al. (2012) Foot-and-Mouth Disease Virus 3C Protease Cleaves NEMO To Impair Innate Immune Signaling. J Virol 86: 9311-9322.*
17. *Fliss PM, Jowers TP, Brinkmann MM, Holstermann B, Mack C, et al. (2012) Viral mediated redirection of NEMO/IKKgamma to autophagosomes curtails the inflammatory cascade. PLoS Pathog 8: e1002517.*
18. *Alloul N, Sherman L (1999) The E2 protein of human papillomavirus type 16 is translated from a variety of differentially spliced polycistronic mRNAs. J Gen Virol 80 (Pt 1): 29-37.*
19. *Sherman L, Alloul N (1992) Human papillomavirus type 16 expresses a variety of alternatively spliced mRNAs putatively encoding the E2 protein. Virology 191: 953-959.*
20. *Liu Y, Fallon L, Lashuel HA, Liu Z, Lansbury PT, Jr. (2002) The UCH-L1 gene encodes two opposing enzymatic activities that affect alpha-synuclein degradation and Parkinson's disease susceptibility. Cell 111: 209-218.*
21. *Trompouki E, Hatzivassiliou E, Tsichritzis T, Farmer H, Ashworth A, et al. (2003) CYLD is a deubiquitinating enzyme that negatively regulates NF-kappaB activation by TNFR family members. Nature 424: 793-796.*
22. *Shembade N, Ma A, Harhaj EW (2010) Inhibition of NF-kappaB signaling by A20 through disruption of ubiquitin enzyme complexes. Science 327: 1135-1139.*
23. *Kayagaki N, Phung Q, Chan S, Chaudhari R, Quan C, et al. (2007) DUBA: a deubiquitinase that regulates type I interferon production. Science 318: 1628-1632.*
24. *Kovalenko A, Chable-Bessia C, Cantarella G, Israel A, Wallach D, et al. (2003) The tumour suppressor CYLD negatively regulates NF-kappaB signalling by deubiquitination. Nature 424: 801-805.*
25. *Li S, Zheng H, Mao AP, Zhong B, Li Y, et al. (2010) Regulation of virus-triggered signaling by OTUB1- and OTUB2-mediated deubiquitination of TRAF3 and TRAF6. J Biol Chem 285: 4291-4297.*
26. *Wertz IE, O'Rourke KM, Zhou H, Eby M, Aravind L, et al. (2004) De-ubiquitination and ubiquitin ligase domains of A20 downregulate NF-kappaB signalling. Nature 430: 694-699.*
27. *Zhang SQ, Kovalenko A, Cantarella G, Wallach D (2000) Recruitment of the IKK signalosome to the p55 TNF receptor: RIP and A20 bind to NEMO (IKKgamma) upon receptor stimulation. Immunity 12: 301-311.*
28. *Sebban-Benin H, Pescatore A, Fusco F, Pascuale V, Gautheron J, et al. (2007) Identification of TRAF6-dependent NEMO polyubiquitination sites through analysis of a new NEMO mutation causing incontinentia pigmenti. Hum Mol Genet 16: 2805-2815.*

29. *Takami Y, Nakagami H, Morishita R, Katsuya T, Cui TX, et al. (2007) Ubiquitin carboxyl-terminal hydrolase L1, a novel deubiquitinating enzyme in the vasculature, attenuates NF-kappaB activation. Arterioscler Thromb Vasc Biol 27: 2184-2190.*
30. *Hiscott J, Nguyen TL, Arguello M, Nakhaei P, Paz S (2006) Manipulation of the nuclear factor-kappaB pathway and the innate immune response by viruses. Oncogene 25: 6844-6867.*
31. *Mohamed MR, McFadden G (2009) NFkB inhibitors: strategies from poxviruses. Cell Cycle 8: 3125-3132.*
32. *Chen RA, Ryzhakov G, Cooray S, Randow F, Smith GL (2008) Inhibition of IkappaB kinase by vaccinia virus virulence factor B14. PLoS Pathog 4: e22.*
33. *Stack J, Haga IR, Schroder M, Bartlett NW, Maloney G, et al. (2005) Vaccinia virus protein A46R targets multiple Toll-like-interleukin-1 receptor adaptors and contributes to virulence. J Exp Med 201: 1007-1018.*
34. *Alff PJ, Sen N, Gorbunova E, Gavrilovskaya IN, Mackow ER (2008) The NY-1 hantavirus Gn cytoplasmic tail coprecipitates TRAF3 and inhibits cellular interferon responses by disrupting TBK1-TRAF3 complex formation. J Virol 82: 9115-9122.*
35. *Wu S, Xie P, Welsh K, Li C, Ni CZ, et al. (2005) LMP1 protein from the Epstein-Barr virus is a structural CD40 decoy in B lymphocytes for binding to TRAF3. J Biol Chem 280: 33620-33626.*
36. *Scheffner M, Whitaker NJ (2003) Human papillomavirus-induced carcinogenesis and the ubiquitin-proteasome system. Semin Cancer Biol 13: 59-67.*
37. *Isaacson MK, Ploegh HL (2009) Ubiquitination, ubiquitin-like modifiers, and deubiquitination in viral infection. Cell Host Microbe 5: 559-570.*
38. *Chen F, Sugiura Y, Myers KG, Liu Y, Lin W (2010) Ubiquitin carboxyl-terminal hydrolase L1 is required for maintaining the structure and function of the neuromuscular junction. Proc Natl Acad Sci U S A 107: 1636-1641.*
39. *Fang Y, Fu D, Shen XZ (2010) The potential role of ubiquitin c-terminal hydrolases in oncogenesis. Biochim Biophys Acta 1806: 1-6.*
40. *Boone DL, Turer EE, Lee EG, Ahmad RC, Wheeler MT, et al. (2004) The ubiquitin-modifying enzyme A20 is required for termination of Toll-like receptor responses. Nat Immunol 5: 1052-1060.*
41. *Wilkins C, Gale M, Jr. (2010) Recognition of viruses by cytoplasmic sensors. Curr Opin Immunol 22: 41-47.*
42. *Rolen U, Kobzeva V, Gasparjan N, Ovaa H, Winberg G, et al. (2006) Activity profiling of deubiquitinating enzymes in cervical carcinoma biopsies and cell lines. Mol Carcinog 45: 260-269.*
43. *zur Hausen H (2009) Papillomaviruses in the causation of human cancers - a brief historical*

account. Virology 384: 260-265.

44. Park JS, Kim EJ, Kwon HJ, Hwang ES, Namkoong SE, et al. (2000) Inactivation of interferon regulatory factor-1 tumor suppressor protein by HPV E7 oncoprotein. Implication for the E7-mediated immune evasion mechanism in cervical carcinogenesis. J Biol Chem 275: 6764-6769.
45. Huang SM, McCance DJ (2002) Down regulation of the interleukin-8 promoter by human papillomavirus type 16 E6 and E7 through effects on CREB binding protein/p300 and P/CAF. J Virol 76: 8710-8721.
46. Spitkovsky D, Hehner SP, Hofmann TG, Moller A, Schmitz ML (2002) The human papillomavirus oncoprotein E7 attenuates NF-kappa B activation by targeting the Ikappa B kinase complex. J Biol Chem 277: 25576-25582.
47. Barnard P, McMillan NA (1999) The human papillomavirus E7 oncoprotein abrogates signaling mediated by interferon-alpha. Virology 259: 305-313.
48. Baldwin AS (2001) Control of oncogenesis and cancer therapy resistance by the transcription factor NF-kappaB. J Clin Invest 107: 241-246.
49. An J, Mo D, Liu H, Veena MS, Srivatsan ES, et al. (2008) Inactivation of the CYLD deubiquitinase by HPV E6 mediates hypoxia-induced NF-kappaB activation. Cancer Cell 14: 394-407.
50. Fischer DF, Gibbs S, van De Putte P, Backendorf C (1996) Interdependent transcription control elements regulate the expression of the SPRR2A gene during keratinocyte terminal differentiation. Mol Cell Biol 16: 5365-5374.
51. Ashida H, Kim M, Schmidt-Supprian M, Ma A, Ogawa M, et al. (2010) A bacterial E3 ubiquitin ligase IpaH9.8 targets NEMO/IKKgamma to dampen the host NF-kappaB-mediated inflammatory response. Nat Cell Biol 12: 66-73; sup pp 61-69.

SUPPLEMENTARY INFORMATION

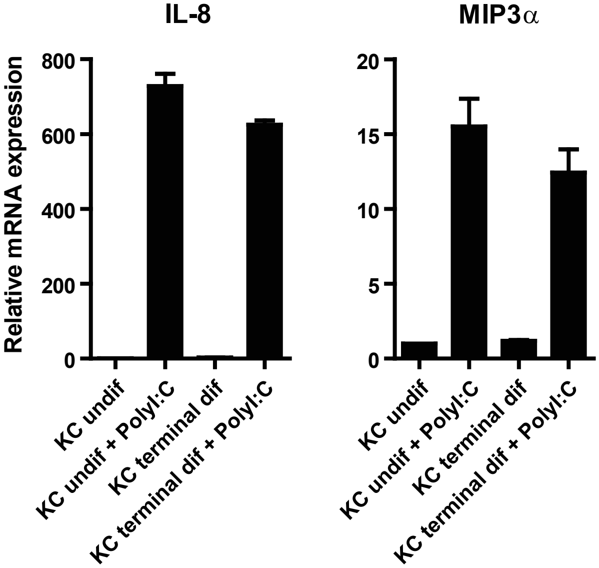

Figure S1. Cytokine production by poly(I:C)-stimulated terminally differentiated keratinocytes.
IL-8 and MIP3α expression levels in unstimulated or poly(I:C)-stimulated uninfected KCs as examined by real-time PCR. KC were either left undifferentiated (undif) or terminally differentiated (terminal dif) with methylcellulose containing Ca2+. Gene expression was normalized using GAPDH.

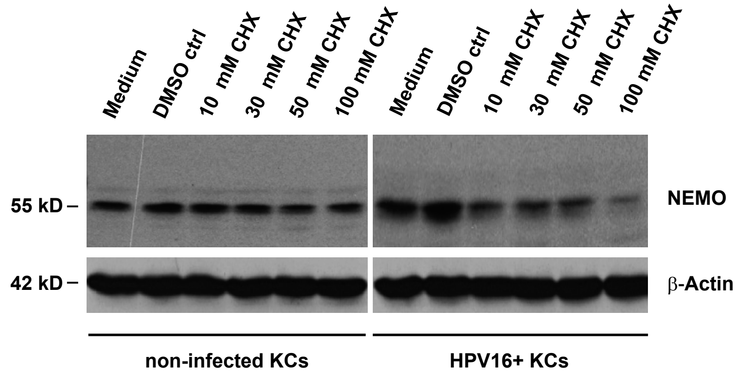
Medium
DMSO ctrl
10 mM CHX
30 mM CHX
50 mM CHX
100 mM CHX
Medium
DMSO ctrl
10 mM CHX
30 mM CHX
50 mM CHX
100 mM CHX
55 kD
42 kD
NEMO
β-Actin
non-infected KCs
HPV16+ KCs

Figure S2. NEMO degradation depends on the expression of UCHL1.
NEMO degradation is enhanced in HPV16+ KCs but not in non-infected KCs. Monolayer cultures were treated with different concentrations of cycloheximide (CHX) for 24 hours. Whole cell extracts were analyzed by WB using antibodies against NEMO and β-actin (control for protein content).

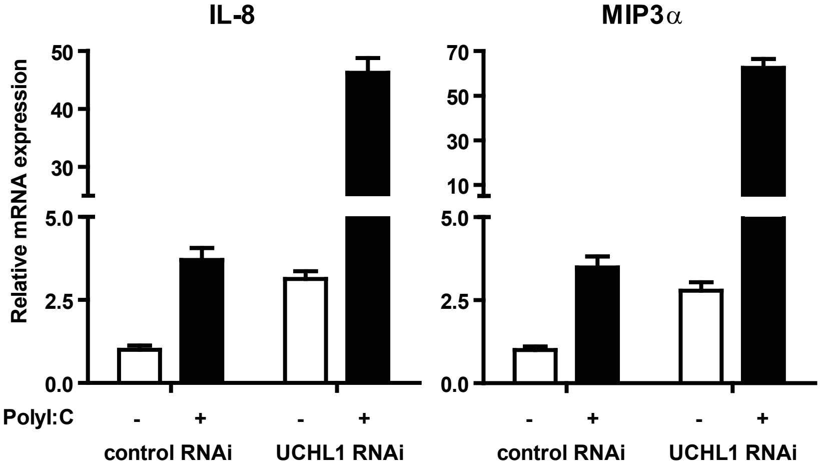

Figure S3. Restored cytokine production after knock down of UCHL1 by RNAi oligos.
HPV16+ keratinocytes were transfected with non-targeting RNAi oligos and oligos targeting UCHL1. Cells were either left unstimulated, or were stimulated with poly(I:C) for 24 hrs. IL-8,and MIP3α mRNA expression was analyzed by qRT-PCR. Gene expression was normalized against GAPDH mRNA levels.

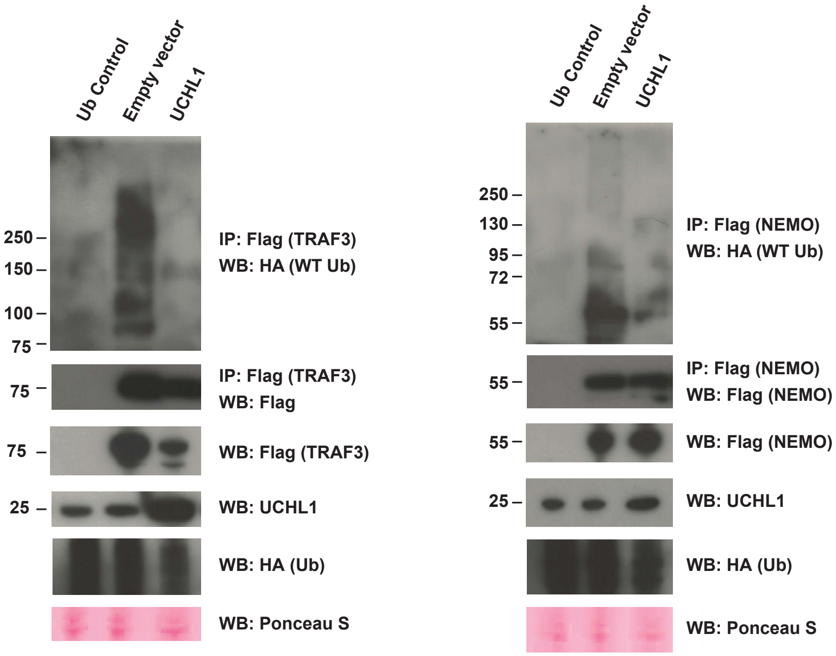
Ub Control
Empty vector
UCHL1
250
150
100
75
IP: Flag (TRAF3)
WB: HA (WT Ub)
75
IP: Flag (TRAF3)
WB: Flag
75
WB: Flag (TRAF3)
25
WB: UCHL1
WB: HA (Ub)
WB: Ponceau S
Ub Control
Empty vector
UCHL1
250
130
95
72
55
IP: Flag (NEMO)
WB: HA (WT Ub)
55
IP: Flag (NEMO)
WB: Flag (NEMO)
55
WB: Flag (NEMO)
25
WB: UCHL1
WB: HA (Ub)
WB: Ponceau S

Figure S4. TRAF3 and NEMO are deubiquitinated by UCHL1.

HEK293T cells were co-transfected with HA-tagged wild-type ubiquitin (WT-Ub) only, with Flag-TRAF3 and HA-tagged wild-type ubiquitin (WT-Ub), and with Flag-TRAF3 and HA-tagged wild-type ubiquitin (WT-Ub) and UCHL1. A similar experiment was performed in which Flag-TRAF3 was replaced by Flag-NEMO (top panels). The bottom four panels show a WB analysis of Flag,Wt-Ub, and UCHL1 of non- immunoprecipitated lysate and a Ponceau S stained loading control for WB.

Table S1. Enrichment of pathways between HPV-positive and uninfected keratinocytes as analyzed by Ingenuity Pathway Analysis (IPA).

Canonical pathway	*p*-value
Purine Metabolism	1.15×10^{-5}
Oxidative Phosphorylation	6.26×10^{-5}
Protein Ubiquitination Pathway	$\mathbf{6.69 \times 10^{-5}}$
Graft-versus-Host Disease Signaling	5.35×10^{-4}
LXR/RXR Activation	7.55×10^{-4}
Mitochondrial Dysfunction	8.22×10^{-4}
Nucleotide Excision Repair Pathway	1.56×10^{-3}
Pyrimidine Metabolism	1.15×10^{-3}
NRF2-mediated Oxidative Stress Response	1.15×10^{-3}
Urea Cycle and Metabolism of Amino Groups	1.15×10^{-3}
Inositol Metabolism	1.15×10^{-3}
Glucocortocoid Receptor Signaling	8.41×10^{-3}
IL-10 Signaling	1.08×10^{-2}
Pentose Phosphate Pathway	1.34×10^{-2}
Glutathione Metabolism	1.43×10^{-2}
D-glutamine and D-glutamate Metabolism	1.46×10^{-2}
Hypoxia Signaling	1.88×10^{-2}
PPAR Signaling	1.94×10^{-2}
Arginine and Purine Metabolism	2.02×10^{-2}
Glutamate Metabolism	2.04×10^{-2}
Role of Cytokine in Mediating Communication between Immune Cells	2.2×10^{-2}
Aldosterone Signaling in Epithelial Cells	2.26×10^{-2}
Cardiac Hypertrophy Signaling	2.61×10^{-2}
Glycosphingolipid Biosynthesis- Neolactoseries	3.07×10^{-2}
Role of BRCA1 in DNA Damage Response	3.36×10^{-2}
Role of CHK Proteins in Cell Cycle Checkpoint Control	3.89×10^{-2}

3

CD40-mediated amplification of local immunity by epithelial cells is impaired by HPV

Tummers B, Goedemans R, Jha V, Meyers C, Melief CJM,
van der Burg SH, Boer JM.

J Invest Dermatol. 2014 Dec;134(12):2918-27.

ABSTRACT

The interaction between the transmembrane glycoprotein surface receptor CD40 expressed by skin epithelial cells (ECs) and its T cell-expressed ligand CD154 was suggested to exacerbate inflammatory skin diseases. However, the full spectrum of CD40-mediated effects by ECs underlying this observation is unknown. Therefore, changes in gene expression after CD40 ligation of ECs were studied by microarrays. CD40-mediated activation for 2 hours stimulated the expression of a coordinated network of immune-involved genes strongly interconnected by *IL8* and *TNF*, while after 24 hours anti-proliferative and anti-apoptotic genes were upregulated. CD40 ligation was associated with the production of chemokines and the attraction of lymphocytes and myeloid cells from peripheral blood mononuclear cells (PBMCs). Thus, CD40-mediated activation of ECs resulted in a highly coordinated response of genes required for the local development and sustainment of adaptive immune responses. The importance of this process was confirmed by a study on the effects of human papilloma virus (HPV) infection to the EC’s response to CD40 ligation. HPV infection clearly attenuated the magnitude of the response to CD40 ligation and the EC’s capacity to attract PBMCs. The fact that HPV attenuates CD40 signalling in ECs indicates the importance of the CD40-CD154 immune pathway in boosting cellular immunity within epithelia.

INTRODUCTION

CD40 is a 48 kDa transmembrane glycoprotein surface receptor also known as the tumour necrosis factor receptor superfamily member 5 (TNFRSF5). It is expressed at the cell surface of antigen presenting cells of the hematopoietic lineage, including B cells, dendritic cells (DCs), Langerhans cells and macrophages, and is also expressed by non-hematopoietic cells, such as endothelial cells (Hollenbaugh *et al.*, 1995), fibroblasts (Fries *et al.*, 1995; Yellin *et al.*, 1995), smooth muscle cells and epithelial cells (Galy and Spits, 1992). The ligand for CD40 is the type II membrane protein CD40L (CD154), which is primarily expressed on activated CD4$^+$ T helper cells. The CD40–CD154 interaction plays a role in both cellular and humoral immune responses. Upon CD40 ligation, DCs mature and become activated to produce high levels of pro-inflammatory cytokines and chemokines, and upregulate MHC class II and co-stimulatory molecules such as CD80 and CD86. Together, these up-regulated molecules facilitate effective priming of CD8$^+$ T cells and stimulate activated CD8$^+$ T cells to become cytotoxic effector cells (Ma and Clark, 2009). In B cells, CD40 ligation induces immunoglobulin isotype switching and differentiation as well as inhibits apoptosis by upregulating anti-apoptotic genes like cIAPs, members of the BCL2 family and MYC (Kehry, 1996; Laman *et al.*, 1996). Deregulation of CD40–CD154 interaction can lead to various clinical conditions (Peters *et al.*, 2009), such as autoimmune diseases, multiple sclerosis, allograft rejections, intraepithelial pre-malignancies and inflammatory skin diseases such as psoriasis and subacute cutaneous lupus erythematosus (Caproni *et al.*, 2007).

In the epidermis, CD40 is expressed at low levels by basal and para-basal layer epithelial cells (ECs). ECs upregulate CD40 expression when stimulated with IFNγ (Denfeld *et al.*, 1996; Gaspari *et al.*, 1996; Peguet-Navarro *et al.*, 1997), that normally is produced by effector cells of the innate immune system and by activated type 1 polarized (IFNγ-producing) CD40L-expressing CD4$^+$ T-helper (Th1) cells that enter the skin (Swamy *et al.*, 2010; van den Bogaard *et al.*, 2013). Indeed, CD40 is highly expressed by ECs in T-cell infiltrated psoriatic lesions (Denfeld *et al.*, 1996). A limited number of *in vitro* studies on CD40 ligation of human primary IFNγ-stimulated ECs showed that these cells express ICAM-1 and secrete RANTES (CCL5), TNFα, IL-6, IL-8 and MCP-1 (CCL2) (Companjen *et al.*, 2002; Denfeld *et al.*, 1996; Gaspari *et al.*, 1996; Pasch *et al.*, 2004; Peguet-Navarro *et al.*, 1997). In addition, there is evidence that CD40-activated ECs stop proliferating and start differentiating (Concha *et al.*, 2003; Grousson *et al.*, 2000; Peguet-Navarro *et al.*, 1997; Villarroel Dorrego *et al.*, 2006). However, the full spectrum of effects mediated by CD40 ligation on the response of ECs is still unknown.

The basal and parabasal layers ECs of squamous epithelia are a well-known target for different viruses (Andrei *et al.*, 2010), including high-risk human papilloma virus (hrHPV). Chronic infections with hrHPV can last for many years, probably as a result of several sophisticated mechanisms employed by hrHPV to evade the hosts' innate immune response (Karim *et al.*, 2011; Karim *et al.*, 2013; Reiser *et al.*, 2011). Interestingly, an *in vivo* model for EC-specific human-CD40 expression and activation showed that CD40 ligation on ECs enhanced DC migration and T cell priming in a mouse model (Fuller *et al.*, 2002), suggesting that ECs boost the activity of cells from the adaptive immune system. HPV-specific cellular immunity, however, develops quite late and slowly during persistent HPV infections (van der Burg and Melief, 2011), posing the question if HPV may also impair pathways typically associated with activation of the adaptive immune response.

To obtain a better understanding of the outcome between the interaction of epithelial cells and CD40 ligand-expressing CD4$^+$ Th1 cells, we analysed the genome-wide expression profiles of CD40-stimulated undifferentiated primary ECs. We observed that ECs react in a very coordinated fashion to CD40 ligation with the induction of mainly immune-related genes and the attraction of immune cells. The parallel analysis of hrHPV-infected primary ECs revealed that hrHPV did not grossly change the gene expression pattern but attenuated the magnitude of the CD40-stimulated immune response, resulting in an impaired immune cell attraction. These data strengthen the notion that the CD40-CD154 pathway plays an important role in protective epithelial immune responses.

RESULTS

CD40 upregulation and functionality on epithelial cells

To study how ECs respond to CD40 ligation on a genome-wide scale, we mimicked the CD40 – CD154 interaction between ECs and IFNγ-secreting CD4$^+$ T cells. Basal CD40 levels on cultured ECs are too low for efficient *in vitro* ligation with CD154, however ECs upregulate the expression of CD40 when stimulated with IFNγ (Denfeld *et al.*, 1996; Gaspari *et al.*, 1996; Peguet-Navarro *et al.*, 1997). Therefore, we measured by flow cytometry the CD40 expression on primary undifferentiated ECs stimulated with increasing concentrations of IFNγ for 72 hours. In line with previous reports, CD40 expression was enhanced by IFNγ at all concentrations but became optimal at a concentration equal or more than 50 IU/ml IFNγ for the primary ECs obtained from 4 different healthy donors (Figure 1a and b). Therefore, this dose was used in our subsequent studies.

ECs were reported to secrete the pro-inflammatory chemokines IL8 (CXCL8) and RANTES (CCL5) upon CD40 ligation (Denfeld *et al.*, 1996; Gaspari *et al.*, 1996; Pasch *et al.*, 2004; Peguet-Navarro *et al.*, 1997). Indeed, this was also observed for CD40 expressing ECs stimulated with CD154-expressing L-cells (CD40L) as compared to ECs cultured with control L-cells (Figure 1c and d), showing that our ECs expressed functionally active CD40. To determine the optimal time points for measuring the response of CD40-ligated ECs on a genome-wide scale, ECs were stimulated for up to 24 hours with CD40L and the peak gene expression of *IL8* and *RANTES* was determined. The highest expression of *IL8* was detected after 2 hours (Figure 1e), *RANTES* peaked after 24 hours of CD40 ligation (Figure 1f). We concluded that these two time-points were most suited for studying early and late responses of ECs to CD40 ligation.

Epithelial cells upregulate genes involved in immune signalling and proliferation after CD40 ligation

The effects of CD40 ligation on four freshly isolated uninfected primary EC cultures from healthy donors of foreskin, vaginal or cervical origin were studied by genome-wide expression profiling. These ECs are the natural target for hrHPV, which is most commonly transmitted by sexual contact. We

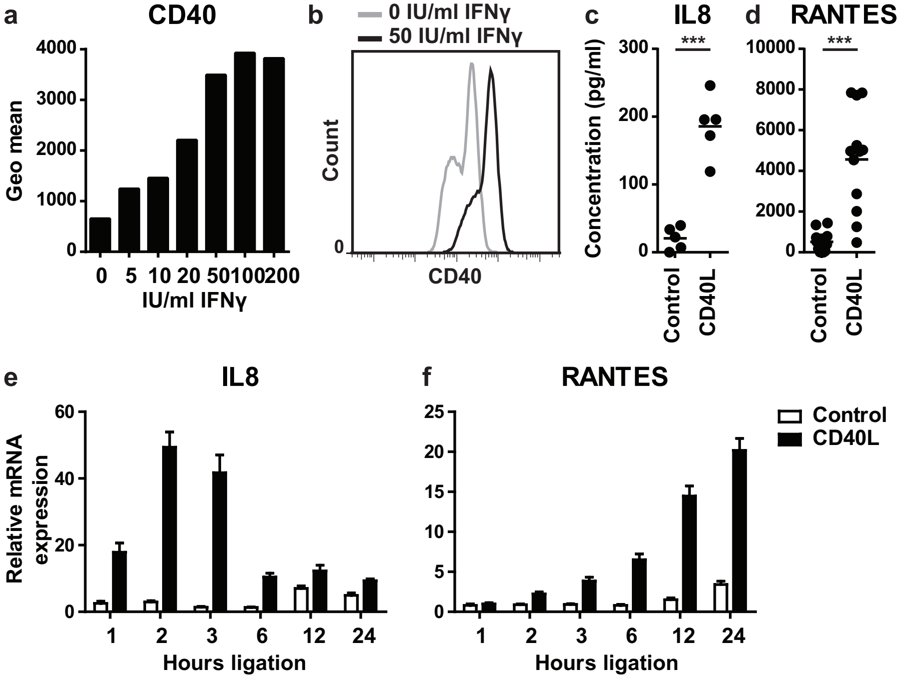

Figure 1. Epithelial cells produce cytokines and chemokines upon CD40 ligation
*(a) CD40 upregulation on vaginal ECs upon stimulation with 0, 5, 10, 20, 50, 100 or 200 IU/ml IFNγ for 3 days. The height of the bars represent the CD40 mean fluorescence intensity as determined by flow cytometry. (b) Histogram of CD40 expression on vaginal ECs stimulated 3 days with 0 and 50 IU/ml IFNγ. ELISA for IL8 (c) and RANTES (d) in cleared supernatants from IFNγ-pre-stimulated foreskin, vaginal and cervical EC cultures (n=5-12) co-cultured for 24 hours with Control or CD40L-expressing L cells in presence of IFNγ. *** indicates $p<0.0005$. RT-qPCR of IL8 (e) and RANTES (f) expression by IFNγ-pre-stimulated vaginal ECs co-cultured with L-Control or L-CD40L cells in presence of IFNγ for 0, 1, 2, 3, 6, 12 or 24 hours. Gene expression was normalized using GAPDH as the calibrator gene. Fold changes over 0 hours co-culture were calculated and depicted. These data are representative for two to three independent experiments.*

verified that the cells were activated via CD40 by confirming the increased expression of *IL8* (2 hours) and *RANTES* (24 hours) (Supplemental figure S1) and subsequently subjected the samples to microarray analysis. Plots with microarray log2 intensities confirmed that *IL8* and *RANTES* were upregulated after 2 and 24 hours, respectively (Supplemental figure S1) and confirmed the results obtained by quantitative PCR.

Using a False Discovery Rate (FDR) ≤0.05 the response to CD40 ligation in the four primary EC cultures was analyzed for genes that were at least two-fold up- or down-regulated (log2-fold change filter (LogFC) ≥1) after 2 or 24 hours of stimulation. The response obtained in EC cultures with control cells was used to correct the results obtained with CD40-ligated ECs for both the time of co-culture with L-cells and total cell density. In total 60 probes showed differential expression, representing 49 differentially expressed genes. Twenty-four genes were upregulated after 2 hours and twenty-nine genes after 24 hours, five genes were upregulated at both time points. One gene (*MMP3*) was significantly downregulated after 24 hours (Figure 2a, Supplemental table S1).

By Ingenuity Pathways Analysis (IPA), we explored if these 49 differentially expressed genes were enriched for biological pathways and how they were connected. IPA enrichment analysis showed that the 24 genes differentially expressed after 2 hours CD40 ligation were mainly involved in 'Cellular movement', especially 'Leukocyte migration', 'Cell-to-cell signalling and interaction', and 'Cell death and survival'. The highest upregulated gene was *IL8*, followed by *CCL20*, *TNFAIP3*, *TNF*, *CXCL1*, *EFNA1* (*TNFAIP4*), *IL36G* and *UBD*, all having a LogFC≥2. At 24 hours post-stimulation the highest upregulated genes were *CCL5* (*RANTES*), *UBD*, *MMP9*, *C15orf48*, *SOD2*, *SerpinA3* and *BIRC3* (*cIAP*2). The 30 genes differentially expressed at this time-point are involved in 'Cellular movement', 'Cell death and survival pathways', 'Post-translational modification', and 'Protein degradation'.

According to the IPA knowledge database 37 of these 49 differentially expressed genes formed a network (117 connections) including 23 out of the 24 genes differentially expressed after 2 hours, and 19 out of the 30 genes differentially expressed after 24 hours (Figure 2b and c). The most interconnected genes within the center of the network were *TNF* and *IL8*, both upregulated only after 2 hours of CD40 ligation. These data indicated that CD40 stimulation of epithelial cells results in a very coordinated reaction; first highly connected immune-involved genes that are able to recruit leukocytes or regulate cytokine expression are upregulated, and subsequently genes involved in the regulation of cell death and survival are upregulated.

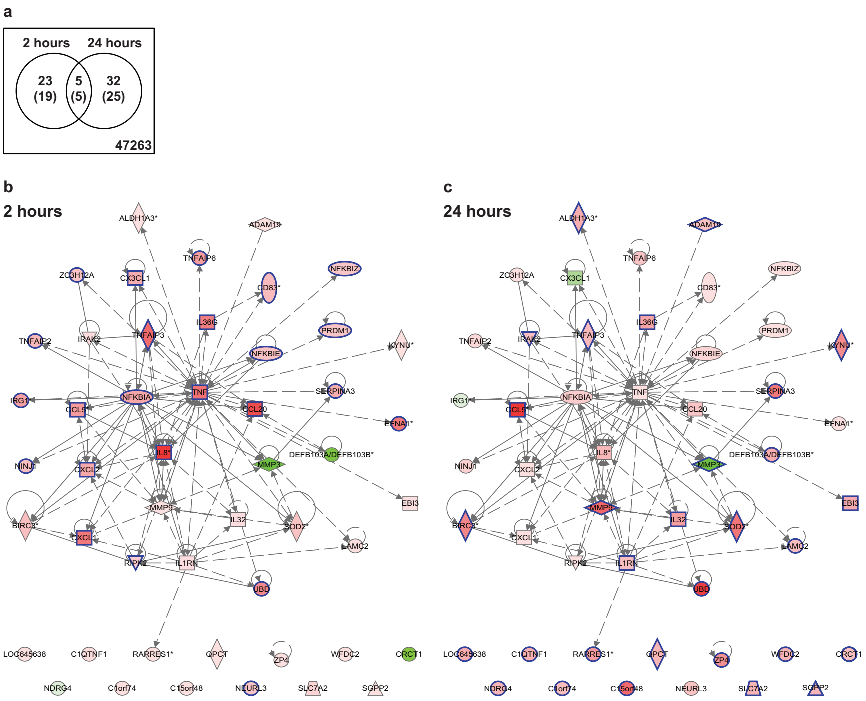
a
2 hours
24 hours
23
(19)
5
(5)
32
(25)
47263
b
2 hours
ALDH1A3*
ADAM19
TNFAIP6
NFKBIZ
ZC3H12A
CX3CL1
CD83*
IL36G
PRDM1
TNFAIP2
IRAK2
TNFAIP3
KYNU*
NFKBIE
SERPINA3
IRG1
CCL5
NFKBIA
TNF
CCL20
EFNA1*
IL8*
DEFB103A/DEFB103B*
NINJ1
CXCL2
MMP3
EBI3
BIRC3*
MMP9
IL32
SOD2*
CXCL1
LAMC2
RIPK2
IL1RN
UBD
LOC645638
C1QTNF1
RARRES1*
QPCT
ZP4
WFDC2
CRCT1
NDRG4
C1orf74
C15orf48
NEURL3
SLC7A2
SGPP2
c
24 hours
ALDH1A3*
ADAM19
TNFAIP6
NFKBIZ
ZC3H12A
CX3CL1
CD83*
IL36G
PRDM1
TNFAIP2
IRAK2
TNFAIP3
KYNU*
NFKBIE
SERPINA3
IRG1
CCL5
NFKBIA
TNF
CCL20
EFNA1*
IL8*
DEFB103A/DEFB103B*
NINJ1
CXCL2
MMP3
EBI3
BIRC3*
MMP9
IL32
SOD2*
CXCL1
LAMC2
RIPK2
IL1RN
UBD
LOC645638
C1QTNF1
RARRES1*
QPCT
ZP4
WFDC2
CRCT1
NDRG4
C1orf74
C15orf48
NEURL3
SLC7A2
SGPP2

Figure 2. CD40 stimulation stimulates a highly coordinated immune response by ECs
(a) Venn diagram depicting the overlap between 49 signature genes (60 microarray probes) differentially expressed at 2 and/or 24 hours L-CD40L stimulation versus L-Control stimulation with adjusted p-value≤0.05 and absolute log2-fold change≥1. Networks with expression changes at 2 (b) and 24 (c) hours were constructed of 49 connected CD40L signature genes using interaction data curated from literature and high-throughput screens by Ingenuity Pathways Analysis. The colours show the degree of upregulation (red) or downregulation (green) in the L-CD40L condition versus the L-Control condition. The genes meeting the adjusted p-value≤0.05 and absolute log2-fold change≥1 thresholds, shown in the Venn diagram in (a), are indicated by blue borders.

CD40 ligation amplifies immune cell attraction to epithelial cells.

Many of the genes that were expressed by ECs after CD40 stimulation belonged to the ’Leukocyte migration‘ group, indicating that CD40-CD154 interactions between T cells and ECs may serve primarily to boost the attraction of immune cells. Therefore, as a second functional assay to study the impact of CD40 ligation, we assessed the capacity of ECs to induce immune cell migration after stimulation with CD40L or control cells. The culture supernatants were isolated and used in a trans-well system with PBMCs seeded in the top wells. To confirm that CD40 ligation is associated with the production of chemokines belonging to the “Leukocyte migration” group, the production of the representative cytokines IL8 and RANTES were measured. Their increased secretions are representative for the production of several chemoattractants following CD40 stimulation (Figure 3a). Indeed, higher numbers of PBMCs migrated towards the supernatants from CD40-ligated ECs when compared to supernatants of control ECs (Figure 3b and c). Analysis of the fraction of lymphocytes and myeloid cells in the migrated PBMCs suggested that the myeloid fraction in the total pool of migrated PBMCs was slightly more increased (Figure 3b). These data indicate that CD40 stimulation of ECs mainly results in the secretion of pro-inflammatory cytokines that aid ECs in the attraction of PBMCs.

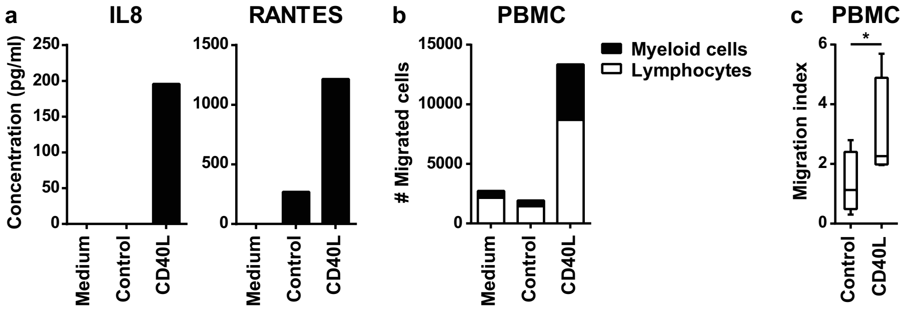

Figure 3. CD40 ligation induces immune cell migration towards epithelial cells
*Example of a representative experiment of the (a) production of IL8 and RANTES in cleared supernatants of vaginal EC donors used for the migration assay by ELISA, and (b) PBMC migration towards these cleared supernatants from vaginal EC donors prepared for the migration assay. PBMC numbers were determined by flow cytometry in presence of FACS counting beads and subsequently gated on lymphocyte or monocyte fractions. Within the total cell numbers (total bar) the fractions of lymphocytes (white) and myeloid cells (black) are depicted. (c) Migration index of total PBMC towards indicated supernatants of ECs of foreskin or vaginal origin of four independent experiments. * indicates $p<0.05$.*

Persistent infection with hrHPV attenuates the intensity of the CD40-induced gene expression

High-risk HPVs are known to deregulate the response of epithelial cells to TNF (Termini *et al.*, 2008). In view of the cellular mediators shared between the TNF- and the CD40-pathway, we studied if a persistent infection with hrHPV influences the gene expression pattern of CD40-stimulated ECs by genome wide expression analysis. We confirmed the expression of CD40 after IFNγ stimulation at the cell surface of hrHPV-positive ECs as well as the expression of *IL8* after 2 hours and *RANTES* after 24 hours of CD40 ligation (Supplemental figure S1a, b and c) and the secretion of these cytokines in the supernatant of hrHPV-infected ECs (Figure 5a). The gene expression profiles of four hrHPV-positive primary EC cultures, stably harbouring HPV16 or HPV18 episomes, were compared with those of the four uninfected primary EC cultures. The expression of *IL8* and *RANTES* of HPV-infected ECs after CD40-stimulation was verified by qPCR (Supplemental figure S1e). The log2 intensity plots of these genes as measured by microarray (Supplemental figure S1f), showed that the results obtained by both methods were comparable.

We studied differential gene expression in HPV-positive epithelial cells after CD40 ligation. At 2 hours, HPV-positive ECs differentially expressed 13 genes, 11 of which overlapped with the 24 genes differentially expressed in uninfected ECs (Figure 4a). At 24 hours, HPV-positive ECs differentially expressed 19 genes, 10 of which overlapped with the 30 genes differentially expressed in uninfected ECs (Figure 4b). This was a first indication that HPV does not grossly alter the reaction to CD40. All differentially expressed genes, 65 in total, were analyzed by IPA and the resulting network (159 connections) was highly similar to the network of genes expressed by CD40-stimulated non-infected ECs (Supplemental figure S3, Supplemental table S1). There were no specific clusters of genes that were either up- or down-regulated in HPV-positive ECs but not in uninfected ECs (Supplemental figure S2), rather the expression intensities of the differentially expressed genes were attenuated in HPV-positive ECs. Focusing on the immune-related genes (Figure 4c), revealed that the presence of hrHPV in ECs impaired the expression of twelve immune-related genes after 2 hours of CD40 stimulation, whereas one gene (*BDKRB1*) was enhanced. After 24 hours of stimulation, hrHPV impaired the expression of eight genes and upregulated seven immune-related genes in ECs. A closer look into the seven upregulated genes was carried out. Three genes, *IL7R*, *LTB* and *SAA1*, showed similar upregulation in the uninfected ECs but did not reach our significance and fold change thresholds (Supplemental figure S4). The remaining four genes, *CXCL9*, *CXCL10*, *CXCL11* and *RSAD2*, were already strongly upregulated in uninfected ECs compared with HPV-positive ECs in response to the IFNγ pre-stimulation, and were not further increased by additional CD40 ligation (Supplemental figure S4). In HPV-positive ECs, CD40 ligation resulted in the upregulation of these genes to levels similar as in uninfected ECs (Supplemental figure S4).

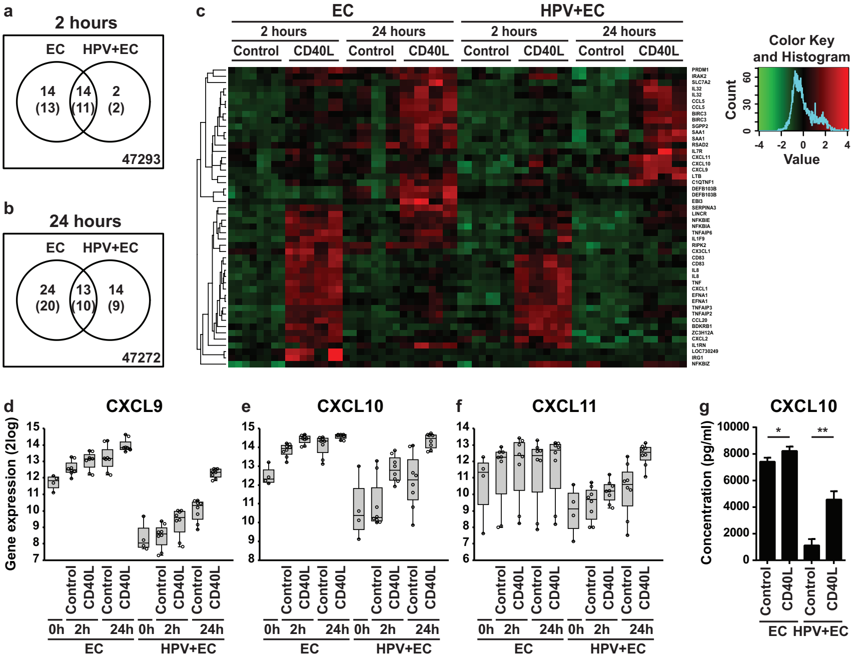

Figure 4. HPV infection results in an attenuated response of ECs to CD40 ligation
*Venn diagrams showing the overlapping genes between ECs and HPV-positive ECs in their response to L-CD40L versus L-Control stimulation for 2 (a) and 24 (b) hours; significance thresholds as in Figure 2a, numbers in brackets represent unique genes. (c) Heat-map of differentially expressed immune-involved genes as determined by IPA. Expression ratios for each condition compared to the 0h time point per cell line were mean-centered and scaled over all conditions. The genes were hierarchically clustered using cosine similarity and average linking. Microarray intensities for CXCL9 (d), 10 (e) and 11 (f) represented in a box plot. (g) CXCL10 concentration as measured by ELISA in supernatants of 24 hours IFNγ-stimulated and L-Control or L-CD40L co-cultured foreskin ECs and HPV-positive foreskin ECs (n=3). * indicates p<0.05 and ** p<0.005.*

hrHPV impairs CD40-ligation mediated immune cell attraction to epithelial cells.

The T cell-attracting chemokines CXCL9, 10 and 11 are known to be induced by IFNγ in various cell types, including ECs (Kanda *et al.*, 2007; Kanda and Watanabe, 2007; Kawaguchi *et al.*, 2009; Ohta *et al.*, 2008; Sauty *et al.*, 1999). Although CD40 stimulation salvaged the expression levels of *CXCL9*, *CXCL10* and *CXCL11* in HPV-positive ECs to similar levels found in non-infected ECs (Figure 4d, e and f), ELISA assays showed that hrHPV-positive ECs still secreted lower levels of CXCL9 and CXCL10 than non-infected ECs (Figure 4g and not shown). On average the CD40-ligated HPV-positive ECs also produced lower amounts of IL8 and RANTES (Figure 5a) albeit that in some experiments the levels approached that of non-infected ECs. To obtain a broader view on the impact of HPV to CD40L-induced immune activation, also their capacity to attract PBMCs was tested. Notwithstanding the production of the earlier tested cytokines, no increased attraction of PBMCs to the supernatants of CD40L-stimulated HPV-positive ECs was observed (Figure 5b and c). This indicates that also the production of other chemokines within the 'Leukocyte migration' group, those that are key in the attraction of PBMCs, must have been impaired in HPV-positive ECs. In independent experiments, the absolute numbers of migrated PBMCs differed per primary EC culture and PBMC donor used, however, the increase in PBMC attraction following CD40 ligation was consistently and significantly higher in uninfected ECs (Figure 3c), but not in hrHPV+ ECs (Figure 5c). Together these data show that hrHPV does not grossly alter, but rather attenuates the intracellular response of epithelial cells to CD40 ligation, resulting in a hampered ability of the HPV-positive ECs to attract immune cells.

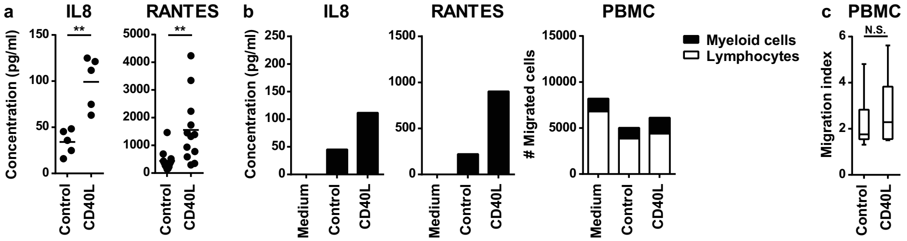

Figure 5. HPV infection hampers the enhanced attraction of immune cells by CD40-stimulated epithelial cells

*(a) ELISA for IL8 and RANTES in cleared supernatants from IFNγ-pre-stimulated HPV-positive foreskin, vaginal and cervical EC cultures (n=5-12) co-cultured for 24 hours with Control or CD40L-expressing L cells in presence of IFNγ. ** indicates $p<0.005$ using unpaired Welch corrected t-test. (b) Example of a representative experiment of the production of IL8 and RANTES in cleared supernatants of vaginal EC donors used for the migration assay by ELISA, and PBMC migration towards these cleared supernatants from vaginal EC donors prepared for the migration assay. (c) Migration index of total PBMC towards indicated HPV-positive foreskin, vaginal and cervical EC supernatants of four independent experiments. N.S. indicates p=not significant.*

DISCUSSION

We studied the response of epithelial cells to CD40 ligation, a major immune trigger of B and T cell immunity, and a major cue for leukocyte migration towards the skin. Stimulation of ECs via CD40 resulted in a highly coordinated regulation of predominantly immune-related genes involved in the attraction, sustainment and amplification of adaptive immune responses as well as resulted in the attraction of immune cells. Interestingly, hrHPV infection did not qualitatively alter the gene expression profile of CD40-stimulated EC, instead the extent of the response was attenuated. The fact that HPV attenuates CD40 signalling in ECs indicates the importance of the CD40-CD154 immune pathway in boosting immunity in epithelia.

Microarray expression studies showed that CD40 ligation of non-hematopoietic cells, such as endothelial cells (Pluvinet *et al.*, 2008), pancreatic cells (Klein *et al.*, 2008), renal proximal tubule epithelial cells (Li and Nord, 2005), smooth muscle cells (Stojakovic *et al.*, 2007), microglia (Ait-Ghezala *et al.*, 2005) and epithelial cells (this report), generally results in the upregulation of genes involved in immunity and inflammatory responses, cell fate and cell adhesion. The response of ECs to CD40 stimulation is alike that of muscle cells and pancreatic cells. Endothelial cells seem to have a broader response as they also upregulate genes involved in the viral immune surveillance system, e.g. the 2’-5’-oligoadenylate/RNase L system and guanylate-binding proteins (GBP1-4), potentially to keep the vasculature from harmful consequences and prevent the spread of systemic viral infection in the host (Pluvinet *et al.*, 2008). Epithelial cells are well equipped with viral sensors which can launch an antiviral response upon infection (Karim et al., 2011), and the CD40 pathway may help to establish efficient adaptive B and T cell immunity to expand the precision of protection after the initial innate immune cell response.

Interestingly, we found that late CD40-mediated responses in ECs involved the upregulation of the anti-apoptosis genes *cIAP2* and *BCL3* as well as the negative regulator of proliferation *RARRES1*. These observations may explain earlier findings that epithelial cells do not go into apoptosis but rather stop proliferating after CD40 ligation (Peguet-Navarro *et al.*, 1997). We are currently exploring this further. The response of ECs to CD40 stimulation is paralleled by

B cells, which respond to CD40 ligation by preventing apoptosis through the upregulation of several anti-apoptotic genes, including *cIAPs*, *MYC* and *BCL2* members (Kehry, 1996; Laman *et al.*, 1996).

CD40 stimulation of dendritic cells (DCs) has been thoroughly studied as it plays a key role in the activation, maturation and T-cell priming capacity of DC. Upon CD40 stimulation DCs produce pro-inflammatory cytokines and chemokines, upregulate HLA class I and II as well as the co-stimulatory molecules CD86 and CD80 (Ma and Clark, 2009). This allows DC to convey the appropriate signals to T cells required for them to become effector cells. Candidate gene studies showed that ECs can express CD40, HLA class I and II, CD86, but not CD80 (Black *et al.*, 2007; Ortiz-Sanchez *et al.*, 2007; Romero-Tlalolini *et al.*, 2013) as well as the co-stimulatory molecules CD83 and ICAM-1 and a number of cytokines after being exposed to IFNγ and CD40 activation (Companjen *et al.*, 2002; Denfeld *et al.*, 1996; Gaspari *et al.*, 1996; Pasch *et al.*, 2004; Peguet-Navarro *et al.*, 1997). This may allow CD40-stimulated ECs to process and present antigen to effector/memory CD4$^+$ and CD8$^+$ T cells (Black *et al.*, 2007) as well as to amplify immune responses. However, it is not likely that such activated ECs function as professional antigen-processing cells (APCs) as it was shown that CD40L-activated ECs fail to prime allogeneic T-cell reactions, underlining the difference of CD40 ligation on professional and non-professional APCs (Grousson *et al.*, 2000).

The pathogenesis of skin diseases such as psoriasis is based on an influx of immune cells into psoriatic lesions where cytokine levels are elevated. Our results sustain the notion that tissue-infiltrating T cells may exacerbate the disease via the production of IFNγ and the interaction with CD40 on ECs. The resulting cytokines may amplify the immune response via the attraction of more immune cells thereby forming a loop in EC stimulation and cytokine production. The involvement of ECs in the exacerbation of disease has been questioned as CD40 expression on epithelial cells *in vivo* can be weak (Ohta and Hamada, 2004). However, we and others have shown that CD40 expression is rapidly upregulated (at least temporarily) under the influence of physiological doses of IFNγ and thus weak steady state expression does not preclude robust action under conditions of immune activation.

HPV attenuates the extent of the epithelial cells' response to CD40 ligation, suggesting that HPV interferes with CD40 ligation-induced signal transduction and subsequent canonical and non-canonical NFκB activation (Gommerman and Summers deLuca, 2011; Hostager and Bishop, 2013; Ma and Clark, 2009). Several research groups have reported that hrHPV deregulates NFκB activation following the activation of pattern recognition receptors (PRRs) (Karim *et al.*, 2011; Reiser *et al.*, 2011) or the TNF receptor (Termini *et al.*, 2008). We and others have previously shown that hrHPV attenuates the PRR-induced (Karim *et al.*, 2013) and TNFR-induced (Takami *et al.*, 2007) NFκB pathway activation by upregulating UCHL1, a cellular deubiquitinase/E3 ligase. Therefore, the expression of UCHL1, or other non-identified modulators, may explain how HPV mediates the attenuation of CD40 ligation-induced gene expression.

Surprisingly, PBMCs were more attracted to supernatants of non-CD40-ligated HPV-positive ECs than to uninfected ECs, implying that supernatants of HPV-positive ECs contain higher cytokine levels than supernatants of uninfected ECs. However, not only in this study, but also in previous studies (Karim *et al.*, 2011; Karim *et al.*, 2013), we observed that hrHPV generally downregulates the basal expression and secretion of many pro-inflammatory cytokines. Recent literature has shown that metabolism intermediates can act as inflammatory signals (Tannahill *et al.*, 2013), implying that a simple difference in cell density can affect basal immune cell attraction. Although both the HPV-positive and uninfected ECs have been treated exactly the same throughout the experiments, HPV-positive ECs proliferate faster than uninfected ECs, and as such the supernatants may contain higher metabolite levels to mediate CD40-independent PBMC attraction towards HPV-positive cells. In hrHPV+ ECs, despite the higher basal numbers of attracted PBMC, CD40 stimulation does not result in an increased number of PBMC attracted whereas in uninfected ECs this is the case.

In conclusion, epithelial cells show a coordinated response to CD40 ligation, mainly inducing the expression of genes involved in leukocyte migration, cell-to-cell signalling and interaction, as well as cell death and survival. HPV attenuates the extent of CD40-signalling, resulting in lower amounts of chemoattractants produced and a failure to enhance immune cell migration.

These data suggest that progression of inflammatory skin diseases may be driven by highly programmed immune activation scenario's in epithelial cells, that have their evolutionary basis in the epithelial cells' response to infections.

MATERIALS & METHODS

Ethics Statement

The use of discarded human foreskin, cervical and vaginal keratinocyte tissues to develop cell lines for these studies was approved by the Institutional Review Board at the Pennsylvania State University College of Medicine and by the Institutional Review Board at Pinnacle Health Hospitals. The Medical Ethical Committee of the Leiden University Medical Center approved the human tissue sections (healthy foreskin, healthy cervix, HPV16- or 18-positive cervical neoplasias) used for staining. All sections and cell lines were derived from discarded tissues and de-identified, therefore no informed consent was necessary.

Cell culture

Primary cultures of human epithelial cells (ECs) were established from foreskin, vaginal and cervical tissues as previously described (Karim *et al.*, 2011) and grown in keratinocyte serum-free medium (K-SFM; Medium 154 supplemented with HKGS kit, Invitrogen, Breda, The Netherlands). The cells morphologically and biochemically resembled ECs in both monolayer and organotypic raft cultures, as indicated by keratin expression, hemidesmosome and desmosome structures, and ability to differentiate to full thickness epithelium (McLaughlin-Drubin *et al.*, 2004; Meyers *et al.*, 1997). Using the microarray data, the cells were verified to express high levels of keratin (KRT) 10, 14, 17, and 19, and low levels of KRT18 (Supplemental figure S5), a signature specific for keratinocytes (Bononi *et al.*, 2012; Moll *et al.*, 2008). Epithelial cell lines stably maintaining the full episomal HPV genome following electroporation (HPV-positive ECs) were grown in monolayer culture using E medium in the presence of mitomycin C treated J2 3T3 feeder cells (McLaughlin-Drubin *et al.*, 2004; Meyers *et al.*, 1997) for two passages and were then adapted to K-SFM for one passage before experimentation. Since primary ECs have a limited life span and do not survive long enough to undergo a mock electroporation procedure similar to that used to obtain HPV-positive ECs, normal undifferentiated primary epithelial cells were used as control. J2 3T3 mouse fibroblasts and L-cells were cultured in Dulbecco's modified Eagle's medium supplemented with 8% fetal bovine serum, 2mM l-glutamine and 1%

penicillin-streptomycin (complete DMEM medium) (Gibco-BRL, Invitrogen, Breda, The Netherlands).

CD40 ligation on epithelial cells

Uninfected ECs or HPV-positive ECs were seeded at $1.5x10^5$ cells/well in 6-wells plates in K-SFM and allowed to attach for 24 hours, after which the cells received fresh K-SFM containing 50 IU/ml IFNγ (Immunotools, Friesoythe, Germany) for 72 hours. Control or CD40L-expressing L-cells were harvested, irradiated (4800 – 5200 rad) and resuspended in K-SFM containing 50 IU/ml IFNγ. L-cells were co-cultured with ECs in a 1:1 ratio for indicated time points, after which the supernatant was collected, the L-cells were removed and the RNA of the ECs was harvested. CD40L expression and functionality of the L-cells were validated as was the percentage of residual L-cells after co-culture (<1%; data not shown).

RNA expression analyses and ELISA

Total RNA was isolated using the NucleoSpin RNA II kit (Machery-Nagel, Leiden, The Netherlands) according to the manufacturer's instructions. Total RNA (0.5 – 1.0 µg) was reverse transcribed using the SuperScript III First Strand synthesis system from Invitrogen. TaqMan PCR was performed using TaqMan Universal PCR Master Mix and pre-designed, pre-optimized primers and probe mix for *RANTES* (*CCL5*), *IL8*, and *GAPDH* (Applied Biosystems, Foster City, USA). Threshold cycle numbers (Ct) were determined using the CFX PCR System (BioRad, Veenendaal, The Netherlands) and the relative quantities of cDNA per sample were calculated using the ΔΔCt method using *GAPDH* as the calibrator gene. ELISA's for CCL2, RANTES, IL8 and CXCL10 were performed according to the manufacturer's instruction (PeproTech, London, United Kingdom). Statistical differences in cytokine production were evaluated using a Welch-corrected t-test, correcting for possible unequal variances between the groups.

Gene expression profiling

Four primary EC cultures were used, HVK (vaginal), HCK (cervical), HFK_1 and HFK_2 (both foreskin), as well as four EC cell lines stably maintaining episomal HPV16 or 18, HVK16 (vaginal), HVK18 (vaginal), HCK18 (cervical), and HPV16 (foreskin). Cells were harvested at five conditions: 0 hrs, 2 hrs and 24 hrs of 50 IU/ml IFNγ in combination with either L-Control or L-CD40L cells. Stimulated 2 hrs and 24 hrs samples were generated in duplo. Total RNA for these 72 samples was isolated as stated above. The microarray experiment was performed by ServiceXS according to their protocols (ServiceXS, Leiden, The Netherlands). Briefly, total RNA was analyzed by Lab-on-a-Chip. All RNA showed a RIN score of >9.5. Total RNA was reverse-transcribed, amplified and biotin labeled. cRNA was hybridized to Illumina Human HT-12 v4 BeadChips in a randomized fashion and scanned with the Illumina iScan. Samples passed quality control as assessed by Illumina GenomeStudio software. Values for missing bead types on the HumanHT-12 BeadChip were estimated using the k-Nearest Neighbor (k-NN) algorithm (Troyanskaya *et al., 2001) in Illumina's BeadStudio Gene Expression Module (v3.3+).*

Microarray data preprocessing

The expression array data was analyzed using R2.14.1 and Bioconductor (R Development Core Team, 2008). The data were normalized using the Bioconductor package lumi version 2.6.0 (Du *et al.*, 2008; Lin *et al.*, 2008), resulting in log2-transformed normalized intensities. Quality control plots were generated using limma version 3.10.2 (Smyth, 2005) and mpm version 1.0-22 (Wouters, 2011; Wouters *et al.*, 2003). Uninfected and HPV-positive ECs correlated in separate blocks, and within these blocks the next level similarity was at the cell line level, and within cell line at the exposure level, indicating that the data behaved as expected (data not shown). All microarray data is MIAME compliant and the raw data has been deposited in the MIAME compliant database Gene Expression Omnibus with accession number GSE54181, as detailed on the MGED Society website http://www.mged.org/Workgroups/MIAME/miame.html.

Analysis of differentially gene expression

Differentially expressed genes were identified using maanova version 1.24.0 (Wu; Wu *et al.*, 2003). We modelled the cell line effect as a random effect and indicated the technical replicates in the model. We calculated test statistics for testing the null hypotheses of no difference in expression between L-CD40L-stimulated and L-Control stimulated cells at 2 and 24 hours for uninfected epithelial cells as well as HPV-positive epithelial cells for each gene. We applied the Fs statistic, which uses a shrinkage estimator for gene-specific variance components based on the James-Stein estimator. To correct for multiple testing, false discovery rates (FDR) were calculated using the q-value method (Dabney; Storey, 2002). The ranking and selection of the genes is based on these adjusted p-values.

Functional genomics analyses

The networks were constructed using Ingenuity Pathways Analysis (IPA version 17199142; Ingenuity systems, Inc., www.ingenuity.com). The list of differentially expressed genes was used to generate the network. All edges are supported by at least one reference from the literature, from a textbook, or from canonical information stored in the Ingenuity Pathway Knowledge Base.

Boxplot representations

Boxplots are drawn as a box, containing the 1st quartile up to the 3rd quartile of the data values. The median is represented as a line within the box. Whiskers represent the values of the outer 2 quartiles. These whiskers are however maximized at 1.5 times the size of the box (a.k.a. inter quartile distance). If 1 or more values outside of the whiskers are present, then this is indicated with a single mark ‘o’ next to the implicated whisker. Plots were generated using the webtool R2: microarray analysis and visualization platform (http://r2.amc.nl).

Migration assays

IFNγ pre-stimulated (HPV-positive) ECs were co-cultured with L-cells for 3 hours after which the L-cells were removed. The ECs were cultured a subsequent 24 hours with fresh K-SFM. Cleared (HPV-positive) EC supernatants were added to the lower compartment of a transwell plate (Corning). The upper compartment was filled with PBMCs, which were allowed to migrate for 16 hours, after which the cells in the lower compartment were counted by flow cytometry in the presence of counting beads (Invitrogen) according to the manufacturer’s protocol. Myeloid cells and lymphocytes were differentiated by their respective size in the FSC/SCC plot (data not shown). To normalize for biological differences between PBMC donors and EC cultures, a migration index was calculated of the total number of PBMCs migrated towards the indicated stimulation over the medium control. The statistical significance of differences in migration towards supernatants of EC cultures stimulated with CD40L or control L-cells was assessed using a paired t-test.

Flow cytometry

Expression of CD40 on epithelial cells was analyzed by flow cytometry using FITC-coupled Mouse-anti-human CD40 (BD Biosciences, Breda, The Netherlands). 50.000 cells/live gate were recorded using the BD FACS Calibur with Cellquest software (BD Bioscience) and data were analyzed using Flowjo (Treestar, Olten, Switzerland).

Conflict of interest

CM has received speaker honoraria from Merck, Quest Diagnostics, GSK, and Bristol-Myers. CM has performed research funded by Merck, The Phillip Morris External Research Program, NexMed, GSK, OriGenix, and Interferon Sciences Inc.

Acknowledgments

This work was supported by the Netherlands Organization for Health Research (NOW/ZonMw) TOP grant 91209012. The funders had no role in study design, data collection and analysis, decision to publish, or preparation of the manuscript.

REFERENCES

Ait-Ghezala G, Mathura VS, Laporte V, et al. (2005) Genomic regulation after CD40 stimulation in microglia: relevance to Alzheimer's disease. Brain research Molecular brain research 140:73-85.

Andrei G, Duraffour S, Van den Oord J, et al. (2010) Epithelial raft cultures for investigations of virus growth, pathogenesis and efficacy of antiviral agents. Antiviral research 85:431-49.

Black AP, Ardern-Jones MR, Kasprowicz V, et al. (2007) Human keratinocyte induction of rapid effector function in antigen-specific memory CD4+ and CD8+ T cells. European journal of immunology 37:1485-93.

Bononi I, Bosi S, Bonaccorsi G, et al. (2012) Establishment of keratinocyte colonies from small-sized cervical intraepithelial neoplasia specimens. Journal of cellular physiology 227:3787-95.

Caproni M, Torchia D, Antiga E, et al. (2007) The CD40/CD40 ligand system in the skin of patients with subacute cutaneous lupus erythematosus. The Journal of rheumatology 34:2412-6.

Companjen AR, van der Wel LI, Boon L, et al. (2002) CD40 ligation-induced cytokine production in human skin explants is partly mediated via IL-1. International immunology 14:669-76.

Concha M, Vidal MA, Moreno I, et al. (2003) Evidence for modulation of human epidermal differentiation and remodelling by CD40. The British journal of dermatology 148:1105-14.

Dabney A qvalue: Q-value estimation for false discovery rate control. (R package version 1.28.0).

Denfeld RW, Hollenbaugh D, Fehrenbach A, et al. (1996) CD40 is functionally expressed on human keratinocytes. European journal of immunology 26:2329-34.

Du P, Kibbe WA, Lin SM (2008) lumi: a pipeline for processing Illumina microarray. Bioinformatics 24:1547-8.

Fries KM, Sempowski GD, Gaspari AA, et al. (1995) CD40 expression by human fibroblasts. Clinical immunology and immunopathology 77:42-51.

Fuller BW, Nishimura T, Noelle RJ (2002) The selective triggering of CD40 on keratinocytes in vivo enhances cell-mediated immunity. European journal of immunology 32:895-902.

Galy AH, Spits H (1992) CD40 is functionally expressed on human thymic epithelial cells. Journal of immunology 149:775-82.

Gaspari AA, Sempowski GD, Chess P, et al. (1996) Human epidermal keratinocytes are induced to secrete interleukin-6 and co-stimulate T lymphocyte proliferation by a CD40-dependent mechanism. European journal of immunology 26:1371-7.

Gommerman JL, Summers deLuca L (2011) LTbetaR and CD40: working together in dendritic cells to optimize immune responses. Immunological reviews 244:85-98.

Grousson J, Ffrench M, Concha M, et al. (2000) CD40 ligation alters the cell cycle of differentiating keratinocytes. The Journal of investigative dermatology 114:581-6.

Hollenbaugh D, Mischel-Petty N, Edwards CP, et al. (1995) Expression of functional CD40 by vascular endothelial cells. The Journal of experimental medicine 182:33-40.

Hostager BS, Bishop GA (2013) CD40-Mediated Activation of the NF-kappaB2 Pathway. Frontiers in immunology 4:376.

Kanda N, Shimizu T, Tada Y, et al. (2007) IL-18 enhances IFN-gamma-induced production of CXCL9, CXCL10, and CXCL11 in human keratinocytes. European journal of immunology 37:338-50.

Kanda N, Watanabe S (2007) Prolactin enhances interferon-gamma-induced production of CXC ligand 9 (CXCL9), CXCL10, and CXCL11 in human keratinocytes. Endocrinology 148:2317-25.

Karim R, Meyers C, Backendorf C, et al. (2011) Human papillomavirus deregulates the response of a cellular network comprising of chemotactic and proinflammatory genes. PloS one 6:e17848.

Karim R, Tummers B, Meyers C, et al. (2013) Human papillomavirus (HPV) upregulates the cellular deubiquitinase UCHL1 to suppress the keratinocyte’s innate immune response. PLoS pathogens 9:e1003384.

Kawaguchi S, Ishiguro Y, Imaizumi T, et al. (2009) Retinoic acid-inducible gene-I is constitutively expressed and involved in IFN-gamma-stimulated CXCL9-11 production in intestinal epithelial cells. Immunology letters 123:9-13.

Kehry MR (1996) CD40-mediated signaling in B cells. Balancing cell survival, growth, and death. Journal of immunology 156:2345-8.

Klein D, Timoneri F, Ichii H, et al. (2008) CD40 activation in human pancreatic islets and ductal cells. Diabetologia 51:1853-61.

Laman JD, Claassen E, Noelle RJ (1996) Functions of CD40 and its ligand, gp39 (CD40L). Critical reviews in immunology 16:59-108.

Li H, Nord EP (2005) CD40/CD154 ligation induces mononuclear cell adhesion to human renal proximal tubule cells via increased ICAM-1 expression. American journal of physiology Renal physiology 289:F145-53.

Lin SM, Du P, Huber W, et al. (2008) Model-based variance-stabilizing transformation for Illumina microarray data. Nucleic acids research 36:e11.

Ma DY, Clark EA (2009) The role of CD40 and CD154/CD40L in dendritic cells. Seminars in immunology 21:265-72.

McLaughlin-Drubin ME, Christensen ND, Meyers C (2004) Propagation, infection, and neutralization of authentic HPV16 virus. Virology 322:213-9.

Meyers C, Mayer TJ, Ozbun MA (1997) Synthesis of infectious human papillomavirus type 18 in differentiating epithelium transfected with viral DNA. Journal of virology 71:7381-6.

Moll R, Divo M, Langbein L (2008) The human keratins: biology and pathology. Histochemistry and cell biology 129:705-33.

Ohta K, Shigeishi H, Taki M, et al. (2008) Regulation of CXCL9/10/11 in oral keratinocytes and fibroblasts. Journal of dental research 87:1160-5.

Ohta Y, Hamada Y (2004) In situ Expression of CD40 and CD40 ligand in psoriasis. Dermatology 209:21-8.

Ortiz-Sanchez E, Chavez-Olmos P, Pina-Sanchez P, et al. (2007) Expression of the costimulatory molecule CD86, but not CD80, in keratinocytes of normal cervical epithelium and human papillomavirus-16 positive low squamous intraepithelial lesions. International journal of gynecological cancer : official journal of the International Gynecological Cancer Society 17:571-80.

Pasch MC, Timar KK, van Meurs M, et al. (2004) In situ demonstration of CD40- and CD154-positive cells in psoriatic lesions and keratinocyte production of chemokines by CD40 ligation in vitro. The Journal of pathology 203:839-48.

Peguet-Navarro J, Dalbiez-Gauthier C, Moulon C, et al. (1997) CD40 ligation of human keratinocytes inhibits their proliferation and induces their differentiation. Journal of immunology 158:144-52.

Peters AL, Stunz LL, Bishop GA (2009) CD40 and autoimmunity: the dark side of a great activator. Seminars in immunology 21:293-300.

Pluvinet R, Olivar R, Krupinski J, et al. (2008) CD40: an upstream master switch for endothelial cell activation uncovered by RNAi-coupled transcriptional profiling. Blood 112:3624-37.

R Development Core Team (2008) R: a language and enviroment for statistical computing. R Foundation for Statistical

Computing, Vienna, Austria. ISBN 3-900051-07-0. URL http://wwwR-projectorg.

Reiser J, Hurst J, Voges M, et al. (2011) High-risk human papillomaviruses repress constitutive kappa interferon transcription via E6 to prevent pathogen recognition receptor and antiviral-gene expression. Journal of virology 85:11372-80.

Romero-Tlalolini MA, Chavez Olmos P, Garrido E (2013) Differential DNA methylation patterns in the CD86 gene controls its constitutive expression in keratinocytes. Biochemical and biophysical research communications 438:54-60.

Sauty A, Dziejman M, Taha RA, et al. (1999) The T cell-specific CXC chemokines IP-10, Mig, and I-TAC are expressed by activated human bronchial epithelial cells. Journal of immunology 162:3549-58.

Smyth GK (2005) Limma: linear models for microarray data. In: Bioinformatics and Computational Biology Solutions using R and Bioconductor (Gentleman R, Carey V, Dudoit S, Irizarry R, Huber W, eds), New York: Springer.

Stojakovic M, Krzesz R, Wagner AH, et al. (2007) CD154-stimulated GM-CSF release by vascular smooth muscle cells elicits monocyte activation--role in atherogenesis. Journal of molecular medicine 85:1229-38.

Storey J (2002) A direct approach to false discovery rates. Journals of the Royal Statistical Society Series B:479-98.

Swamy M, Jamora C, Havran W, et al. (2010) Epithelial decision makers: in search of the 'epimmunome'. Nature immunology 11:656-65.

Takami Y, Nakagami H, Morishita R, et al. (2007) Ubiquitin carboxyl-terminal hydrolase L1, a novel deubiquitinating enzyme in the vasculature, attenuates NF-kappaB activation. Arteriosclerosis, thrombosis, and vascular biology 27:2184-90.

Tannahill GM, Curtis AM, Adamik J, et al. (2013) Succinate is an inflammatory signal that induces IL-1beta through HIF-1alpha. Nature 496:238-42.

Termini L, Boccardo E, Esteves GH, et al. (2008) Characterization of global transcription profile of normal and HPV-immortalized keratinocytes and their response to TNF treatment. BMC medical genomics 1:29.

Troyanskaya O, Cantor M, Sherlock G, et al. (2001) Missing value estimation methods for DNA microarrays. Bioinformatics 17:520-5.

van den Bogaard EH, Tjabringa GS, Joosten I, et al. (2013) Crosstalk between Keratinocytes and T Cells in a 3D Microenvironment: A Model to Study Inflammatory Skin Diseases. The Journal of investigative dermatology.

van der Burg SH, Melief CJ (2011) Therapeutic vaccination against human papilloma virus induced malignancies. Current opinion in immunology 23:252-7.

Villarroel Dorrego M, Whawell SA, Speight PM, et al. (2006) Transfection and ligation of CD40 in human oral keratinocytes affect proliferation, adhesion and migration but not apoptosis in vitro. Clinical and experimental dermatology 31:266-71.

Wouters L (2011) Exploratory graphical analysis of multivariate data, specifically gene expression data with different projection methods: principal component analysis, correspondence analysis, spectral map analysis (http://CRAN.R-project.org/package=mpm).

Wouters L, Gohlmann HW, Bijnens L, et al. (2003) Graphical exploration of gene expression data: a comparative study of three multivariate methods. Biometrics 59:1131-9.

Wu H maanova: Tools for analyzing Micro Array experiments. (http://research.jax.org/faculty/churchill).

Wu H, Kerr MK, Cui XQ, et al. (2003) MAANOVA: A Software Package for the Analysis of Spotted cDNA Microarray Experiments. In: The Analysis of Gene Expression Data: An Overview of Methods and Software (Parmigiani G, Garret ES, Irizarry RA, Zeger SL, eds), New York: Springer, 313–41.

Yellin MJ, Winikoff S, Fortune SM, et al. (1995) Ligation of CD40 on fibroblasts induces CD54 (ICAM-1) and CD106 (VCAM-1) up-regulation and IL-6 production and proliferation. Journal of leukocyte biology 58:209-16.

4

The interferon-related developmental regulator (IFRD1) is used by Human papillomavirus (HPV) to suppress NFκB activation

Tummers B, Goedemans R, Pelascini LPL, Jordanova ES, van Esch EMG,
Meyers C, Melief CJM, Boer JM, van der Burg SH.

Nat Commun. 2015 Mar 13;6:6537.

ABSTRACT

High-risk human papillomaviruses (hrHPVs) infect keratinocytes and successfully evade host immunity despite the fact that keratinocytes are well equipped to respond to innate and adaptive immune signals. Using non-infected and freshly established or persistent hrHPV-infected keratinocytes we show that hrHPV impairs the acetylation of NFκB/RelA K310 in keratinocytes. As a consequence, keratinocytes display a decreased pro-inflammatory cytokine production and immune cell attraction in response to stimuli of the innate or adaptive immune pathways. HPV accomplishes this by augmenting the expression of interferon-related developmental regulator 1 (IFRD1) in an EGFR-dependent manner. Restoration of NFκB/RelA acetylation by IFRD1 shRNA, Cetuximab treatment or the HDAC1/3 inhibitor entinostat increases basal and induced cytokine expression. Similar observations are made in IFRD1-overexpressing HPV-induced cancer cells. Thus, our study reveals an EGFR-IFRD1 mediated viral immune evasion mechanism which can also be exploited by cancer cells.

INTRODUCTION

High-risk human papillomaviruses (hrHPVs) are absolutely species-specific small double-stranded DNA viruses that primarily target undifferentiated keratinocytes (KCs) of squamous epithelia via micro-wounds and abrasions. HrHPV infections can last up to two years despite viral activity in infected KCs, the expression of viral antigens and the presence of KC-expressed pattern recognition receptors (PRR)[1-4] that should lead to activation of innate and adaptive immune responses. This indicates that hrHPV has evolved mechanisms to transiently evade innate and adaptive immune mechanisms. Ultimately, the majority of hrHPV infections are controlled by the immune system, in particular by type 1 (IFNγ and TNFα) cytokine producing T cells[5]. In case of immune failure, hrHPV causes cancer of the anogenital and/or head and neck regions[6].

Upon infection, hrHPV alters the immune-related response of keratinocytes to various innate and adaptive immune stimuli resulting in impaired expression of interferon (IFN)-stimulated genes (ISG), interferon regulatory transcription factor (IRF)-induced genes, and NFκB-induced genes[3,7-12], suggesting that HPV hampers STAT1 and NFκB activation. HPV-infected KCs display downregulated basal expression of *STAT1* and lowered STAT1 protein levels explaining the impaired expression of ISGs[13-16]. Furthermore, soon after infection HPV upregulates the cellular deubiquitinase ubiquitin carboxy-terminal hydrolase L1 (UCHL1) to impair PRR-induced NFκB activation by upstream interference with TRAF3, TRAF6 and NEMO[8]. The upregulation of UCHL1 however can not explain how the virus manages to suppress the KCs response to adaptive immune signals[12]. In addition, repressing UCHL1 does not fully restore NFκB signaling via PRR[8], suggesting that one or more additional mechanisms are in play to suppress NFκB signaling.

In this study, we analyze NFκB activation and subsequent cytokine/chemokine production following IFNγ and TNFα stimulation in uninfected and HPV-infected primary KCs. Our study reveals that RelA-acetylation, needed for NFκB transcriptional activity[17], is impaired in hrHPV-infected KCs. The HPV-induced overexpression of the cellular protein interferon-related developmental regulator 1 (IFRD1) is shown to be instrumental in this process and involves

HDAC1 and/or 3. The augmented expression of IFRD1 is the result of the HPV-mediated upregulation of EGFR. Blocking of IFRD1 protein expression by shRNA or via the anti-EGFR antibody Cetuximab restores NFκB/RelA-mediated cytokine expression. Additional data suggest that IFRD1 may have a similar role in suppressing cytokine/chemokine production in HPV-positive cervical cancer cells.

RESULTS

HrHPV impairs the KCs cytokine response to IFNγ and TNFα

To evaluate if the KCs immune response following the exposure to IFNγ and/or TNFα is attenuated by hrHPV, we utilized a system that resembles the natural infection with hrHPV as closely as possible. Primary KCs stably maintaining the hrHPV genome as episomes (hrHPV+ KCs) display similar growth properties as non-transfected KC, and upon culture in organotypic raft cultures, mimic HPV infection *in vivo* as documented by genome amplification, late gene expression, and virus production during the differentiation dependent life cycle of HPV[18-20].

The presence of HPV type 16 (HPV16) was clearly associated with an impaired capacity to respond to IFNγ and to TNFα as shown by the lower mRNA expression and production of the IFNγ and/or TNFα-induced pro-inflammatory cytokines CCL2, RANTES (CCL5), IL8 and the chemokines CXCL9, 10 and 11 by KCs (Figure 1AB). Not only did the presence of HPV16 impair the production of cytokines, also the migration of peripheral blood mononuclear cells (PBMCs) to supernatants of IFNγ and TNFα-stimulated HPV16+ KCs was greatly impaired (Figure 1C).

These data suggest that hrHPV, besides impairing the innate immune response of KCs[8], also suppresses the KCs response to the adaptive immune signals provided by IFNγ and TNFα.

The hrHPV-mediated deregulated expression of STAT1[13-16] may explain the impaired cytokine expression by hrHPV-positive KCs upon IFNγ stimulation but not the impaired response to TNFα (IL8) or to IFNγ and TNFα (RANTES). Previously, we showed that hrHPV hampers phosphorylation of the NFκB subunit RelA (p65) upon stimulation with the innate pattern recognition receptor (PRR) ligand Poly(I:C)[8]. As TNFα stimulation rapidly induces the phosphorylation of RelA[17], we tested whether hrHPV also hampers rapid TNFα-induced RelA phosphorylation by stimulating KCs and HPV16+ KCs for 0, 5, 15 or 30 minutes with TNFα. Western blotting showed that RelA was rapidly phosphorylated similarly in KCs and HPV16+ KCs, peaking after 15 minutes of TNFα stimulation (Figure 1D), indicating that the impairment of TNFα-induced responses seen in HPV16+ KCs was not due to altered RelA phosphorylation after short-term TNFα stimulation. Activated NFκB translocates to the nucleus where it is modified to regulate its DNA binding ability and transcriptional activity. Acetylation of the RelA subunit at lysine 310 (K310) is crucial in this process[17]. Strikingly, acetylated RelA K310 protein levels were lower in the HPV16+ KCs than in uninfected KCs, both in the absence of stimulation and after short-term TNFα stimulation (Figure 1D). The lowered basal RelA K310 acetylation state was verified in three independent primary KC and two independent HPV16+ KC cultures (Figure 1E), indicating that HPV hampers the activity of NFκB already at steady-state levels. This was also reflected in a lowered basal cytokine gene expression in unstimulated HPV16+ KCs (Figure 1F).

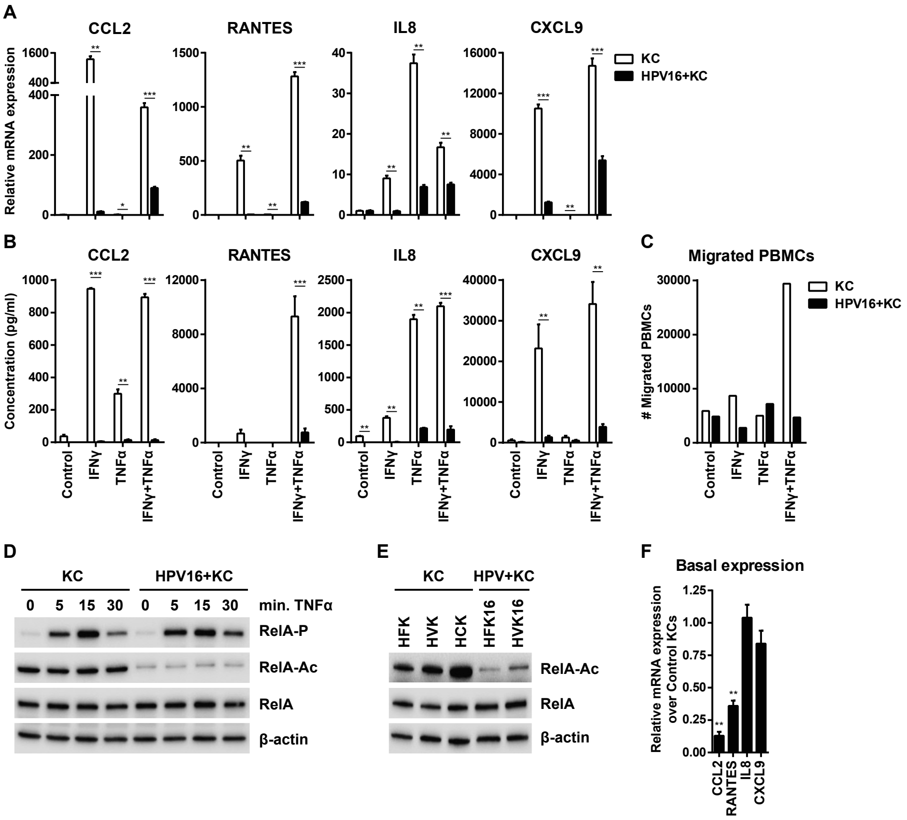

Figure 1: HPV16 impairs IFNγ and TNFα-induced cytokine production and RelA K310 acetylation in KCs

(A) RT-qPCR of CCL2, RANTES, IL8 and CXCL9 expression by 24 hours control, IFNγ and/or TNFα-stimulated undifferentiated KCs or HPV16+ KCs. Gene expression was normalized using GAPDH as the calibrator gene. Fold changes over control-stimulated undifferentiated KCs were calculated and depicted.
(B) ELISA for CCL2, RANTES, IL8 and CXCL9 in cleared supernatants of 24 hours control, IFNγ and/or TNFα-stimulated undifferentiated KCs or HPV16+ KCs.
(C) PBMCs migration towards cleared supernatants of 24 hours control, IFNγ and/or TNFα-stimulated KCs or HPV16+ KCs. A representative example of 3 different donors is shown.
(D) RelA phosphorylation, acetylation and total levels in KCs and HPV16+ KCs stimulated with TNFα for 0, 5, 15 and 30 minutes.
(E) RelA acetylation and total levels at steady-state in three human primary keratinocyte (KC) donor pools originating from human foreskin keratinocytes (HFK), human vaginal keratinocytes (HVK) or human cervical keratinocytes (HCK) and two HPV16+ genome transfected primary KC pools foreskin (HFK16) or vaginal (HVK16) origin.
(F) RT-qPCR of CCL2, RANTES, IL8 and CXCL9 in HPV16+ KCs and KCs. Gene expression was normalized using GAPDH as the calibrator gene. Gene expression in HPV16+ KCs was standardized over KCs.
*All data are representative for at least three independent experiments. Error bars indicate SD. P-values were determined via Welch-corrected unpaired t tests. * p<0.05, ** p<0.01, *** p<0.001.*

HrHPV upregulates IFRD1 to impair RelA K310 acetylation

Acetylation of RelA K310 can be regulated by the lysine acetyl transferases (KAT) PCAF (KAT2B), CBP (KAT3A), p300 (KAT3B), and TIP60 (KAT5) as well as the histone deacetylases (HDAC) 1 and 3[17]. Since our results imply that hrHPV has a mechanism either to deacetylate or impair the acetylation of RelA, we screened our validated micro array data[12] for genes involved in regulating RelA K310 acetylation. High-risk HPV did not significantly influence *histone deacetylase* (*HDAC1* to *11*) or *sirtuin* (*SIRT1* to *7*) expression (Figure 2A). The only significantly upregulated gene was the lysine acetyl transferase *CREBBP* (*KAT3A*), confirming previous observations stating that HPV upregulates CREBBP to enhance expression from episomal DNA[21,22]. However, as CREBBP acetylates RelA its upregulation can not explain the observed lower levels of RelA K310 acetylation in hrHPV-infected KCs under steady state conditions. Interestingly, the micro array data also showed the upregulation of Interferon-related developmental regulator 1 (*IFRD1*) (Figure 2B), which previously was shown to complex HDAC1[23] and HDAC3 to RelA causing its deacetylation at lysine 310 in the mouse myoblast cell line C2C12[24]. We hypothesized that it may fulfill a similar role in human KCs. Therefore, RT-qPCR and western blotting was used to confirm that *IFRD1* gene expression (Figure 2C left) and IFRD1 protein levels (Figure 2D left) were elevated in two independent HPV16+ KC cultures. Knock-down of the polycistronic mRNA of HPV16 by a siRNA against HPV16 E2 in HPV16+ KCs resulted in the reduction of HPV16 *E1*, *E2*, *E6* and *E7* expression (Supplementary Fig. S1), *IFRD1* mRNA (Figure 2C middle) and IFRD1 protein levels (Figure 2D middle), indicating that the augmented IFRD1 levels in hrHPV+ KCs are the result of the presence of hrHPV. Reciprocally, when undifferentiated KCs were infected with native HPV16 virions, *IFRD1* mRNA (Figure 2C right) and IFRD1 protein (Figure 2D right) levels were clearly enhanced after 2 days of infection. Furthermore, immunohistochemistry of HPV-positive vulvar lesions revealed the presence of IFRD1 in the nuclei of cells positive for HPV16 E2 (reflecting HPV-infected cells)[25], but not in the nuclei of already transformed KCs (identified through p16 staining[25,26] or undifferentiated (E2 and p16 negative) healthy tissue (Figure 2E).

We then asked if the hrHPV-induced increased levels of IFRD1 affected RelA K310 acetylation also in human undifferentiated KCs. Indeed, when lentivirus-delivered siRNA against *IFRD1* was used to lower IFRD1 protein expression a concomitant increase in the steady-state levels of acetylated RelA K310 in HPV16+ KCs was seen when compared to control knock-down HPV16+ KCs (Figure 2F; Supplementary Fig. S2A). Furthermore, a small increase in total RelA protein levels was observed. The gain in acetylated RelA K310 translated into a higher basal expression and secretion of cytokines in IFRD1 KD cells (Figure 2GHI), indicating that IFRD1 is involved in the deregulation of steady-state inflammatory gene expression levels in HPV16+ KCs. The dampening effect of *IFRD1* on the NFκB-regulated cytokine expression became even more apparent when the KCs were stimulated with both IFNγ and TNFα (Figure 2HI). The cytokine levels produced after stimulation were much higher in IFRD1 KD HPV16+ KCs than in control KD HPV16+ KCs. Moreover, *IFRD1* knock-down augmented the ability of HPV16+ KCs to attract PBMCs (Figure 2J). The main results were recapitulated in HPV18-infected KCs (Supplementary Fig. S3), suggesting that IFRD1 may form a general mechanism exploited by any hrHPV type.

As the effect of IFRD1 occurred directly at the level of RelA, the influence of IFRD1 on the response of HPV16+ KCs to Poly(I:C) stimulation, previously shown by us to be impaired in hrHPV-infected KCs[8], was also tested. Knock-down of *IFRD1* resulted in an enhanced expression of *CCL2, RANTES, IL8*

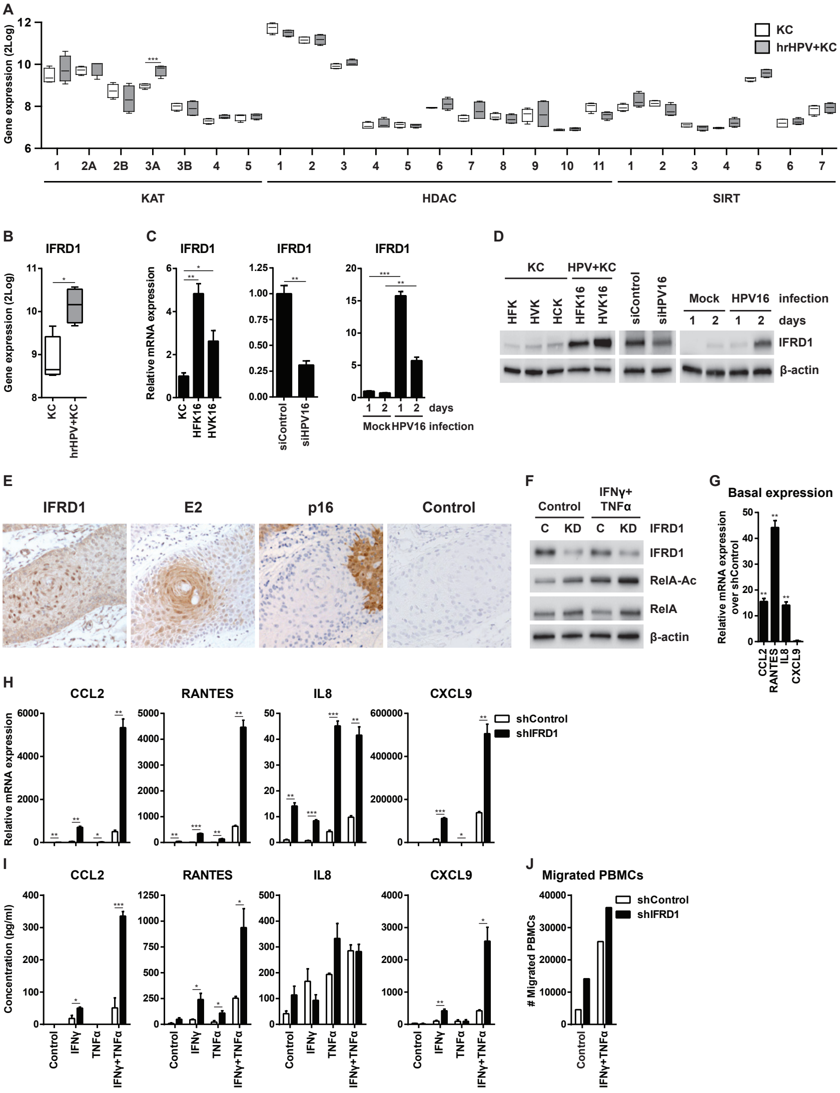

Figure 2: HrHPV upregulates IFRD1 to impair RelA K310 acetylation and basal cytokine expression
Microarray intensities for (A) all KATs, HDACs and SIRTs, and (B) IFRD1 in 4 independent KCs and 4 independent hrHPV+ KCs represented in a box plot. The box contains the 1st quartile up to the 3rd quartile, the median is represented as a line, whiskers represent the values of the outer 2 quartiles.

(C) IFRD1 mRNA expression of one representative control primary KC culture and two HPV16+ KC culture (left panel), in HFK16 cells transfected with siControl or siHPV16 (middle panel) and in primary KCs that are either mock infected or infected with native HPV16 virions (right panel), as measured by RT-qPCR.
(D) IFRD1 protein expression in three human primary keratinocyte (KC) donor pools originating from human foreskin keratinocytes (HFK), human vaginal keratinocytes (HVK) or human cervical keratinocytes (HCK) and two HPV16+ genome transfected primary KC pools foreskin (HFK16) or vaginal (HVK16) origin (left panel) in HFK16 cells transfected with siControl or siHPV16 (middle panel) and in primary KCs that are either mock infected or infected with native HPV16 virions (right panel), as measured by western blot.
(E) Immunohistochemical staining for IFRD1, HPV16 E2, p16 and negative antibody control of a vulvar intraepithelial neoplasia (VIN) lesion, one representative donor of two shown. Counterstaining was done using hematoxylin. Arrows indicate sites where E2 and nuclear IFRD1 are expressed. Scale bar 500 µm.
(F) IFRD1, RelA K310 acetylation and total RelA levels in 24 hours non- or IFNγ and TNFα-stimulated control or IFRD1 knock-down (KD) HPV16+ KCs.
(G) RT-qPCR of CCL2, RANTES, IL8 and CXCL9 expression in steady-state control or IFRD1 KD HPV16+ KCs.
(H) RT-qPCR of CCL2, RANTES, IL8 and CXCL9 expression in 24 hours non- or IFNγ and/or TNFα-stimulated control or IFRD1 KD HPV16+ KCs.
(I) ELISA for CCL2, RANTES, IL8 and CXCL9 in cleared supernatants of 24 hours non- or IFNγ and/or TNFα-stimulated control or IFRD1 KD HPV16+ KCs.
(J) PBMCs migration towards cleared supernatants of 24 hours non- or IFNγ and TNFα-stimulated control or IFRD1 KD HPV16+ KCs. A representative example of 3 different donors is shown.
*These data are representative for at least three independent experiments. Error bars indicate SD. P-values were determined via Welch-corrected unpaired t tests. * p<0.05, ** p<0.01, *** p<0.001.*

and *CXCL9* following PRR stimulation with Poly(I:C) (Supplementary Fig. S4).

Thus, hrHPV upregulates the expression of *IFRD1* soon after infection, thereby effectively decreasing the basal levels of transcriptionally active RelA and as a consequence the levels of pro-inflammatory cytokines induced via various innate and adaptive immune-mediated NFκB stimulatory pathways.

EGFR-signaling mediates the increased expression of IFRD1

Growth factors, such as NGF, FGF or EGF, have previously been shown to induce the expression of *Tis* family genes, which also includes *IFRD1,* in rat neocortical astrocytes and chromaffin cell line PC12, mouse C243 and IEC-18, and mammary epithelial cells[27]. The hrHPV E5 protein is known to affect different aspects of EGF receptor (EGFR) signaling and expression[28]. Verification of EGFR expression in our model showed that *EGFR* mRNA expression (Figure 3A) and membrane-bound protein expression (Figure 3B) were higher in hrHPV+ KCs than in non-infected KCs. When we transfected cDNA for E2 (as control), E5 or a mix of several other HPV proteins, only E5 enhanced *EGFR* expression (Figure 3C). To test if EGFR signaling had a similar effect on IFRD1 in human primary KCs, the clinically used anti-EGFR antibody Cetuximab was employed to block EGFR signaling. Indeed, *IFRD1* expression decreased in HPV16+ KCs, but not in uninfected KCs, when treated with Cetuximab (Figure 3D). IFRD1 protein levels also decreased dose-dependently in both Cetuximab-treated non-infected KCs and HPV16+ KCs (Figure 3E). Notably, the isotype control antibody Rituximab (anti-CD20) had no effect (Figure 3DE). Thus EGFR signaling does not only induce *IFRD1* gene expression but also stabilizes IFRD1 protein levels. Relative density analysis revealed that in Cetuximab-treated HPV16+ KCs the protein levels of IFRD1 decreased while concomitantly the levels of RelA K310 acetylation increased in a dose-dependent fashion. Total RelA levels were unaffected (Figure 3F). These results indicated that the HPV-induced expression of IFRD1 is mediated via the EGFR signaling pathway and implied that Cetuximab treatment may enhance the hrHPV+ KCs pro-inflammatory cytokine response to immune stimuli. Indeed, upon IFNγ and TNFα stimulation Cetuximab-treated HPV16+ KCs expressed higher levels of indicated cytokine genes than Rituximab-treated cells (Figure 3G) as well as higher levels of secreted cytokines (Figure 3H). In uninfected KCs treatment with Cetuximab decreased the already low levels of IFRD1 protein, and although this led to increased cytokine gene expression after IFNγ and TNFα-stimulation no additional increase in the already high levels of secreted cytokines was observed (Figure 3GH). The absence of cytokine production in Cetuximab-treated HPV16+ KC and uninfected KCs that were not stimulated with IFNγ and TNFα shows that binding of Cetuximab to EGFR *per se* does not result in the stimulation of cytokine production (Figure 3GH).

As EGFR signaling involves the downstream partners PI3K, mTOR, MEK1, RAF and JNK, we selectively inhibited these proteins using small molecule inhibitors in HPV16+ KCs and observed that selective inhibition of mTOR (Rapamycin), MEK1 (PD98059) and RAF (GW5074) but not PI3K (LY94002) or JNK (SP60025) resulted in decreased expression of IFRD1 (Figure 3I). Thus EGFR-mediated upregulation of IFRD1 is fundamental to the impaired NFκB-induced cytokine response of hrHPV-infected KCs to innate and adaptive immune stimuli.

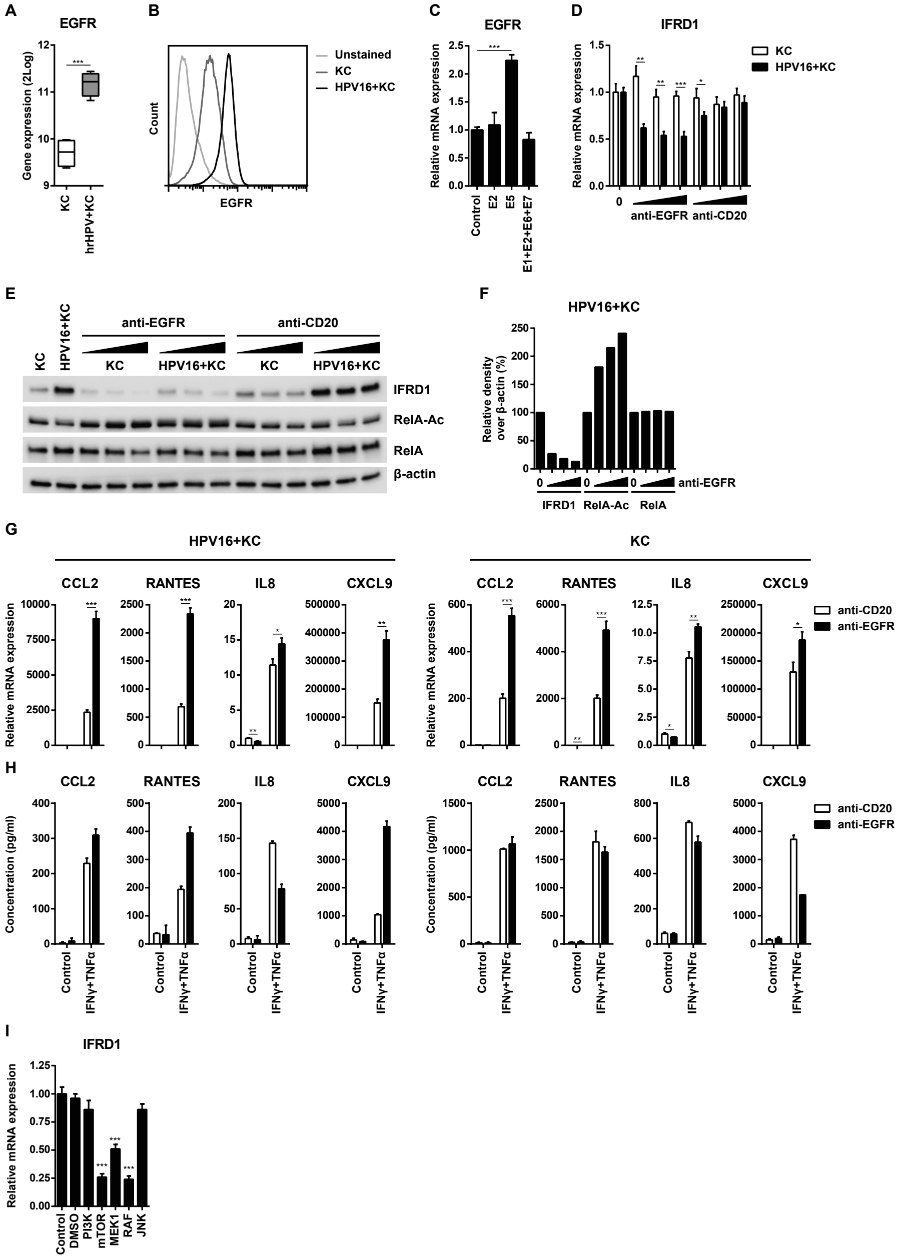
A
EGFR
Gene expression (2Log)
KC
hrHPV+KC
B
Count
EGFR
Unstained
KC
HPV16+KC
C
EGFR
Relative mRNA expression
Control
E2
E5
E1+E2+E6+E7
D
IFRD1
Relative mRNA expression
KC
HPV16+KC
anti-EGFR
anti-CD20
E
KC
HPV16+KC
anti-EGFR
anti-CD20
KC
HPV16+KC
KC
HPV16+KC
IFRD1
RelA-Ac
RelA
β-actin
F
HPV16+KC
Relative density over β-actin (%)
anti-EGFR
IFRD1
RelA-Ac
RelA
G
HPV16+KC
KC
CCL2
RANTES
IL8
CXCL9
Relative mRNA expression
anti-CD20
anti-EGFR
H
CCL2
RANTES
IL8
CXCL9
Concentration (pg/ml)
Control
IFNγ+TNFα
anti-CD20
anti-EGFR
I
IFRD1
Relative mRNA expression
Control
DMSO
PI3K
mTOR
MEK1
RAF
JNK

Figure 3: Blocking EGFR-signaling decreases IFRD1 levels and rescues cytokine production by hrHPV+ KCs

(A) Microarray intensities for EGFR in KCs (n=4) and hrHPV+ KCs (n=4) represented in a box plot.

(B) Histogram of EGFR surface protein expression on KCs and HPV16+ KCs as determined by flow cytometry.

(C) RT-qPCR of EGFR expression in KCs transfected with cDNA for E2, E5, E1+E2+E6+E7, or empty control.

(D) RT-qPCR of IFRD1 expression in KCs and HPV16+ KCs treated for 72 hours with 0, 0.1, 1 or 10 μg ml^{-1} anti-EGFR or anti-CD20.

(E) IFRD1, RelA K310 acetylation and total RelA levels in KCs and HPV16+ KCs treated for 72 hours with 0, 0.1, 1 or 10 μg ml^{-1} anti-EGFR or anti-CD20.

(F) Quantified protein levels of IFRD1, RelA K310 acetylation, and RelA over β-Actin in HPV16+ KCs treated for 72 hours with 0, 0.1, 1 or 10 μg ml^{-1} anti-EGFR (western blot 2D). The expression levels of the 0 μg/ml treated HPV+ KCs were set as 100%.

(G) RT-qPCR of CCL2, RANTES, IL8 and CXCL9 expression in 24 hours non- or IFNγ and TNFα-stimulated, anti-CD20 or anti-EGFR-treated HPV16+ KCs (left) and KCs (right).

(H) ELISA for CCL2, RANTES, IL8 and CXCL9 in cleared supernatants of 24 hours non- or IFNγ and TNFα-stimulated, anti-CD20 or anti-EGFR-treated HPV16+ KCs (left) and KCs (right).

(I) RT-qPCR of IFRD1 expression in HPV16+ KCs treated with inhibitors of PI3K (LY94002, 25 μM), mTOR (Rapamycin, 50 nM), MEK1 (PD98059, 50 μM), RAF (GW5074, 20 μM), and JNK (SP60025, 20 μM). Gene expression was normalized using GAPDH as the calibrator gene. Fold changes over Control were calculated and depicted.

*These data are representative for at least three independent experiments, except for figure H which was performed once. Error bars indicate SD. P-values were determined via Welch-corrected unpaired t tests. * p<0.05, ** p<0.01, *** p<0.001.*

HDAC1/3 inhibition stimulates cytokine production

IFRD1-mediated RelA deacetylation required the recruitment of HDAC1 and/or 3 to the RelA-IFRD1 complex in the mouse myoblast cell line C2C12[24]. To test if these HDACs played a similar role in human hrHPV+ KCs, the effect of HDAC inhibition was tested in HPV16+ KCs and non-infected KCs. A dose-titration of the HDAC1/3-specific inhibitor entinostat (MS-275), and the prototypic pan-HDAC inhibitors trichostatin A (TSA), sodium butyrate (NaBu) and the FDA-approved vorinostat (SAHA) was performed to study RelA K310 acetylation. All pan-HDAC inhibitors increased RelA acetylation in KCs at the lowest concentration used (Figure 4A & Supplementary Fig. S2B) but at higher doses cells suffered from toxic effects as observed by microscopy. However, HPV16+ KCs did survive entinostat treatment, and clearly this HDAC1/3 inhibitor increased RelA K310 acetylation in HPV16+ KCs (Figure 4A & Supplementary Fig. S2B). This indicated that HDAC1 and/or 3 are indeed specifically involved in the deacetylation of RelA in hrHPV+ KCs. Entinostat treatment of HPV16+ KCs not only restored RelA K310 acetylation but also released the suppressive effect of IFRD1 on cytokine production. Treated HPV16+ KCs displayed a

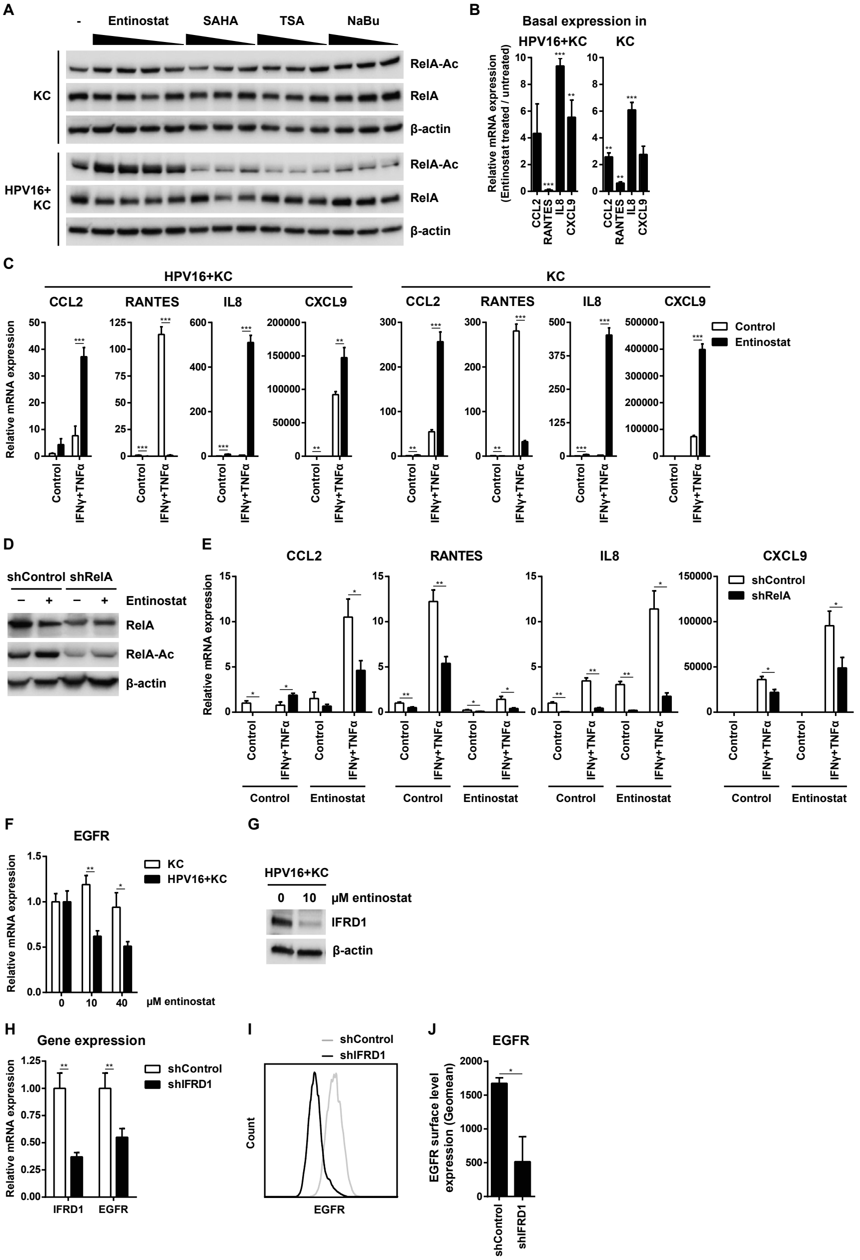
A
-
Entinostat
SAHA
TSA
NaBu
KC
RelA-Ac
RelA
β-actin
HPV16+
KC
RelA-Ac
RelA
β-actin
B
Basal expression in
HPV16+KC
KC
Relative mRNA expression
(Entinostat treated / untreated)
CCL2
RANTES
IL8
CXCL9
C
HPV16+KC
KC
CCL2
RANTES
IL8
CXCL9
Relative mRNA expression
Control
IFNγ+TNFα
Control
Entinostat
D
shControl
shRelA
Entinostat
RelA
RelA-Ac
β-actin
E
CCL2
RANTES
IL8
CXCL9
shControl
shRelA
Relative mRNA expression
Control
IFNγ+TNFα
Control
Entinostat
F
EGFR
Relative mRNA expression
KC
HPV16+KC
0
10
40
μM entinostat
G
HPV16+KC
0
10
μM entinostat
IFRD1
β-actin
H
Gene expression
Relative mRNA expression
shControl
shIFRD1
IFRD1
EGFR
I
shControl
shIFRD1
Count
EGFR
J
EGFR
EGFR surface level
expression (Geomean)
shControl
shIFRD1

Figure 4: Entinostat treatment reveals involvement of HDAC1/3 in RelA deacetylation in HPV16+ KCs
(A) RelA K310 acetylation and total RelA levels in KCs and HPV16+ KCs treated with decreasing doses of entinostat (40, 20, 10 and 2 μM), SAHA (10, 5 and 1 μM), TSA (5, 1 and 0.333 μM) or NaBu (10, 5 and 1 mM).
RT-qPCR of CCL2, RANTES, IL8 and CXCL9 expression in steady-state (B) or 24 hours non- or IFNγ and TNFα-stimulated (C) control or entinostat (10 μM) pre-treated HPV16+ KCs.
(D) Total RelA levels and RelA K310 acetylation non- or entinostat-treated control or RelA knock-down (KD) HPV16+ KCs.
(E) RT-qPCR of CCL2, RANTES, IL8 and CXCL9 expression in 24 hours non- or IFNγ and TNFα-stimulated non- or entinostat-treated control or RelA knock-down (KD) HPV16+ KCs.
(F) RT-qPCR of EGFR expression in KCs and HPV16+ KCs treated with increasing doses of entinostat (0, 10 or 40 μM). Gene expression was normalized using GAPDH as the calibrator gene.
(G) IFRD1 in control or entinostat (10 μM) pre-treated HPV16+ KCs.
(H) RT-qPCR of IFRD1 and EGFR expression in control or IFRD1 KD HPV16+ KCs. Gene expression was normalized using GAPDH as the calibrator gene.
Histogram (I) and Geo mean (J) of EGFR expression on control or IFRD1 KD HPV16+ KCs as determined by flow cytometry. SEM of two independent experiments.
*These data are representative for at least two independent experiments. Error bars indicate SD. P-values were determined via Welch-corrected unpaired t tests. * p<0.05, ** p<0.01, *** p<0.001.*

higher basal expression for 3 out of 4 tested cytokines when compared to their untreated counterparts (Figure 4B). Moreover, when stimulated with IFNγ and TNFα both KCs and HP16V+ KCs displayed a higher expression of *CCL2*, *IL8* and *CXCL9*, although the expression of *RANTES* was abrogated (Figure 4C). To confirm the involvement of RelA in this process, RelA was knocked-down in HPV+ KCs (Figure 4D), after which the cells were treated with entinostat and stimulated with IFNy and TNFa. Indeed, RelA acetylation and cytokine production was increased in the control knock-down cells after stimulation with IFNy and TNFa when treated with entinostat (Figure 4DE). However, when RelA was knocked-down in HPV16+ KCs, the cytokine expression was abrogated despite treatment with entinostat (Figure 4E).

Previously, it was shown that HDAC inhibition abrogates EGFR expression[29,30], indicating that *EGFR* expression is dependent on acetylation events. Indeed, entinostat treatment dose-dependently abrogated *EGFR* expression in hrHPV+ KCs, but did not influence the expression in KCs (Figure 4F). Furthermore, entinostat treatment resulted in a reduced level of IFRD1 protein in hrHPV+ KCs (Figure 4G), which made us wonder if IFRD1 could regulate EGFR expression. Therefore, *IFRD1* was knocked-down in hrHPV+ KCs and this resulted in lower *EGFR* expression (Figure 4H) and a lower level of membrane-bound EGFR than control-treated hrHPV+ KCs (Figure 4IJ), indicating that IFRD1 can control *EGFR* expression.

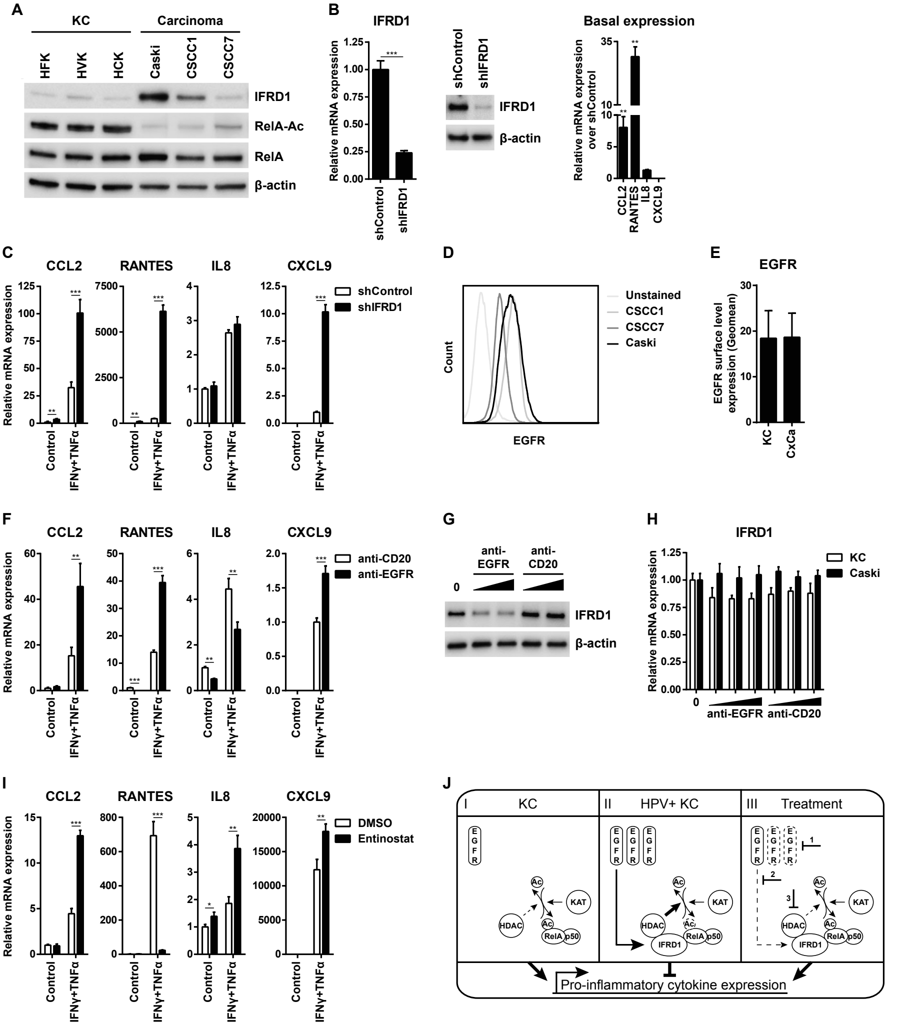

Figure 5: Role of IFRD1 in hrHPV+ cervical cancer cells

(A) IFRD1, RelA acetylation and total RelA levels at steady-state in three KC donors and three HPV16-induced CxCa lines.

(B) RT-qPCR of IFRD1, CCL2, RANTES, IL8 and CXCL9 expression and IFRD1 protein levels in

steady-state control or IFRD1 KD Caski cells.
(C) RT-qPCR of IFRD1, CCL2, RANTES, IL8 and CXCL9 expression in 24 hours non- or IFNγ and TNFα-stimulated control or IFRD1 KD Caski cells.
(D) Histogram of EGFR expression on three HPV16-induced CxCa lines.
(E) Geo mean of EGFR expression on KCs and CxCa as determined by flow cytometry. SEM of two independent experiments.
(F) RT-qPCR of CCL2, RANTES, IL8 and CXCL9 expression in 24 hours non- or IFNγ and TNFα-stimulated anti-CD20 or anti-EGFR-treated Caski cells.
(G) IFRD1 and RelA K310 acetylation status in Caski cells treated for 72 hours with 0, 1 or 10 μg ml^{-1} anti-EGFR (Cetuximab) or anti-CD20 (Rituximab).
(H) RT-qPCR of IFRD1 expression in KCs and Caski cells treated for 72 hours with 0, 0.1, 1 or 10 μg ml^{-1} anti-EGFR or anti-CD20.
(I) RT-qPCR of CCL2, RANTES, IL8 and CXCL9 expression in 24 hours non- or IFNγ and TNFα-stimulated control (DMSO) or entinostat-treated Caski cells.
(J) Schematic representation of IFRD1-mediated RelA (de-)acetylation. I) In KCs, RelA acetylation is positively regulated by KATs, resulting in the production of pro-inflammatory cytokines. HDACs may suppress this process. II) In HPV+ KCs, elevated EGFR levels can induce the expression of IFRD1, which can mediate RelA deacetylation by forming a bridge between RelA and HDAC1 and/or 3, hampering pro-inflammatory gene expression. III) Interfering with EGFR signaling (1 and 2) or HDAC function (3) may lower IFRD1 levels, restoring the RelA acetylation balance, augmenting pro-inflammatory gene expression.
*Error bars indicate SD. P-values were determined via Welch-corrected unpaired t tests. * $p<0.05$, ** $p<0.01$, *** $p<0.001$.*

IFRD1 hampers the response of cancer cells to IFNγ and TNFα

To evaluate if an increased expression of IFRD1 could also play a role in HPV16-induced squamous cell carcinoma, we analyzed the cell line Caski, as well as the two early passage cervical cancer cell lines, CSCC1 and CSCC7[31]. IFRD1 protein expression differed between the cell lines (Figure 5A), but was increased in Caski and CSCC1 when compared to normal KCs. RelA K310 acetylation was lower in all three cervical cancer cell lines than in uninfected KCs (Figure 5A & Supplementary Fig. S2C). For the Caski and CSCC1 lines this may be explained by the presence of upregulated IFRD1. However, the lack of RelA K310 acetylation in the CSCC7 line indicates that besides IFRD1 also other mechanisms can alter the acetylation of RelA K310 in these squamous cancer cells.

Because IFRD1 was upregulated in the Caski and CSCC1 cells we studied the effects of IFRD1 using these cell lines. IFRD1 knock-down in the CSCC1 cells did not alter basal cytokine expression levels (Supplementary Fig. S5A), but IFRD1 knock-down in the Caski cells resulted in a direct increase of the basal expression levels of *CCL2* and *RANTES* (Figure 5B). Furthermore, both cell lines showed increased cytokine gene levels upon IFNγ and TNFα stimulation when IFRD1 was knocked-down as compared to their control knock-down counterparts (Figure 5C and Supplementary Fig. S5B).

CSCC1 and Caski cells express EGFR (Figure 5D) at a level that is similar to that of uninfected KCs (Figure 5E). However the downstream signaling pathway is known to be constitutively higher in HPV-induced cancer cells[32]. As a consequence, the treatment of Caski and CSCC1 cancer cells with the anti-EGFR antibody Cetuximab resulted in a higher production of IFNγ and TNFα-induced cytokines than when the cancer cells were treated with the control anti-CD20 antibody Rituximab (Figure 5F and Supplementary Fig. S5C). The enhanced response to IFNγ and TNFα was associated with a concomitant decrease in IFRD1 protein levels (Figure 5G), but not mRNA expression (Figure 5H), upon EGFR blockade. Similarly, treatment of Caski and CSCC1 cancer cells with entinostat resulted in a higher production of *CCL2*, *IL8* and *CXCL9* by the cancer cells when stimulated with IFNγ and TNFα than DMSO carrier control treated cells (Figure 5I and Supplementary Fig. S5D). Congruent with our earlier observations, *RANTES* levels diminished after entinostat treatment. These results suggest that IFRD1 may also play a role in suppressing the response of cancer cells to immune stimuli such as IFNγ and TNFα.

DISCUSSION

Using a unique *in vitro* model we here show that hrHPV infection leads to the upregulated expression of endogenous IFRD1 to deregulate the K310 acetylation of NFκB/RelA. As a result hrHPV-infected KCs display an impaired production of pro-inflammatory cytokines and chemokines, and a reduced capacity to attract immune cells. The increased expression of IFRD1 in hrHPV+ KCs is mediated by EGFR signaling via mTOR, RAF and/or MEK1. Knock-down of *IFRD1* with siRNA or indirectly via blockade of EGFR with the clinically used EGFR-specific antibody Cetuximab, resulted in decreased IFRD1 mRNA and protein levels, increased NFκB/RelA K310 acetylation and enhanced expression and production of pro-inflammatory cytokines and chemokines by hrHPV+ KCs. The use of entinostat indicated that HDAC1 and/or 3 are involved in lowering K310 acetylation of NFκB/RelA. These conclusions are schematically represented in figure 5J.

EGFR activation on epithelial cells has been shown to result in a decreased production of CCL2, RANTES and CXCL10 and increased production of IL8. Inhibition of EGFR signaling with blocking antibodies or tyrosine kinase inhibitors can reverse the effect on these cytokines as well as result in an increased epithelial immune infiltrate *in vivo*[33-35]. Interestingly, virus-induced EGFR-activation has been implicated as novel mechanism for respiratory viruses to suppress antiviral host responses[33]. The exact underlying mechanism on EGFR-mediated immune suppression remained unclear, albeit that ERK1/2 signaling was shown to be involved in regulating cytokine production and skin inflammation[36]. Using the EGFR blocking antibody Cetuximab in the absence of an additional EGFR stimulus such as TGFα we found similar effects on the cytokine production of HPV16+ KCs. In KCs the expression of EGFR and IFRD1 are tightly linked as EGFR inhibition reduced the expression and protein levels of IFRD1, via mTOR, RAF and/or MEK1, but not PI3K or JNK. This fits with the involvement of ERK1/2 in regulating cytokine production (Pastore et al., 2005) since RAF and MEK1 are just upstream of these kinases. Based on our data, the previously observed EGFR activation-induced suppression of cytokine production and immune cell infiltration of epithelia can be explained by upregulation of IFRD1 and subsequent suppression of NFκB signaling. Our data suggest that EGFR-driven overexpression of IFRD1 may also play a role in deregulating NFκB-signaling in HPV-induced tumor cells. Knock-down of IFRD1 results in an increased production of pro-inflammatory cytokines and chemokines by tumor cells when stimulated with IFNγ and TNFα. Furthermore, blocking of the EGFR by Cetuximab resulted in a decrease of IFRD1 protein levels as well as increased cytokine production. The HPV oncoproteins are also known to directly intervene with NFκB signaling. Studies with transfected or transformed cells – resembling protein expression in tumor cells – show that E6 and/or E7 proteins inhibit basal and TNFα-inducible NFκB activity[37] by influencing NFκB localization[38,39] and activation[40-43].

Studies in immunosuppressed patients and healthy individuals show a key role for the adaptive immune response, in particular that of a strong type 1 (IFNγ and TNFα)-associated HPV early antigen-specific T cells in the protection against progressive disease[5]. This notion is sustained by the clinical responses of patients treated with HPV-specific therapeutic vaccines[5]. Ample reasons, therefore, for HPV to also develop strategies preventing KCs to respond to these cytokines. Our data shows that HPV deploys multiple strategies to interfere with induced RelA-associated NFκB signaling. HPV utilizes the cellular deubiquitinase UCHL1 to interfere with TRAF3, TRAF6 and NEMO function[8] and here we show that HPV also upregulates the expression of endogenous IFRD1 to deregulate the K310 acetylation of NFκB. Furthermore, the E7 protein of hrHPV has been shown to bind HDAC1 and prevent acetylation of histones, thereby suppressing TLR9 signaling[44], but E7 can also displace HDACs resulting in enhanced hypoxia-inducible factor 1α transcriptional activity[45]. It is not unusual for viruses to target NFκB activation[46,47], and hampering RelA acetylation is a common strategy. For instance, the N-terminus of the orf virus (ORFV) protein 002 inhibits acetylation of RelA by blocking phosphorylation of RelA S276 and subsequent recruitment of acetylases p300 and CBP[48], and the A238L protein of African swine fever virus (ASFV) hampers RelA K310 acetylation by inhibiting RelA-p300 interaction[49]. We here postulate that hrHPV does not hamper KATs in acetylating RelA, but rather recruits a mediator to enhance HDAC-mediated RelA deacetylation. Together with our observation that HPV lowers basal cytokine expression in resting KCs due to the presence of IFRD1, we suggest that impairment of immune driven RelA-associated

NFκB-responsive gene expression is crucial for the virus to persist. This viral strategy has not been reported before, but as discussed above may also be employed by respiratory viruses that activate EGFR[33].

All together, our data indicate that HPV upregulates EGFR to drive IFRD1 expression as a tool to decrease basal and adaptive-immune system driven cytokine expression. This may allow hrHPV to evade the host's immune response. It is highly likely that this mechanism plays a role in other viral infections too and even extents to tumors.

METHODS

Ethics Statement

The use of discarded human foreskin, cervical and vaginal keratinocyte tissues to develop cell lines for these studies was approved by the Institutional Review Board at the Pennsylvania State University College of Medicine and by the Institutional Review Board at Pinnacle Health Hospitals. The Medical Ethical Committee of the Leiden University Medical Center approved the human tissue sections (healthy foreskin, healthy cervix, HPV16- or 18-positive cervical neoplasias) used for staining. All sections and cell lines were derived from discarded tissues and de-identified, therefore no informed consent was necessary.

Cell culture

Primary cultures of human epithelial keratinocytes (KCs) were established from foreskin, vaginal, vulva and cervical tissues as previously described[3] and grown in keratinocyte serum-free medium (K-SFM; Medium 154 supplemented with HKGS kit, Invitrogen, Breda, The Netherlands). KCs stably maintaining the full episomal HPV genome following electroporation (HPV-positive KCs) were grown in monolayer culture using E medium in the presence of mitomycin C (Sigma-Aldrich) treated J2 3T3 feeder cells[19,20] for two passages and were then adapted to K-SFM for one passage before experimentation. J2 3T3 mouse fibroblasts, Caski, CSCC1, CSCC7 and SiHa cell-lines were cultured in Iscove's modified Dulbecco's medium supplemented with 8% fetal bovine serum, 2 mM l-glutamine and 1% penicillin-streptomycin (complete IMDM medium) (Gibco-BRL, Invitrogen, Breda, The Netherlands).

HPV16 infection of non-infected keratinocytes

Primary basal layer human foreskin keratinocytes were seeded 75.000 cells per well to 24-wells plates and allowed to attach for 48 hours. Cells received fresh medium (Mock infected) or medium containing native HPV16 isolated from raft cultures at MOI 100 for 24 hours. Cells were washed and harvested for either RT-qPCR or western blotting analysis.

IFRD1 and RelA knock-down in HPV-positive KCs

shRNA's were obtained from the MISSION TRC-library of Sigma-Aldrich (Zwijndrecht, The Netherlands). The MISSION shRNA clones are sequence-verified shRNA lentiviral plasmids (pLKO.1-puro) provided as frozen bacterial glycerol stocks (Luria Broth, carbenicillin at 100 µg/ml and 10% glycerol) in *E. coli* for propagation and downstream purification of the shRNA clones. pLKO.1 contains the puromycin selection marker for transient or stable transfection. The construct against IFRD1 (NM_001550) was TRCN0000156194:

CCGGCAGTTCTGAAACAGTTTCTTTCTCGAGAAAGAAACTGTTTCAGAACTGTTTTT, RelA (NM_021975) was TRCN0000014687: CCGGCCTGAGGCTATAACTCGCCTACTCGAGTAGGCGAGTTATAGCCTCAGGTTTTT, and the control was: SHC004 (MISSION TRC2-pLKO puro TurboGFP shRNA Control vector): CCGGCGTGATCTTCACCGACAAGATCTCGAGATCTTGTCGGTGAAGATCACGTTTTT. HPV16-positive KCs at ~60% confluence were transduced with lentivirus at MOI 5-10 over night, after which medium was replaced. At least 72 hours post-transduction cells were stimulated as indicated and target gene expression was assayed by RT-qPCR or western blotting.

HPV knock-down in HPV-positive KCs

SilencerSelect siRNA against HPV16 E2 (AACACUACACCCAUAGUACAUtt) was designed using siRNA Target Finder software (Ambion, Invitrogen). Blast search revealed that the designed E2 siRNA does not match with the known human transcriptome. E2 and Negative control #2 (NC2) siRNA (sequence not provided by manufacturer) were purchased from Ambion. HPV16+ KCs were transfected with 50 nM siRNA E2 or NC2 using Lipofectamine 2000 (Invitrogen) according to the manufacturer's instructions. 48 hours post-transfection cells were harvested or stimulated as indicated and target gene expression was assayed by RT-qPCR or western blotting.

Transfection of HPV genes into non-infected keratinocytes

Non-infected primary KCs were seeded 50.000 cells per well to 24-wells plates and allowed to attach over night. Cells were transfected with 500 ng DNA using Lipofectamine (invitrogen), according to the manufacturer's instructions. Cells were maintained in E-medium. 72 hours post-transfection cells were harvested and target gene expression was assayed by RT-qPCR.

EGFR signaling blocking

Subconfluent cells were cultured in respective complete growth medium in presence of Cetuximab (0.1, 1 or 10 µg ml^{-1}; Merck serono), Rituximab (0.1, 1 or 10 µg ml^{-1}; Roche), rapamycin (50 nM; Calbiochem), PD98059 (50 µM; Sigma-Aldrich), GW5074 (20 µM; Sigma-Aldrich), LY94002 (25 µM; Sigma-Aldrich) or SP60025 (20 µM; Sigma-Aldrich). Medium was changed every 2-3 days. After at least 72 hours, cells were stimulated as indicated and target gene expression was assayed by RT-qPCR or western blotting.

HDAC inhibition

Subconfluent cells were cultured in presence of a dilution series of entinostat (MS-175; 40, 20, 10 and 2 µM; Selleckchem BioConnect), vorinostat (suberoylanilide hydroxamic acid (SAHA); 10, 5 and 1 µM; Sigma-Aldrich), trichostatin A (TSA; 5, 1 and 0.333 µM; Sigma-Aldrich) or Sodium Butyrate (NaBu; 10, 5 and 1 mM; Sigma-Aldrich) in respective complete growth medium over night. Medium was changed for respective complete growth medium, cells were stimulated as indicated and target gene expression was assayed by RT-qPCR or western blotting. Since treatment with 10 µM entinostat showed a good increase in RelA K310 acetylation without signs of toxicity, subsequent experiments were performed using this dose.

Migration assays

(HPV-positive) KCs were stimulated as indicated for 24 hours. Cleared (HPV-positive) KC supernatants were added to the lower compartment of a transwell plate (Corning). The upper compartment was filled with peripheral blood mononuclear cells (PBMCs) isolated from buffy coats (Sanquin). PBMCs were allowed to migrate for 16 hours, after which the cells in the lower compartment were counted by flow cytometry in the presence of counting beads (Invitrogen) according to the manufacturer’s instructions. Myeloid cells and lymphocytes were differentiated by their respective size in the FSC/SSC plot (data not shown).

RNA expression analyses and ELISA

The microarray data[12] is accessible in the Gene Expression Omnibus database (accession number GSE54181). Plots were generated using the webtool R2: microarray analysis and visualization platform (http://r2.amc.nl).

Total RNA was isolated using the NucleoSpin RNA II kit (Machery-Nagel, Leiden, The Netherlands) according to the manufacturer's instructions. Total RNA (0.5 – 1.0 µg) was reverse transcribed using the SuperScript III First Strand synthesis system from Invitrogen. TaqMan PCR was performed using TaqMan Universal PCR Master Mix and pre-designed, pre-optimized primers and probe mix for CCL2, RANTES (CCL5), IL8 (CXCL8), CXCL9 and GAPDH (Applied Biosystems, Foster City, USA). Threshold cycle numbers (Ct) were determined using the CFX PCR System (BioRad, Veenendaal, The Netherlands) and the relative quantities of cDNA per sample were calculated using the ΔΔCt method using GAPDH as the calibrator gene.

ELISA's for CCL2, RANTES, IL8 and CXCL9 were performed according to the manufacturer's instruction (PeproTech, London, United Kingdom).

Flow cytometry

Expression of EGFR on keratinocytes was analyzed by flow cytometry using PE-coupled Mouse-anti-human EGFR (1:20, BD Biosciences, Breda, The Netherlands). Per live gate, 50.000 cells were recorded using the BD FACS Calibur with Cellquest software (BD Bioscience) and data were analyzed using Flowjo (Treestar, Olten, Switzerland).

Western blot analysis

For Western blotting, polypeptides were resolved by SDS–polyacrylamide gel electrophoresis (SDS–PAGE) and transferred to a nitrocellulose membrane (Bio-Rad, Veenendaal, The Netherlands). Immunodetection was achieved with anti-p65 (1:1000, sc-372, Santa Cruz), anti-phospho-p65 (Ser536; 1:1000, #3033 Cell Signaling Technology (CST)), anti-acetyl-p65 (Lys310; 1:1000, #3045 CST), anti-IFRD1 (1:400, T2576 Sigma-Aldrich), β-actin (1:10,000, Sigma-Aldrich) primary antibodies, and HRP-coupled anti-mouse (1:5000; CST) and HRP-coupled anti-rabbit (1:5000, CST) secondary antibodies. Chemoluminescence reagent (Bio-Rad) was used as substrate and signal was scanned using the Chemidoc and accompanying Software (Bio-Rad) to quantify the intensity of the bands as a measure of the amount of protein of interest in the blot. The relative amount was determined by calculating the ratio of each protein over that of the density measured for the housekeeping protein β-actin.

Immunohistochemistry

4 μm formalin fixed, paraffin embedded tissue sections from two random VIN cases were deparaffinised and rehydrated using graded concentrations of ethanol to distilled water. Endogenous peroxidise activity was blocked with 0.03% H_2O_2/MeOH for 20 minutes. Antigen retrieval was performed in boiling EDTA buffer (pH 9.0) for 12 minutes. After 2 hours of cooling down to RT, slides were washed twice in distilled water and twice in phosphate-buffered saline (PBS). Subsequently, incubation was performed overnight at room temperature with the primary IFRD1 antibody (T2576 Sigma-Aldrich; 1:500 in PBS containing 1% bovine serum albumin); p16 (CINTEC, diluted 1:5) and E2 (1:50) (provided by Dr. F. Thierry). Second, sections were incubated with BrightVision polyhorseradish peroxidase anti-mouse/rabbit/rat IgG (Immunologic BV, Duiven, The Netherlands) for 30 minutes at room temperature. Washing between incubations was performed 3 times for 5 minutes in PBS. Immune complexes were visualized by applying a 0.05M tris-HCl buffer (pH 7.6) containing 0.05% of 3,3′-diamino-benzidine-tetrahydrochloride and 0.0018% of H_2O_2. After 10 minutes, the reaction was stopped by rinsing with demineralised water. Finally, the tissue sections were counterstained with Mayer’s haematoxylin before addition of a cover slip.

Statistical analysis

Statistical analysis were performed using GraphPad InStat version 3.00. P-values were determined via Welch-corrected unpaired *t* tests. * $p<0.05$, ** $p<0.01$, *** $p<0.001$.

Conflict of interest

CM has received speaker honoraria from Merck, Quest Diagnostics, GSK, and Bristol-Myers. CM has performed research funded by Merck, The Phillip Morris External Research Program, NexMed, GSK, OriGenix, and Interferon Sciences Inc. Authors declare no other financial interests.

Author contributions

BT, RG, ESJ, CJMM, JMB and SHvdB designed the experiments. BT, RG, LPLP and ESJ performed the experiments. LPLP, EMGMvE and CM made viruses and cells. BT and SHvdB wrote the paper. CJMM, JMB and SHvdB supervised the project. All authors discussed the data.

Acknowledgements

This work was supported by the Netherlands Organization for Health Research (NOW/ZonMw) TOP grant 91209012. The funders had no role in study design, data collection and analysis, decision to publish, or preparation of the manuscript.

REFERENCES

1. *Doorbar, J. Molecular biology of human papillomavirus infection and cervical cancer. Clinical science 110, 525-541, doi:10.1042/CS20050369 (2006).*
2. *Frazer, I. H. Interaction of human papillomaviruses with the host immune system: a well evolved relationship. Virology 384, 410-414, doi:10.1016/j.virol.2008.10.004 (2009).*
3. *Karim, R. et al. Human papillomavirus deregulates the response of a cellular network comprising of chemotactic and proinflammatory genes. PloS one 6, e17848, doi:10.1371/journal.pone.0017848 (2011).*
4. *Richardson, H. et al. The natural history of type-specific human papillomavirus infections in female university students. Cancer epidemiology, biomarkers & prevention : a publication of the American Association for Cancer Research, cosponsored by the American Society of Preventive Oncology 12, 485-490 (2003).*
5. *van der Burg, S. H. & Melief, C. J. Therapeutic vaccination against human papilloma virus induced malignancies. Current opinion in immunology 23, 252-257, doi:10.1016/j.coi.2010.12.010 (2011).*
6. *zur Hausen, H. Papillomaviruses and cancer: from basic studies to clinical application. Nature reviews. Cancer 2, 342-350, doi:10.1038/nrc798 (2002).*
7. *Hasan, U. A. et al. TLR9 expression and function is abolished by the cervical cancer-associated human papillomavirus type 16. Journal of immunology 178, 3186-3197 (2007).*
8. *Karim, R. et al. Human papillomavirus (HPV) upregulates the cellular deubiquitinase UCHL1 to suppress the keratinocyte's innate immune response. PLoS pathogens 9, e1003384, doi:10.1371/journal.ppat.1003384 (2013).*
9. *Reiser, J. et al. High-risk human papillomaviruses repress constitutive kappa interferon transcription via E6 to prevent pathogen recognition receptor and antiviral-gene expression. Journal of virology 85, 11372-11380, doi:10.1128/JVI.05279-11 (2011).*
10. *Sunthamala, N. et al. E2 proteins of high risk human papillomaviruses down-modulate STING and IFN-kappa transcription in keratinocytes. PloS one 9, e91473, doi:10.1371/journal.pone.0091473 (2014).*
11. *Termini, L. et al. Characterization of global transcription profile of normal and HPV-immortalized keratinocytes and their response to TNF treatment. BMC medical genomics 1, 29, doi:10.1186/1755-8794-1-29 (2008).*
12. *Tummers, B. et al. CD40-Mediated Amplification of Local Immunity by Epithelial Cells Is Impaired by HPV. The Journal of investigative dermatology, doi:10.1038/jid.2014.262 (2014).*
13. *Chang, Y. E. & Laimins, L. A. Microarray analysis identifies interferon-inducible genes and*

Stat-1 as major transcriptional targets of human papillomavirus type 31. Journal of virology 74, 4174-4182 (2000).

14. *Hong, S., Mehta, K. P. & Laimins, L. A. Suppression of STAT-1 expression by human papillomaviruses is necessary for differentiation-dependent genome amplification and plasmid maintenance. Journal of virology 85, 9486-9494, doi:10.1128/JVI.05007-11 (2011).*
15. *Nees, M. et al. Papillomavirus type 16 oncogenes downregulate expression of interferon-responsive genes and upregulate proliferation-associated and NF-kappaB-responsive genes in cervical keratinocytes. Journal of virology 75, 4283-4296, doi:10.1128/JVI.75.9.4283-4296.2001 (2001).*
16. *Zhou, F., Chen, J. & Zhao, K. N. Human papillomavirus 16-encoded E7 protein inhibits IFN-gamma-mediated MHC class I antigen presentation and CTL-induced lysis by blocking IRF-1 expression in mouse keratinocytes. The Journal of general virology 94, 2504-2514, doi:10.1099/vir.0.054486-0 (2013).*
17. *Chen, L. F. & Greene, W. C. Shaping the nuclear action of NF-kappaB. Nature reviews. Molecular cell biology 5, 392-401, doi:10.1038/nrm1368 (2004).*
18. *Conway, M. J. & Meyers, C. Replication and assembly of human papillomaviruses. Journal of dental research 88, 307-317, doi:10.1177/0022034509333446 (2009).*
19. *McLaughlin-Drubin, M. E., Christensen, N. D. & Meyers, C. Propagation, infection, and neutralization of authentic HPV16 virus. Virology 322, 213-219, doi:10.1016/j.virol.2004.02.011 (2004).*
20. *Meyers, C., Mayer, T. J. & Ozbun, M. A. Synthesis of infectious human papillomavirus type 18 in differentiating epithelium transfected with viral DNA. Journal of virology 71, 7381-7386 (1997).*
21. *Lee, D., Lee, B., Kim, J., Kim, D. W. & Choe, J. cAMP response element-binding protein-binding protein binds to human papillomavirus E2 protein and activates E2-dependent transcription. The Journal of biological chemistry 275, 7045-7051 (2000).*
22. *Quinlan, E. J., Culleton, S. P., Wu, S. Y., Chiang, C. M. & Androphy, E. J. Acetylation of conserved lysines in bovine papillomavirus E2 by p300. Journal of virology 87, 1497-1507, doi:10.1128/JVI.02771-12 (2013).*
23. *Gu, Y. et al. Identification of IFRD1 as a modifier gene for cystic fibrosis lung disease. Nature 458, 1039-1042, doi:10.1038/nature07811 (2009).*
24. *Micheli, L. et al. PC4/Tis7/IFRD1 stimulates skeletal muscle regeneration and is involved in myoblast differentiation as a regulator of MyoD and NF-kappaB. The Journal of biological chemistry 286, 5691-5707, doi:10.1074/jbc.M110.162842 (2011).*
25. *Xue, Y. et al. HPV16 E2 is an immediate early marker of viral infection, preceding E7 expression in precursor structures of cervical carcinoma. Cancer research 70, 5316-5325,*

doi:10.1158/0008-5472.CAN-09-3789 (2010).

26. *von Knebel Doeberitz, M., Gissmann, L. & zur Hausen, H. Growth-regulating functions of human papillomavirus early gene products in cervical cancer cells acting dominant over enhanced epidermal growth factor receptor expression. Cancer research 50, 3730-3736 (1990).*
27. *Vietor, I. & Huber, L. A. Role of TIS7 family of transcriptional regulators in differentiation and regeneration. Differentiation; research in biological diversity 75, 891-897, doi:10.1111/j.1432-0436.2007.00205.x (2007).*
28. *Kim, M. K. et al. Human papillomavirus type 16 E5 oncoprotein as a new target for cervical cancer treatment. Biochemical pharmacology 80, 1930-1935, doi:10.1016/j.bcp.2010.07.013 (2010).*
29. *Bruzzese, F. et al. HDAC inhibitor vorinostat enhances the antitumor effect of gefitinib in squamous cell carcinoma of head and neck by modulating ErbB receptor expression and reverting EMT. Journal of cellular physiology 226, 2378-2390, doi:10.1002/jcp.22574 (2011).*
30. *Liu, N. et al. Blocking the class I histone deacetylase ameliorates renal fibrosis and inhibits renal fibroblast activation via modulating TGF-beta and EGFR signaling. PloS one 8, e54001, doi:10.1371/journal.pone.0054001 (2013).*
31. *Heusinkveld, M. et al. M2 macrophages induced by prostaglandin E2 and IL-6 from cervical carcinoma are switched to activated M1 macrophages by CD4+ Th1 cells. Journal of immunology 187, 1157-1165, doi:10.4049/jimmunol.1100889 (2011).*
32. *Feng, W., Duan, X., Liu, J., Xiao, J. & Brown, R. E. Morphoproteomic evidence of constitutively activated and overexpressed mTOR pathway in cervical squamous carcinoma and high grade squamous intraepithelial lesions. International journal of clinical and experimental pathology 2, 249-260 (2009).*
33. *Kalinowski, A. et al. EGFR activation suppresses respiratory virus-induced IRF1-dependent CXCL10 production. American journal of physiology. Lung cellular and molecular physiology 307, L186-196, doi:10.1152/ajplung.00368.2013 (2014).*
34. *Mascia, F., Mariani, V., Girolomoni, G. & Pastore, S. Blockade of the EGF receptor induces a deranged chemokine expression in keratinocytes leading to enhanced skin inflammation. The American journal of pathology 163, 303-312, doi:10.1016/S0002-9440(10)63654-1 (2003).*
35. *Paul, T. et al. Cytokine regulation by epidermal growth factor receptor inhibitors and epidermal growth factor receptor inhibitor associated skin toxicity in cancer patients. European journal of cancer 50, 1855-1863, doi:10.1016/j.ejca.2014.04.026 (2014).*
36. *Pastore, S. et al. ERK1/2 regulates epidermal chemokine expression and skin inflammation. Journal of immunology 174, 5047-5056 (2005).*
37. *Vandermark, E. R. et al. Human papillomavirus type 16 E6 and E 7 proteins alter NF-*

kB in cultured cervical epithelial cells and inhibition of NF-kB promotes cell growth and immortalization. Virology 425, 53-60, doi:10.1016/j.virol.2011.12.023 (2012).

38. *Caberg, J. H. et al. Increased migration of Langerhans cells in response to HPV16 E6 and E7 oncogene silencing: role of CCL20. Cancer immunology, immunotherapy : CII 58, 39-47, doi:10.1007/s00262-008-0522-5 (2009).*
39. *Havard, L., Rahmouni, S., Boniver, J. & Delvenne, P. High levels of p105 (NFKB1) and p100 (NFKB2) proteins in HPV16-transformed keratinocytes: role of E6 and E7 oncoproteins. Virology 331, 357-366, doi:10.1016/j.virol.2004.10.030 (2005).*
40. *Avvakumov, N., Torchia, J. & Mymryk, J. S. Interaction of the HPV E7 proteins with the pCAF acetyltransferase. Oncogene 22, 3833-3841, doi:10.1038/sj.onc.1206562 (2003).*
41. *Bernat, A., Avvakumov, N., Mymryk, J. S. & Banks, L. Interaction between the HPV E7 oncoprotein and the transcriptional coactivator p300. Oncogene 22, 7871-7881, doi:10.1038/sj.onc.1206896 (2003).*
42. *Huang, S. M. & McCance, D. J. Down regulation of the interleukin-8 promoter by human papillomavirus type 16 E6 and E7 through effects on CREB binding protein/p300 and P/CAF. Journal of virology 76, 8710-8721 (2002).*
43. *Spitkovsky, D., Hehner, S. P., Hofmann, T. G., Moller, A. & Schmitz, M. L. The human papillomavirus oncoprotein E7 attenuates NF-kappa B activation by targeting the Ikappa B kinase complex. The Journal of biological chemistry 277, 25576-25582, doi:10.1074/jbc.M201884200 (2002).*
44. *Hasan, U. A. et al. The human papillomavirus type 16 E7 oncoprotein induces a transcriptional repressor complex on the Toll-like receptor 9 promoter. The Journal of experimental medicine 210, 1369-1387, doi:10.1084/jem.20122394 (2013).*
45. *Bodily, J. M., Mehta, K. P. & Laimins, L. A. Human papillomavirus E7 enhances hypoxia-inducible factor 1-mediated transcription by inhibiting binding of histone deacetylases. Cancer research 71, 1187-1195, doi:10.1158/0008-5472.CAN-10-2626 (2011).*
46. *Hiscott, J., Nguyen, T. L., Arguello, M., Nakhaei, P. & Paz, S. Manipulation of the nuclear factor-kappaB pathway and the innate immune response by viruses. Oncogene 25, 6844-6867, doi:10.1038/sj.onc.1209941 (2006).*
47. *Le Negrate, G. Viral interference with innate immunity by preventing NF-kappaB activity. Cellular microbiology 14, 168-181, doi:10.1111/j.1462-5822.2011.01720.x (2012).*
48. *Ning, Z. et al. The N terminus of orf virus-encoded protein 002 inhibits acetylation of NF-kappaB p65 by preventing Ser(276) phosphorylation. PloS one 8, e58854, doi:10.1371/journal.pone.0058854 (2013).*
49. *Granja, A. G., Sabina, P., Salas, M. L., Fresno, M. & Revilla, Y. Regulation of inducible nitric oxide synthase expression by viral A238L-mediated inhibition of p65/RelA acetylation and p300 transactivation. Journal of virology 80, 10487-10496, doi:10.1128/JVI.00862-06 (2006).*

SUPPLEMENTARY INFORMATION

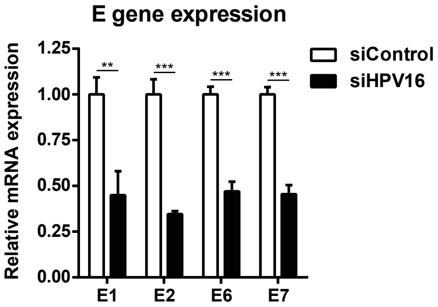

Figure S1: HPV16 E gene expression after HPV16 knock-down in HPV16+ KCs
E1, E2, E6 and E7 expression in HFK16 cells transfected with siControl or siHPV16.
*Error bars indicate SD. P-values were determined via Welch-corrected unpaired t tests. ** p<0.01, *** p<0.001*

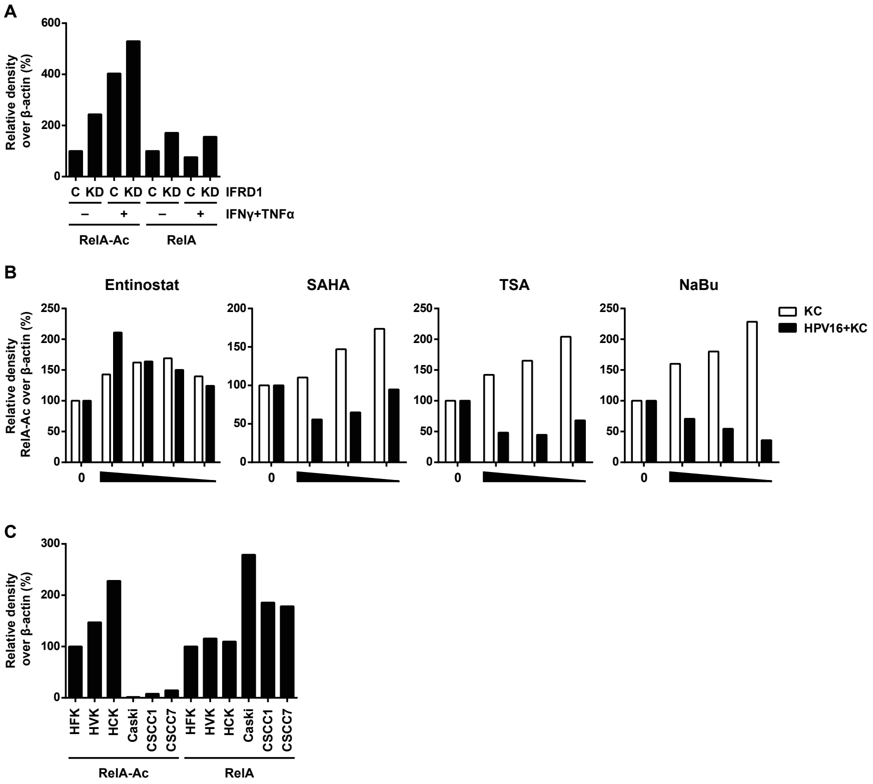

Figure S2: Western blot quantifications of RelA acetylation

(A) Quantified protein levels of RelA K310 acetylation and RelA over β-Actin in 24 hours non- or IFNγ and TNFα-stimulated control or

IFRD1 knock-down (KD) HPV16+ KCs. The expression levels of the control-treated HPV16+ KCs were set as 100%.

(B) Quantified protein levels of RelA K310 acetylation over β-Actin in KCs and HPV16+ KCs treated with decreasing doses of

entinostat (40, 20, 10 and 2 µM), SAHA (10, 5 and 1 µM), TSA (5, 1 and 0.333 µM) or NaBu (10, 5 and 1 mM) (western blot Figure 4A).

The expression levels of the control-treated HPV16+ KCs were set as 100%.

(C) Quantified protein levels of RelA K310 acetylation and RelA over β-Actin in in three KC donors and three HPV16-induced CxCa lines.

The expression levels of the HFK were set as 100%.

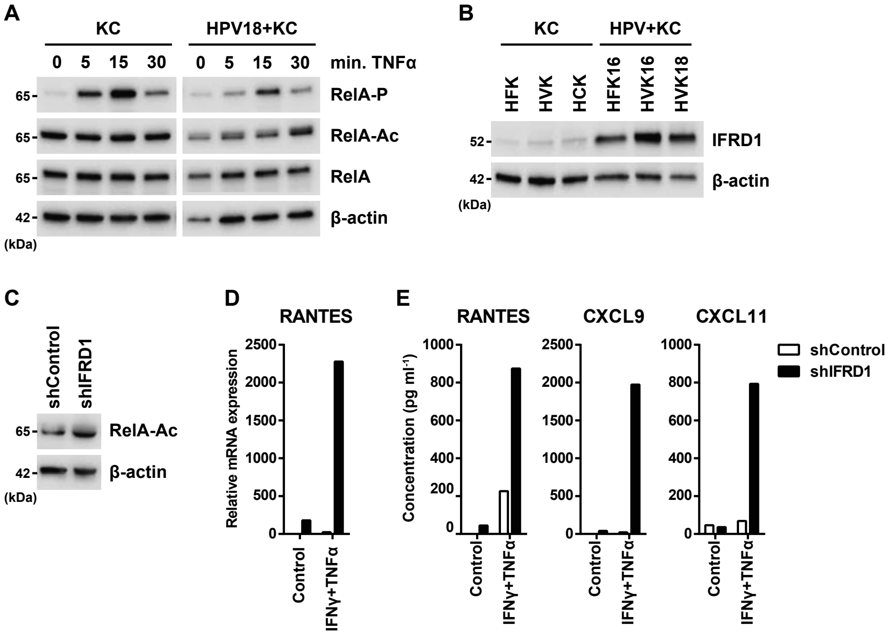

Figure S3: RelA acetylation, IFRD1 expression and IFRD1 knock-down effects in HPV18+ KCs

(A) RelA phosphorylation, acetylation and total levels in KCs and HPV18+ KCs stimulated with TNFα for 0, 5, 15 and 30 minutes.

(B) IFRD1 levels in three KC donor pools, two HPV16+ KC lines and one HPV18+ KC line.

(C) RelA acetylation levels in control or IFRD1 knock-down HPV18+ KCs.

(D) RT-qPCR of RANTES expression in 24 hours non- or IFNγ and TNFα-stimulated control or IFRD1 knock-down HPV18+ KCs.

(E) ELISA for RANTES, CXCL9 and CXCL11 in cleared supernatants of 24 hours non- or IFNγ and TNFα-stimulated control or IFRD1 knock-down HPV18+ KCs.

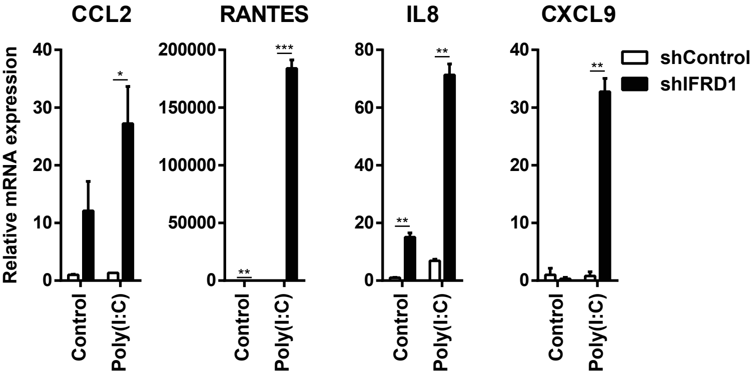

Figure S4: IFRD1 impairs Poly(I:C)-induced cytokine expression
RT-qPCR of CCL2, RANTES, IL8 and CXCL9 expression in 24 hours non- or Poly(I:C)-stimulated control or IFRD1 knock-down HPV16+ KCs.
*These data are representative for at least two independent experiments. Error bars indicate SD. P-values were determined via Welch-corrected unpaired t tests. * p<0.05, ** p<0.01, *** p<0.001.*

Figure S5: The effects of IFRD1 knock-down, anti-EGFR and entinostat on CSCC1

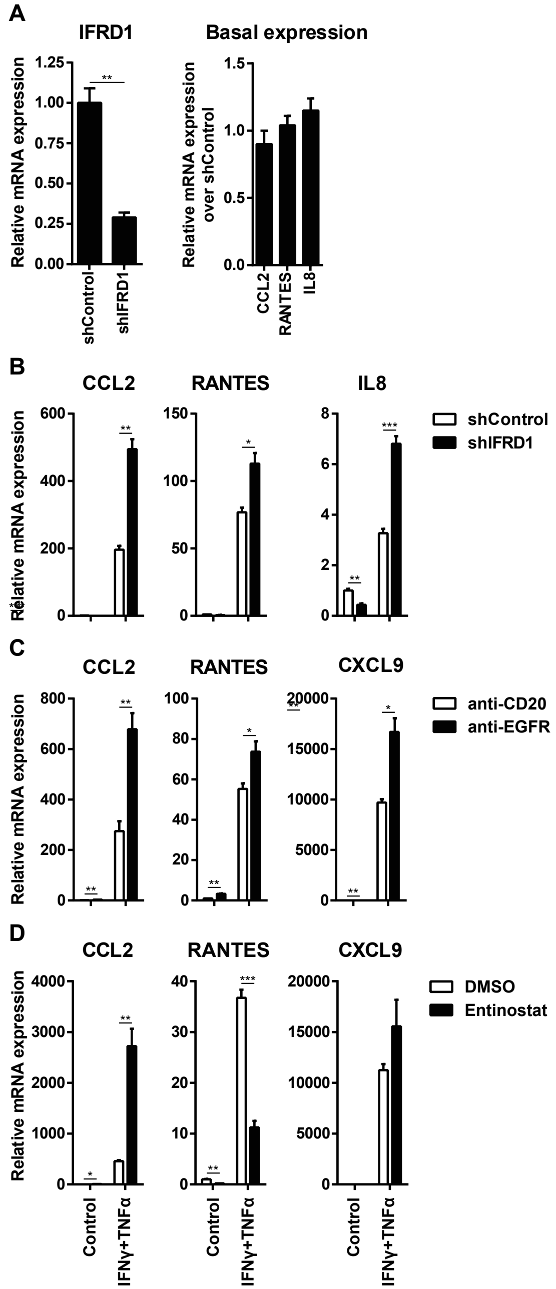

(A) RT-qPCR of IFRD1, CCL2, RANTES, IL8 and CXCL9 expression in steady-state control or IFRD1 knock-down CSCC1 cells.

(B) RT-qPCR of CCL2, RANTES and IL8 expression in 24 hours non- or IFNγ and TNFα-stimulated control or IFRD1 knock-down CSCC1 cells.

(C) RT-qPCR of CCL2, RANTES and CXCL9 expression in 24 hours non- or IFNγ and TNFα-stimulated anti-CD20 or anti-EGFR-treated CSCC1 cells.

(D) RT-qPCR of CCL2, RANTES and CXCL9 expression in 24 hours non- or IFNγ and TNFα-stimulated DMSO (control) or entinostat-treated CSCC1 cells.
These data are representative for at least two independent experiments. Error bars indicate SD. P-values were determined via Welch-corrected unpaired t tests.
** $p<0.05$, ** $p<0.01$, *** $p<0.001$.*

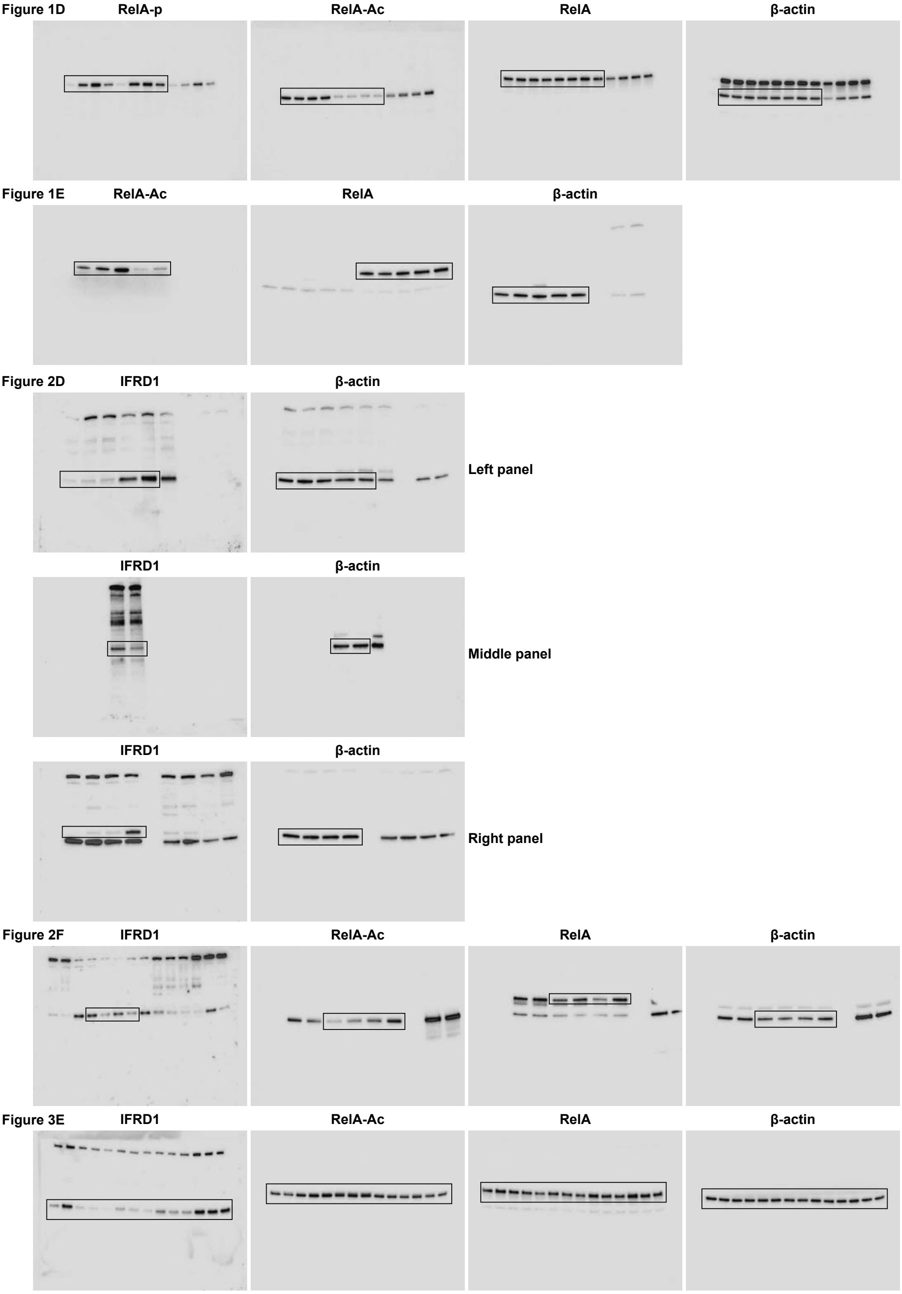
Figure 1D
RelA-p
RelA-Ac
RelA
β-actin
Figure 1E
RelA-Ac
RelA
β-actin
Figure 2D
IFRD1
β-actin
Left panel
IFRD1
β-actin
Middle panel
IFRD1
β-actin
Right panel
Figure 2F
IFRD1
RelA-Ac
RelA
β-actin
Figure 3E
IFRD1
RelA-Ac
RelA
β-actin

Figure S6: Full Western Blot data

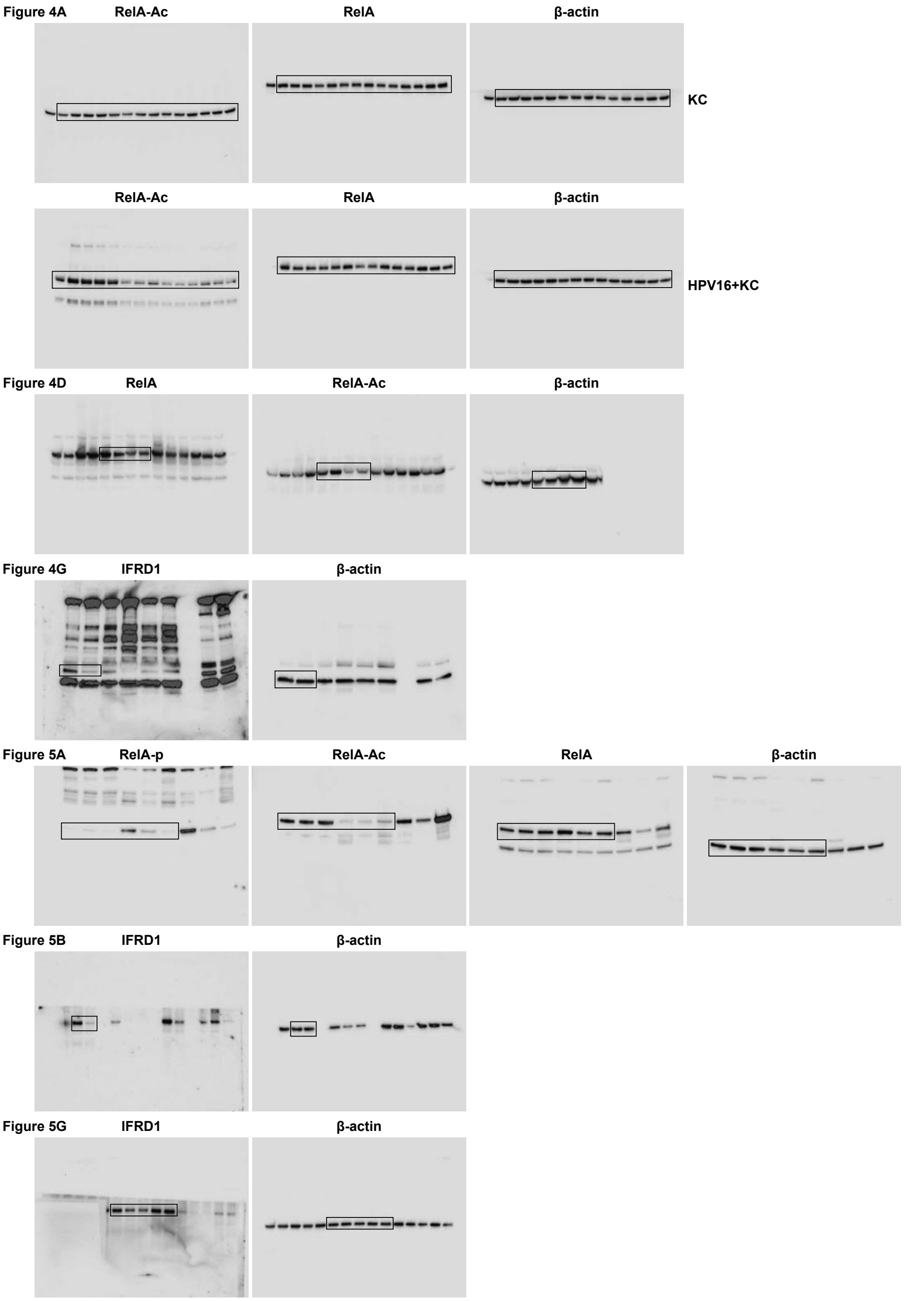
Figure 4A
RelA-Ac
RelA
β-actin
KC
RelA-Ac
RelA
β-actin
HPV16+KC
Figure 4D
RelA
RelA-Ac
β-actin
Figure 4G
IFRD1
β-actin
Figure 5A
RelA-p
RelA-Ac
RelA
β-actin
Figure 5B
IFRD1
β-actin
Figure 5G
IFRD1
β-actin

Figure S6: Full Western Blot data *Continued*

Supplementary Figure 3A

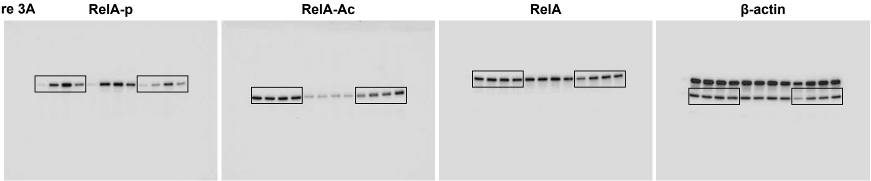
RelA-p
RelA-Ac
RelA
β-actin

Supplementary Figure 3B

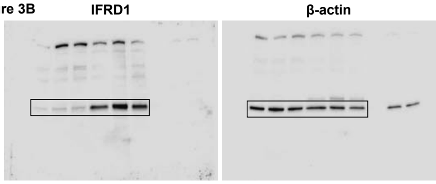
IFRD1
β-actin

Supplementary Figure 3C

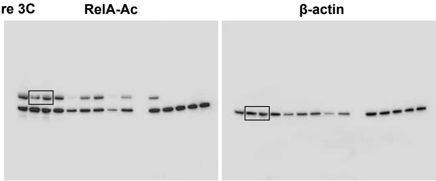
RelA-Ac
β-actin

Figure S6: Full Western Blot data *Continued*
The full blots for all Western blot pictures. Above the blot the used target is indicated. The black boxes represent the depicted parts of the blot.

5

Human papillomavirus (HPV) downregulates the expression of IFITM1 to resist the anti-proliferative effects of IFNγ and TNFα

Bart Tummers, Edith M.G. van Esch, Wenbo Ma, Renske Goedemans,
Laetitia P.L. Pelascini, Roser Vilarrasa-Blasi, Sofia Torreggiani, Craig Meyers,
Cornelis J.M. Melief, Judith M. Boer, Sjoerd H. van der Burg.

Submitted

ABSTRACT

Basal keratinocytes (KCs) are responsible for renewal of the epithelium and are the target cells for high risk human papilloma viruses (hrHPVs) which may cause KCs to become transformed. The immune system has developed means to counteract infections through several mechanisms, including the suppression of viral spread through the proliferation of infected cells via the production of the effector cytokines IFNγ and TNFα. These two cytokines are known to synergize in the suppression of KC proliferation. Using an unique system for freshly established or persistent hrHPV infection, we show that hrHPV renders KCs resistant to the growth inhibitory effects of these cytokines. Furthermore, a comparative analysis of marker expression for senescence (*GLB1*), apoptosis (*BAX* and *BCL2*) and proliferation (*RARRES1* and *PCNA*) showed that hrHPV specifically resists the induction of an anti-proliferative state induced by IFNγ in KCs. hrHPV accomplished this by targeting the expression of the anti-proliferative gene *IFITM1,* the expression of which was down-regulated already at 48 hours after hrHPV infection. Knock-down of *IFITM1* in uninfected KCs confirmed its role in providing resistance to the anti-proliferative effects of IFNγ and TNF, whereas the analysis of *IFITM1*, *RARRES1* and *PCNA* in cells isolated from clinical samples of HPV-positive and – negative (pre-)malignant vulvar cells underlined the relevance of our finding. Thus, our study revealed that hrHPV targets IFITM1 in order to evade the anti-proliferative effects of IFNγ and TNFα.

IMPORTANCE

A persistent infection with high-risk human papillomavirus (hrHPV) may cause cancer. In order to combat viruses the immune system has developed several mechanisms to counteract infections. One such a mechanism is the production of two cytokines, called interferon-gamma and tumor necrosis factor-alpha, which can prevent the proliferation of infected cells and as such can suppress viral spread. However, hrHPV has developed ways to evade the host's immune response for sustained periods of time. We showed that hrHPV accomplishes this by downregulating the expression of a negative regulator of cell growth called interferon-induced transmembrane protein 1 (IFITM1). When the cytokines of the immune system activate IFITM1 in non-infected cells a cellular program is started that stops cell proliferation. Downregulation of IFITM1, allows hrHPV infected cells to evade the anti-proliferative effects of the immune system on hrHPV-infected cells, thus promoting viral spread and the ability of hrHPV-induced lesions to progress.

INTRODUCTION

High-risk human papillomaviruses (hrHPVs) infect undifferentiated keratinocytes (KCs) of squamous epithelia. Persistent infections may lead to cancers of the anogenital region as well as of the head and neck [1]. Studies in healthy individuals, immunosuppressed patients and in patients with spontaneously or vaccine-induced regressions revealed an important role for a strong type 1 (IFNγ and TNFα)-associated HPV early antigen-specific T cell response in the control of HPV [2].

IFNγ is a pleiotropic cytokine that affects immune regulation, immune surveillance, inflammation, tumor suppression, and has antiviral as well as anti-proliferative properties. Binding of IFNγ to its receptor (IFNγR) leads to JAK1/2-mediated STAT1 phosphorylation, dimerization and nuclear translocation, resulting in interferon-stimulated gene expression [3]. TNFα also regulates immune and cell death mechanisms. It activates NFκB and MAP kinase pathways and induces the formation of cell death complexes [4]. hrHPV attenuates immune signalling of the STAT1 [5-8], IRF and NFκB pathways [9-15], resulting in suppressed innate and adaptive antiviral responses.

IFNγ and TNFα are known to synergize in the suppression of KC proliferation [16]. IFNγ induces growth arrest and differentiation [17,18]. TNFα also induces growth arrest but there are conflicting data concerning its capacity to induce cell death of primary KCs [16,19]. In unstimulated KCs, HPV can regulate cell growth via its early (E) proteins. E6 and E7 promote proliferation by directly modulating p53 and p21, however, their expression is regulated by E2, which can also induce apoptosis. E5 can both protect and induce apoptosis. E1^E4 expression results in growth arrest [20,21]. Previously, it was shown that retrovirus-mediated expression of E6 and/or E7 in KCs resulted in downregulation of IFNγ responsive genes and the upregulation of genes associated with cellular proliferation [7,22]. However, the ability of HPV-infected KCs to resist the effects of IFNγ and/or TNFα on proliferation as well as the underlying mechanisms are not well understood.

In this study, we analyzed the influence of HPV on the IFNγ and TNFα-mediated cell growth inhibition of KCs by functional and biochemical analyses. Here we show that hrHPV presence renders KCs more resistant to the anti-proliferative effects of IFNγ and TNFα, via the downregulation of *IFITM1.* Ex-vivo analysis of KCs isolated from clinically obtained control tissue and HPV-induced (pre)malignancies of the vulva confirmed our observations *in situ*.

RESULTS

HPV hampers the anti-proliferative state of KCs upon IFNγ and/or TNFα treatment

We previously reported that hrHPV suppresses the IFNγ and TNFα-induced immune response of KCs. Since IFNγ and TNFα are also known to synergize in the suppression of KC proliferation by inducing growth arrest and differentiation [16-19], we studied the influence of HPV herein. First, our previously reported validated microarray, in which uninfected KCs of four different donors and four different hrHPV-infected KCs were pre-stimulated with IFNγ for 72 hours, and subsequently treated with control or IFNγ for another 24 hours [15], was re-analysed for gene expression of markers indicative for apoptosis, senescence, or proliferation (Figure 1A). Genes indicative for apoptosis (*BAX, BCL2*) and senescence (*GLB1, RGN*) were not differentially expressed, whereas genes indicative for anti-proliferation (*RARRES1*, *SAMD9L*, *TOB1*) were downregulated and pro-proliferative genes (*MCM2*, *MKI67*, *MT1A*, *PCNA*) upregulated in hrHPV+ KCs compared to KCs after stimulation.

To validate the microarray data and investigate the additive role of TNFα, KCs and HPV+ KCs were harvested after 24 hours of IFNγ and TNFα stimulation and the gene expression of markers indicative for apoptosis, senescence, or proliferation were determined by RT-qPCR (Figure 1B). In this setting, uninfected KCs displayed a slight increase in the expression of the senescence marker beta-Galactosidase (*GLB1*), a strong reduction in the expression of the anti-apoptosis marker *BCL2* while the expression level of *BAX* was marginally affected (Figure 1B). Importantly, this analysis confirmed the anti-proliferative state of IFNγ- and TNFα-stimulated KCs since the expression level of *RARRES1*, a marker for anti-proliferation [23,24], was highly upregulated and in parallel, the level of the proliferation marker *PCNA* was decreased.

In hrHPV-positive KCs, the expression levels of *BCL2, GLB1* and *BAX* mirrored that of non-infected KCs, albeit that the basal level of the anti-apoptotic gene *BCL2* was lower in hrHPV+ KCs. Analysis of the genes involved in proliferation revealed that the basal levels of *PCNA* were higher in hrHPV-positive KCs than in uninfected KCs. In contrast to non-infected KCs stimulated with IFNγ and/or TNFα, the hrHPV+ KCs displayed only a marginal

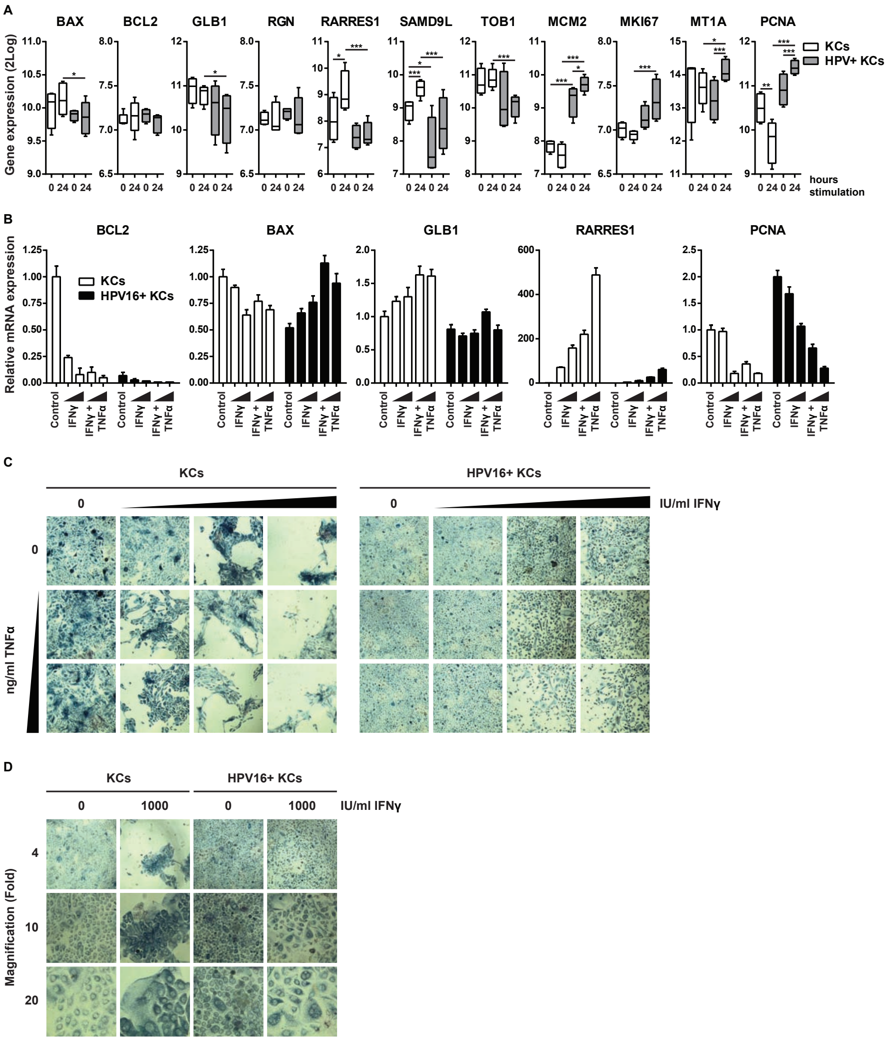

Figure 1: hrHPV resists IFNγ and TNFα-induced growth inhibition
*(A) Microarray intensities for BAX, BCL2, GLB1, RGN, RARRES1, SAMD9L, TOB1, MCM2, MKI67, MT1A and PCNA in 72 hours IFNγ (50 IU/ml) pre-treated four independent KCs and four independent hrHPV+ KCs, stimulated with IFNγ (50 IU/ml) for 0 or 24 hours, represented in a box plot. The box contains the 1st quartile up to the 3rd quartile, the median is represented as a line, whiskers represent the values of the outer 2 quartiles. * p<0.05, ** p<0.01, *** p<0.001.*
(B) RT-qPCR of BCL2, BAX, GLB1, RARRES1 and PCNA in 24 hours Control, IFNγ (50 or 250 IU/ml) or IFNγ and TNFα (50 IU/ml IFNγ + 50 ng/ml TNFα or 250 IU/ml IFNγ + 250 ng/ml TNFα)-treated KCs and HPV16+ KCs. Gene expression was normalized using GAPDH as the calibrator gene. Fold changes over control-stimulated undifferentiated KCs were calculated and depicted.

(C) Microscopy pictures (4x magnification) of 72 hours IFNγ (0, 50, 250 or 1000 IU/ml) and/or TNFα (0, 50 or 250 ng/ml)-treated KCs and HPV16+ KCs.
(D) Microscopy pictures (4x, 10x and 20x magnifications) of 72 hours IFNγ-treated KCs and HPV16+ KCs.
Representative results of three independent experiments.

increase in *RARRES1* expression and the levels of *PCNA* were only reduced to the levels observed in uninfected KCs upon stimulation with a combination of the highest doses of IFNγ and TNFα.

To confirm that hrHPV-positive KCs are indeed less sensitive to the IFNγ and/or TNFα-induced arrest in proliferation, uninfected KCs and hrHPV-positive KCs, seeded into 96 well plates, were treated for four days with increasing doses of IFNγ and/or TNFα. Cell confluence was monitored by phase-contrast microscopy as a measure of proliferation since we and others [25] had observed that KC proliferation can not be quantified via usual proliferation assays (data not shown). As expected, the growth of uninfected KCs was greatly affected by increasing doses of IFNγ. In contrast, hrHPV-positive KCs were much more resistant (Figure 1C). TNFα in itself appeared not to affect the growth of uninfected or HPV-infected KCs, but when combined with IFNγ augmented the reduction in cell density (Figure 1C). We observed that the remaining KCs after treatment displayed a senescence-like morphology [26] following IFNγ stimulation (Figure 1D), fitting well with the upregulated expression of *GLB1* in the uninfected KCs. All together, these data confirm that IFNγ or IFNγ and TNFα affect the growth of uninfected KCs by arresting their proliferation and skewing them to a senesced, pro-apoptotic state. Moreover, our data clearly indicate that hrHPV alters the IFNγ and TNFα-regulated proliferative pathway in KCs by resisting the induction a proliferative arrest.

HPV downregulates the expression of IFITM1

The interferon-induced transmembrane protein 1 (IFITM1) plays an essential role in the anti-proliferative action of IFNγ [27], making it a potential target for hrHPV. Indeed, re-analysis of the data from one of our earlier validated microarrays, in which the basal expression of genes measured in different uninfected and hrHPV infected KCs was compared [28], showed that *IFITM1* expression is downregulated in HPV-positive KCs (Figure 2A).

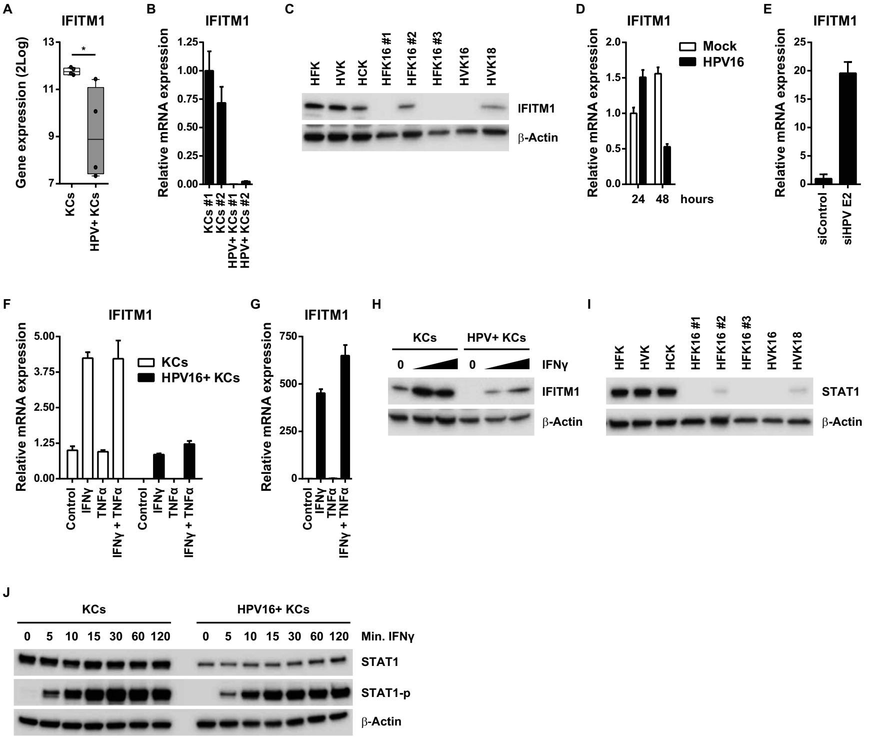

Figure 2: HPV downregulates IFITM1 expression
*(A) Microarray intensities for IFITM1 in four independent KCs and four independent hrHPV+ KCs represented in a box plot. The box contains the 1st quartile up to the 3rd quartile, the median is represented as a line, whiskers represent the values of the outer 2 quartiles. * p<0.05.*
(B) RT-qPCR of IFITM1 expression in two independent KCs and two independent HPV16+ KCs cultures.
(C) Western blot of IFITM1 protein levels in three independent KC, four independent HPV16+ KC, and one HPV18+ KC cultures.
RT-qPCR of IFITM1 expression in KCs infected with mock or HPV16 for 1 or 2 days, as indicated (D), and siControl and siHPV16 E2-transfected HPV16+ KCs (E).
(F) RT-qPCR of IFITM1 expression in 24 hours IFNγ (50 IU/ml) and/or TNFα (50 ng/ml)-stimulated KCs and HPV16+ KCs. Fold changes over control-stimulated undifferentiated KCs were calculated and depicted.
(G) RT-qPCR of IFITM1 expression in 24 hours IFNγ (50 IU/ml) and/or TNFα (50 ng/ml)-stimulated HPV16+ KCs. Fold changes over control-stimulated HPV16+ KCs were calculated and depicted.
(H) IFITM1 protein levels in KC and HPV18+ KC stimulated with IFNγ (0, 100 or 1000 IU/ml).
(I) STAT1 protein levels in three independent KC, four independent HPV16+ KC, and one HPV18+ KC cultures.
(J) STAT1 and phosphorylated STAT1 protein levels in KCs and HPV16+ KCs stimulated with IFNγ (50 IU/ml) as indicated.

Representative results of at least two independent experiments.

This was confirmed by RT-qPCR (Figure 2B) and western blot (Figure 2C) in different independent hrHPV-positive primary KC cultures. To show that the expression of *IFITM1* was genuinely altered by the presence of hrHPV in KCs, undifferentiated KCs were infected with native HPV16 virions resulting in a reduced expression of *IFITM1* two days after infection (Figure 2D). Reciprocally, the knock-down of total HPV16 early gene expression by introduction of siRNA against HPV16 E2 in HPV-positive KCs [14], resulted in the upregulation of *IFITM1* (Figure 2E).

IFNγ induces *de novo* synthesis of *IFITM1* for which STAT1 is required [29-32]. Indeed, IFNγ stimulation of uninfected KCs resulted in approximately 4-fold increase in *IFITM1* after 24 hours (Figure 2F). Strikingly, IFNγ stimulation of hrHPV+ KCs resulted in a much stronger relative increase of *IFITM1* levels (Figure 2G), albeit that these levels still remained lower than those measured in uninfected KCs (Figure 2F). IFITM1 protein levels in IFNγ-stimulated KCs and hrHPV+ KCs confirmed the gene expression data (Figure 2H). These data indicated that hrHPV predominantly regulates the expression of *IFITM1* at the basal level but less at the level of IFNγ-mediated induction of *IFITM1* gene expression. It has been reported that HPV can lower *STAT1* mRNA and protein levels in KCs [5-8], and this was also detected in the hrHPV+ KCs analyzed at the protein level (Figure 2I). Interestingly, the HPV+ KCs with the highest basal IFITM1 protein expression (Figure 2C) also showed the highest STAT1 levels (Figure 2I). Concomitant with the induction of *IFITM1* expression, IFNγ stimulation also stimulated the phosphorylation of STAT1 (Figure 2J). Together this indicates that HPV represses the basal levels of STAT1 but does not interfere with STAT1 signalling in our persistently hrHPV infected KCs. Furthermore, it explains why IFNγ is able to stimulate the expression of *IFITM1*. TNFα did not influence *IFITM1* expression (Figure 2F-G).

IFITM1 downregulation helps to overcome the anti-proliferative effects of IFNγ and TNFα

To study the effects of IFITM1 on KC proliferation in a setting where all additional influences of HPV are ruled out [20,21], *IFITM1* was knocked-down in uninfected KCs (Figure 3A). The KCs were stimulated with IFNγ or a combination of IFNγ and TNFα. *IFITM1* knock-down KCs displayed a less pronounced downregulation of *BCL2* and *PCNA* upon IFNγ stimulation

(Figure 3B). The expression of *RARRES1* was lower at the basal level when *IFITM1* was knocked-down and its IFNγ-induced expression was only affected when KCs were stimulated with a low but not with a higher concentration of IFNγ. Importantly, *IFITM1* knock-down KCs were more resistant to the anti-proliferative effects of IFNγ and the combination of IFNγ and TNFα than control shRNA and non-transduced KCs (Figure 3C).

Thus, HPV is able to resist IFNγ-mediated arrest of proliferation by lowering the basal levels of *IFITM1*.

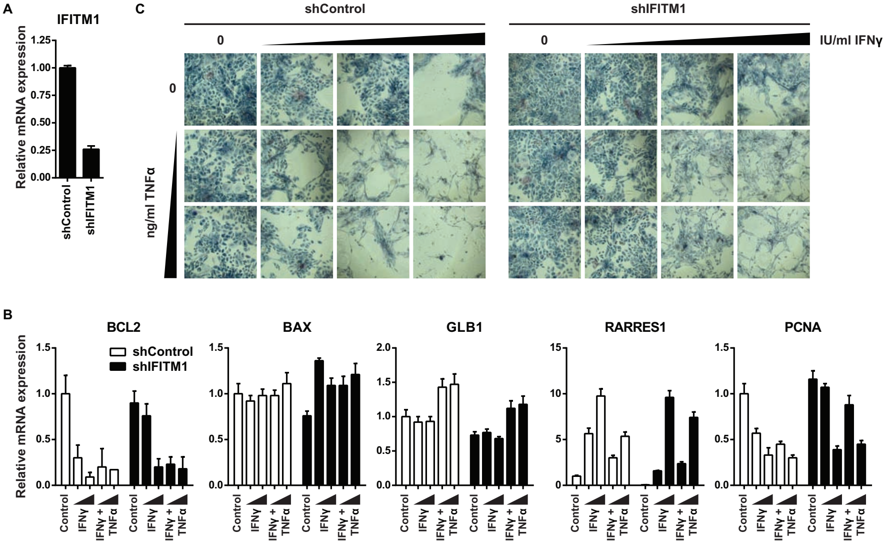

Figure 3: IFITM1 downregulation helps to overcome the anti-proliferative effects of IFNγ and TNFα

(A) RT-qPCR of IFITM1 expression in control and IFITM1 knock-down KCs.

(B) RT-qPCR of BCL2, BAX, GLB1, RARRES1 and PCNA in 24 hours Control, IFNγ (50 or 250 IU/ml) or IFNγ and TNFα (50 IU/ml IFNγ + 50 ng/ml TNFα or 250 IU/ml IFNγ + 250 ng/ml TNFα)-treated control and IFITM1 knock-down KCs.

(C) Microscopy pictures (4x magnification) of 72 hours IFNγ (0, 50, 250 or 1000 IU/ml) and/or TNFα (0, 50 or 250 ng/ml)-treated control and IFITM1 knock-down KCs.

Representative results of three independent experiments.

IFITM1 expression is down in HPV-induced premalignant and malignant vulvar cells.

In order to study the relevancy of these results we analysed the five genetic markers for apoptosis, senescence and proliferation in cells isolated from clinical biopsies taken from women suffering from different stages of HPV-induced (pre)malignancies. The isolated cells were treated with 0 or 100 IU/ml IFNγ for 24 hours and gene expression was analyzed by RT-qPCR. Basal *IFITM1* expression was lower in the cells isolated from a HPV16-induced vulvar intraepithelial neoplasia (VIN) and a HPV16-induced vulvar carcinoma when compared to that in the KCs obtained from control tissue or an HPV-negative vulvar carcinoma (Figure 4A). The levels of *GLB1* and *BAX* were similar between control and HPV16+ vulvar cells, both at the basal level as after IFNγ stimulation. The expression of *BCL2* was lower in the HPV16+ vulvar cells than in controls, but similar to control KCs, the HPV16+ cells displayed a decreased *BCL2* expression upon stimulation with IFNγ (Figure 4B), albeit that control KCs show a stronger decrease. The levels of *PCNA* and *RARRES1* were similar in control cells and HPV16+ vulvar cells, however upon stimulation with IFNγ only the control cells showed a strong decrease in *PCNA* expression and a stronger increase in *RARRES1* when compared to the HPV16+ vulvar cells (Figure 4B). Interestingly, the cells isolated from an HPV-negative vulvar carcinoma reacted more or less similar as control cells, pointing out the HPV-specific component in these analyses. These results indicate that also *in situ* hrHPV+ cells display a reduced expression of *IFITM1* and a concomitant resistance to IFNγ-induced arrest of proliferation.

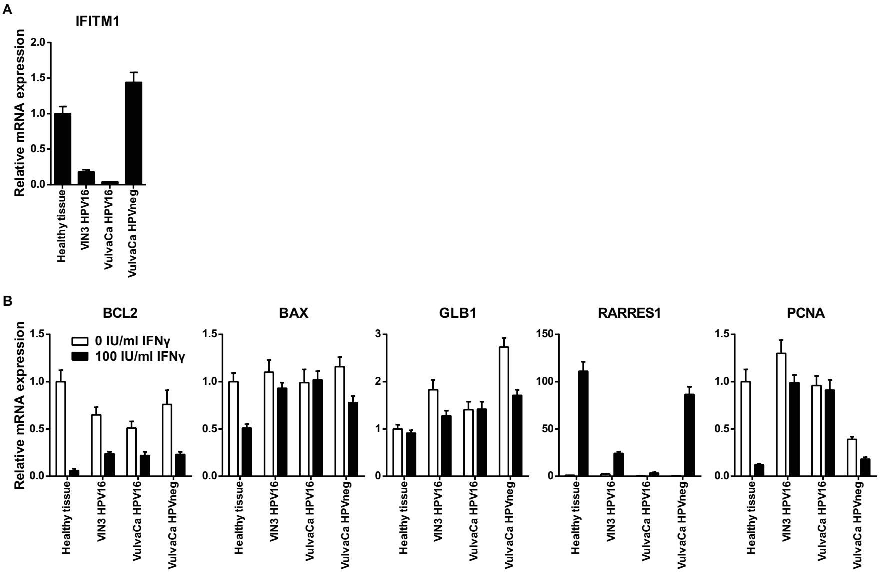

Figure 4: IFITM1 expression is decreased in HPV-induced VIN lesions
(A) RT-qPCR of IFITM1 expression in KCs derived from clinical biopts.
(B) RT-qPCR of BCL2, BAX, GLB1, RARRES1 and PCNA in 24 hours control or IFNγ (100 IU/ml)-stimulated KCs derived from clinical biopts.

DISCUSSION

Using a unique *in vitro* model we here show that hrHPV infection renders KCs resistant to IFNγ and TNFα-induced arrest of cell growth. Analysis of the expression of markers representative for senescence, apoptosis and proliferation of KCs showed that HPV specifically counteracts the arrest in cell proliferation of KCs when stimulated by IFNγ. The resistance of hrHPV+ cells to an IFNγ-mediated proliferative arrest was associated with a strong downregulation in the basal expression of the negative regulator of cell growth *IFITM1* and an impaired IFNγ-mediated increase in the expression of the anti-proliferative *RARRES1* gene. Notably, this basal and IFNγ-stimulated gene profile was also found *ex vivo*, in cells isolated from biopsies of HPV-induced (pre-)malignant vulvar lesions.

The IFNγ-induced increase in expression of both *IFITM1* and *RARRES1* depends on STAT1, which is downregulated by HPV E6 and E7 proteins [5-7]. Basal *IFITM1* expression is downregulated in HPV+ KCs, but *RARRES1* is not, which might be explained by the fact that the basal expression of *RARRES1* in uninfected KCs is already low. Our data confirm the hrHPV-mediated decrease in STAT1 protein levels but also show that hrHPV does not hamper IFNγ-induced STAT1 activation, as reflected by STAT1 phosphorylation and increase in *RARRES1* and *IFITM1* expression in HPV+ KCs. Still, as total STAT1 levels are lower in HPV+ KCs, the amount of available STAT1 to phosphorylate and signal is lower in hrHPV+ KCs potentially explaining why the increase in *RARRES1* and *IFITM1* expression does not reach the levels observed in uninfected KCs. This is also demonstrated in our study showing that the effect of *IFITM1* knock-down on proliferation of uninfected KCs does not resemble the influence of hrHPV on KCs. Whilst the effect of IFITM1 in uninfected KCs is apparent and anti-proliferative as indicated by the retained expression of *PCNA* and *RARRES1* in KCs stimulated with a low dose of IFNγ when *IFITM1* was knocked-down, clearly the downregulation of STAT1 as well as the positive growth signals as delivered by hrHPV [20,21] are missing in these cells. Hence differences in IFNγ-stimulated arrest of proliferation are less noticeable. Thus, whereas the decreased basal level of *IFITM1* is already providing resistance to the IFNγ-stimulated arrest of proliferation, the downregulation of STAT1 is likely to exaggerate this effect.

The downregulation of *IFITM1* clearly is advantageous to hrHPV as it allows infected KCs to expand. Mechanistically, IFITM1 inhibits the phosphorylation of ERK and thus regulates mitogen-activated protein (MAP) kinase signalling [27]. Furthermore, IFITM1 mediates the dephosphorylation of p53 at Thr55 resulting in increased p53 stability and transcriptional activity, as indicated by the upregulated expression of p21. Consequently, arrest occurs in cell cycle progression at the G1 phase and, hence, a halt in proliferation [27]. This is also reflected by the retained *PCNA* expression when *IFITM1* was knocked-down in low dose IFNγ-stimulated KCs. Conceivably, the effect of hrHPV on *IFITM1* in infected KCs extents to HPV-induced cancer cells as we found that cells isolated from an HPV16-induced vulvar tumor, but not cells isolated from a non-HPV induced vulvar tumor, displayed a strongly decreased level of *IFITM1* and a highly impaired response to IFNγ stimulation with respect to the expression of *RARRES1* and *PCNA*.

In conclusion, hrHPV allows infected KCs to resist the IFNγ-induced anti-proliferative state by regulating the expression of (anti-)proliferative genes through regulation of STAT1 and IFITM1. This identifies IFITM1 as one the proteins within the IFNγ-signalling pathway that is targeted by hrHPV to evade the anti-proliferative effects of the immune system on hrHPV-infected cells, thus promoting viral spread and the ability of hrHPV-induced lesions to progress.

MATERIALS & METHODS

Ethics Statement

The use of discarded human foreskin, cervical and vaginal keratinocyte tissues to develop cell lines for these studies was approved by the Institutional Review Board at the Pennsylvania State University College of Medicine and by the Institutional Review Board at Pinnacle Health Hospitals. The Leiden University Medical Ethic Committee approved our study on prospective collection of healthy control tissue and for keratinocyte isolation patients were enrolled in the Circle study, which investigates cellular immunity against HPV-induced neoplasia. All human samples were anonymized.

Cell culture

Primary cultures of human epithelial keratinocytes (KCs) were established from foreskin, vaginal, vulva and cervical tissues as previously described [28] and grown in keratinocyte serum-free medium (K-SFM; Medium 154 supplemented with HKGS kit, Invitrogen, Breda, The Netherlands). KCs stably maintaining the full episomal HPV genome following electroporation (HPV-positive KCs) were grown in monolayer culture using E medium in the presence of mitomycin C (Sigma-Aldrich) treated J2 3T3 feeder cells [33,34] for two passages and were then adapted to K-SFM for one passage before experimentation. J2 3T3 mouse fibroblasts were cultured in Iscove's modified Dulbecco's medium supplemented with 8% fetal bovine serum, 2 mM l-glutamine and 1% penicillin-streptomycin (complete IMDM medium) (Gibco-BRL, Invitrogen, Breda, The Netherlands).

HPV16 knock-down in HPV16-positive KCs and infection of undifferentiated keratinocytes

HPV16-positive KCs were transfected with 50 nM Control or HPV16 E2 siRNA for at least 72 hours as previously described [14]. Primary basal layer human foreskin keratinocytes were infected with native HPV16 at MOI 100 as previously described [14]. Cells were washed and harvested and target gene expression was assayed by RT-qPCR.

IFITM1 knock-down in undifferentiated KCs

shRNA's were obtained from the MISSION TRC-library of Sigma-Aldrich (Zwijndrecht, The Netherlands). The MISSION shRNA clones are sequence-verified shRNA lentiviral plasmids (pLKO.1-puro) provided as frozen bacterial glycerol stocks (Luria Broth, carbenicillin at 100 µg/ml and 10% glycerol) in E. coli for propagation and downstream purification of the shRNA clones. pLKO.1 contains the puromycin selection marker for transient or stable transfection. The construct against IFITM1 (NM_003641) was TRCN0000057499: CCGGCCTCATGACCATTGGATTCAT CTCGAGATGAATCCAATGGTCATGAGGTTTTTG and the control was: SHC004 (MISSION TRC2-pLKO puro TurboGFP shRNA Control vector): CCGGCGTGATCTTCACCGACAAGATCTCGAGATCTTGTCGGTGAAGATCACGT TTTT. KCs at ~60% confluency were transduced with lentivirus at MOI 5-10 over night, after which medium was replaced. At least 72 hours post-transduction cells were harvested, washed and plated as indicated and allowed to attach overnight. Cell were stimulated as indicated and assayed accordingly.

Proliferation assay

KC, HPV+ KCs, control shRNA-expressing KCs, or IFITM1 shRNA-expressing KCs were seeded 5,000 cell/well in 96-well plates and allowed to attach over night. Cells were cultured in presence of indicated concentrations of IFNγ (Immunotools, Friesoythe, Germany) and/or TNFα (Invivogen, Toulouse, France) in 150 µl for 96 hours. 15 µl/well MTT (3-(4,5-dimethylthiazol-2-yl)-2,3-diphenyl-2*H*-tetrazolum bromide) stock solution (5 mg/ml in 0.1 M PBS) was added for 3 hours. When the purple formazan precipitate was clearly visible under the microscope, bright light pictures were made using an Olympus IX51 inverse fluorescence microscope (Olympus, Zoeterwoude, The Netherlands) and ColorView II Peltier-cooled charge-coupled device camera (Olympus), and archived using Cell^F software (Olympus).

RNA expression analyses

All microarray data is accessible in the Gene Expression Omnibus database. The microarray data of Karim *et al.* [28] (accession number GSE21260) compared four independent KC cultures with four independent HPV+ KCs cultures, whereas the microarray data of Tummers et al. [15]

(accession number GSE54181) compared four independent KC cultures with four independent HPV+ KCs cultures that were pre-stimulated with IFNγ for 72 hours after which they were treated with IFNγ in the presence of Control L-cells for 24 hours. Plots were generated using the webtool R2: microarray analysis and visualization platform (http://r2.amc.nl).

KC, HPV+ KCs, control shRNA-expressing KCs, or IFITM1 shRNA-expressing KCs were seeded 150,000 cell/well in 12-well plates and allowed to attach over night. Cells were cultured in presence of indicated concentrations of IFNγ and/or TNFα in 1 ml for 24 hours. Total RNA was isolated using the NucleoSpin RNA II kit (Machery-Nagel, Leiden, The Netherlands) according to the manufacturer's instructions. Total RNA (0.5 – 1.0 µg) was reverse transcribed using the SuperScript III First Strand synthesis system from Invitrogen. TaqMan PCR was performed using TaqMan Universal PCR Master Mix and pre-designed, pre-optimized primers and probe mix for *IFITM1*, *BAX*, *BCL2*, *GLB1*, *RARRES1*, *PCNA* and *GAPDH* (Applied Biosystems, Foster City, USA). Threshold cycle numbers (Ct) were determined using the CFX PCR System (BioRad, Veenendaal, The Netherlands) and the relative quantities of cDNA per sample were calculated using the ΔΔCt method using GAPDH as the calibrator gene. The error bars indicate standard deviations of triple PCR measurements.

Western blot analysis

Polypeptides were resolved by SDS–polyacrylamide gel electrophoresis (SDS–PAGE) and transferred to a nitrocellulose membrane (Bio-Rad, Veenendaal, The Netherlands). Immunodetection was achieved with anti-IFITM1 (1:1000, PA5-20989, Thermo Scientific) anti-STAT1 (1:1000, #9172, Cell Signaling Technology (CST)), anti-phospho-STAT1 (Tyr701, 1:1000, #9167, CST), b-actin (1:10,000, Sigma-Aldrich) primary antibodies, and HRP-coupled anti-mouse (1:5000, CST) and HRP-coupled anti-rabbit (1:5000, CST) secondary antibodies. Chemoluminescence reagent (Bio-Rad) was used as substrate and signal was scanned using the Chemidoc and accompanying Software (Bio-Rad).

Conflict of interest

CM has received speaker honoraria from Merck, Quest Diagnostics, GSK, and Bristol-Myers. CM has performed research funded by Merck, The Phillip Morris External Research Program, NexMed, GSK, OriGenix, and Interferon Sciences Inc.

Acknowledgments

This work was supported by the Netherlands Organization for Health Research (NWO/ZonMw) TOP grant 91209012. The funders had no role in study design, data collection and analysis, decision to publish, or preparation of the manuscript.

REFERENCES

1. *zur Hausen H (2002) Papillomaviruses and cancer: from basic studies to clinical application. Nat Rev Cancer 2: 342-350.*
2. *van der Burg SH, Melief CJ (2011) Therapeutic vaccination against human papilloma virus induced malignancies. Curr Opin Immunol 23: 252-257.*
3. *Platanias LC (2005) Mechanisms of type-I- and type-II-interferon-mediated signalling. Nat Rev Immunol 5: 375-386.*
4. *Cabal-Hierro L, Lazo PS (2012) Signal transduction by tumor necrosis factor receptors. Cell Signal 24: 1297-1305.*
5. *Chang YE, Laimins LA (2000) Microarray analysis identifies interferon-inducible genes and Stat-1 as major transcriptional targets of human papillomavirus type 31. J Virol 74: 4174-4182.*
6. *Hong S, Mehta KP, Laimins LA (2011) Suppression of STAT-1 expression by human papillomaviruses is necessary for differentiation-dependent genome amplification and plasmid maintenance. J Virol 85: 9486-9494.*
7. *Nees M, Geoghegan JM, Hyman T, Frank S, Miller L, et al. (2001) Papillomavirus type 16 oncogenes downregulate expression of interferon-responsive genes and upregulate proliferation-associated and NF-kappaB-responsive genes in cervical keratinocytes. J Virol 75: 4283-4296.*
8. *Zhou F, Chen J, Zhao KN (2013) Human papillomavirus 16-encoded E7 protein inhibits IFN-gamma-mediated MHC class I antigen presentation and CTL-induced lysis by blocking IRF-1 expression in mouse keratinocytes. J Gen Virol 94: 2504-2514.*
9. *Avvakumov N, Torchia J, Mymryk JS (2003) Interaction of the HPV E7 proteins with the pCAF acetyltransferase. Oncogene 22: 3833-3841.*
10. *Bernat A, Avvakumov N, Mymryk JS, Banks L (2003) Interaction between the HPV E7 oncoprotein and the transcriptional coactivator p300. Oncogene 22: 7871-7881.*
11. *Caberg JH, Hubert P, Herman L, Herfs M, Roncarati P, et al. (2009) Increased migration of Langerhans cells in response to HPV16 E6 and E7 oncogene silencing: role of CCL20. Cancer Immunol Immunother 58: 39-47.*
12. *Havard L, Rahmouni S, Boniver J, Delvenne P (2005) High levels of p105 (NFKB1) and p100 (NFKB2) proteins in HPV16-transformed keratinocytes: role of E6 and E7 oncoproteins. Virology 331: 357-366.*
13. *Huang SM, McCance DJ (2002) Down regulation of the interleukin-8 promoter by human papillomavirus type 16 E6 and E7 through effects on CREB binding protein/p300 and P/CAF.*

J Virol 76: 8710-8721.

14. *Karim R, Tummers B, Meyers C, Biryukov JL, Alam S, et al. (2013) Human papillomavirus (HPV) upregulates the cellular deubiquitinase UCHL1 to suppress the keratinocyte's innate immune response. PLoS Pathog 9: e1003384.*
15. *Tummers B, Goedemans R, Jha V, Meyers C, Melief CJ, et al. (2014) CD40-Mediated Amplification of Local Immunity by Epithelial Cells Is Impaired by HPV. J Invest Dermatol.*
16. *Detmar M, Orfanos CE (1990) Tumor necrosis factor-alpha inhibits cell proliferation and induces class II antigens and cell adhesion molecules in cultured normal human keratinocytes in vitro. Arch Dermatol Res 282: 238-245.*
17. *Hancock GE, Kaplan G, Cohn ZA (1988) Keratinocyte growth regulation by the products of immune cells. J Exp Med 168: 1395-1402.*
18. *Saunders NA, Jetten AM (1994) Control of growth regulatory and differentiation-specific genes in human epidermal keratinocytes by interferon gamma. Antagonism by retinoic acid and transforming growth factor beta 1. J Biol Chem 269: 2016-2022.*
19. *Kono T, Tanii T, Furukawa M, Mizuno N, Taniguchi S, et al. (1990) Effects of human recombinant tumor necrosis factor-alpha (TNF-alpha) on the proliferative potential of human keratinocytes cultured in serum-free medium. J Dermatol 17: 409-413.*
20. *Fuentes-Gonzalez AM, Contreras-Paredes A, Manzo-Merino J, Lizano M (2013) The modulation of apoptosis by oncogenic viruses. Virol J 10: 182.*
21. *Hamid NA, Brown C, Gaston K (2009) The regulation of cell proliferation by the papillomavirus early proteins. Cell Mol Life Sci 66: 1700-1717.*
22. *Delvenne P, al-Saleh W, Gilles C, Thiry A, Boniver J (1995) Inhibition of growth of normal and human papillomavirus-transformed keratinocytes in monolayer and organotypic cultures by interferon-gamma and tumor necrosis factor-alpha. Am J Pathol 146: 589-598.*
23. *Ohnishi S, Okabe K, Obata H, Otani K, Ishikane S, et al. (2009) Involvement of tazarotene-induced gene 1 in proliferation and differentiation of human adipose tissue-derived mesenchymal stem cells. Cell Prolif 42: 309-316.*
24. *Wu CC, Tsai FM, Shyu RY, Tsai YM, Wang CH, et al. (2011) G protein-coupled receptor kinase 5 mediates Tazarotene-induced gene 1-induced growth suppression of human colon cancer cells. BMC Cancer 11: 175.*
25. *Marionnet AV, Lizard G, Chardonnet Y, Schmitt D (1997) Comparative evaluation of the antiproliferative effect of cyclosporin A and gamma-interferon on normal and HPV-transformed keratinocytes by cell counting, MTT assay and tritiated thymidine incorporation. Cell Biol Toxicol 13: 115-123.*
26. *Siegrist F, Singer T, Certa U (2009) MicroRNA Expression Profiling by Bead Array Technology in Human Tumor Cell Lines Treated with Interferon-Alpha-2a. Biol Proced Online 11: 113-129.*

6

General discussion

GENERAL DISCUSSION

Keratinocytes are well equipped to recognize and react to invading pathogens, and hrHPV is no exception to this. However, hrHPV initiates several immune evasion mechanisms soon after infecting the KC. The virus interferes with the innate immune response by affecting several signaling pathways that otherwise would prompt anti-viral mechanisms in the host cell. Furthermore, hrHPV interferes with the production of cytokines that are involved in the attraction of immune cells to the infected epithelium. In addition, the virus hides itself from the immune system by suppressing the antigen presentation machinery normally allowing infected cells to be recognized by adaptive immune cells and, if this is not successful, hrHPV still employs means to hamper the response of KC's to signals from the effector molecules used by adaptive immune cells to exert their antiviral function. In this thesis we show that hrHPV attenuates innate immune signaling (**Chapter 2**) and CD40-mediated (**Chapter 3**) and IFNγ and/or TNFα-induced (**Chapter 4**) adaptive immune signaling. For this hrHPV exploits the cellular proteins UCHL1 (**Chapter 2**) and IFRD1 (**Chapter 4**) that act on multiple points in the IRF and NFκB signaling pathways. Moreover, hrHPV downregulates cellular IFITM1 to resist the growth inhibitory effects of IFNγ and/or TNFα (**Chapter 5**). Taken together, our data provide important new insights on how the small hrHPV can persist in the face of host immunity.

HPV exploits cellular proteins to alter canonical NFκB signaling

The canonical NFκB pathway is attacked by hrHPV at multiple positions in the signaling cascade downstream of immune receptors. This indicates that suppression of the NFκB pathway forms a very important target for the virus and implies that this pathway normally would allow the host to resist viral infection. There are several early proteins involved in this process (see Chapter 1). The observations made in this thesis using hrHPV episome-baring KCs revealed that hrHPV exploits the cellular proteins UCHL1 and IFRD1 to interfere with NFκB signaling.

We showed that HPV-induced UCHL1 attenuates PRR-induced type I IFN and pro-inflammatory cytokine expression (Chapter 2). UCHL1 hampered the

IRF pathway by interacting with and deubiquitinating K63-linked polyubiquitin chains from TRAF3, resulting in reduced TBK1 – TRAF3 interaction, IRF3 phosphorylation and *IFNβ* expression (Figure 1). PRR-induced NFκB signaling was also attenuated through binding of UCHL1 to TRAF6, thereby influencing the Ub status of TRAF6 (Figure 2). Furthermore, UCHL1 exacerbated NEMO degradation and UCHL1 can prevent IκBα ubiquitination [1].

That UCHL1 binds and affects the ubiquitination status of TRAF3 and 6 implies that UCHL1 may influence other TRAF proteins as well. Indeed, co-immunoprecipitation (co-IP) experiments of UCHL1 and TRAF1-6 in HEK293T cells showed that UCHL1 can bind to all TRAFs (Tummers, *Unpublished data*) and might therefore be a regulator of TRAF ubiquitination and thus function. Furthermore, our co-IP experiments showed that UCHL1 binds to RIP1. In line with this, UCHL1 may influence adaptive immunity-induced canonical and non-canonical NFκB signaling, since the TRAF proteins and RIP1 mediate these pathways [2]. Indeed, knock-down of UCHL1 in HPV-episome expressing KCs enhanced pro-inflammatory cytokine expression upon IFNγ and/or TNFα or CD40L (Tummers, *Unpublished data*). Furthermore, although the two proteins do not co-immunoprecipitate, UCHL1 mediated the degradation of NEMO (Chapter 2). How UCHL1 does this is currently unknown, but, as TRAF6 facilitates the phosphorylation of the IKK complex by TAB1-TAB2-TAK1, one could speculate that UCHL1 is in close enough proximity to NEMO to facilitate its degradation, suggesting that UCHL1 may have a variety of cellular protein targets.

EGFR activation on epithelial cells has been shown to result in a decreased production of pro-inflammatory cytokines [3-5]. HrHPV upregulates EGFR gene and surface expression via the E5, E6 and E7 proteins (Chapter 4 and [6]), and enhances EGFR signaling via E5 and E6 [7-9]. Blocking the EGFR on our HPV+ KCs using the clinically used anti-EGFR antibody cetuximab augmented the production of IFNγ and TNFα-induced production of pro-inflammatory cytokines, indicating that by elevating EGFR levels and signaling HPV may hamper cytokine production (Chapter 4). Via EGFR signaling through mTOR, RAF and/or MEK1, HPV increased the expression of IFRD1, which mediates RelA K310 deacetylation by HDAC1/3 [10] and, thereby, attenuates the transcriptional activity of NFκB1 (Chapter 4 and Figure 6). IFRD1 knock-down

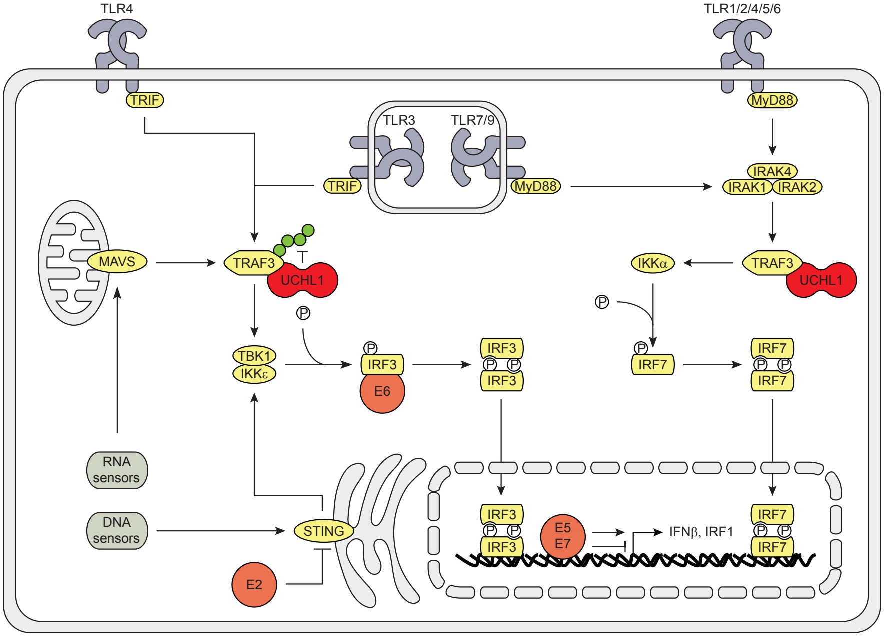
TLR4
TLR1/2/4/5/6
TRIF
MyD88
TLR3
TLR7/9
TRIF
MyD88
IRAK4
IRAK1
IRAK2
MAVS
TRAF3
UCHL1
IKKα
TRAF3
UCHL1
Ⓟ
Ⓟ
TBK1
IKKε
Ⓟ
IRF3
E6
IRF3
Ⓟ Ⓟ
IRF3
Ⓟ
IRF7
IRF7
Ⓟ Ⓟ
IRF7
RNA sensors
DNA sensors
STING
E2
IRF3
Ⓟ Ⓟ
IRF3
E5
E7
IFNβ, IRF1
IRF7
Ⓟ Ⓟ
IRF7

Figure 1: The effects of hrHPV on IRF signaling
Schematic representation of the effects of hrHPV on IRF signaling. All TLRs, except TLR3, activate IRF7 via signaling through MyD88, the IRAK complex, TRAF3 and IKKα. TLR3 and 4 signal via TRIF, cytosolic RNA sensors through MAVS and cytosolic DNA sensors via STING activate IRF3 through TRAF3, TBK1 and IKKε. Activated IRFs dimerize, translocate to the nucleus and initiate gene transcription. HPV utilizes its own encoded E proteins (red) as well as exploits the cellular protein UCHL1 (red) to interfere with these signaling pathways. Green circles on TRAF3 indicate K63-linked poly-ubiquitin chains.

experiments in HPV+ KCs indeed showed that basal RelA acetylation was restored and basal signaling and signaling induced by Poly(I:C), TNFα and the combination of IFNγ and TNFα resulted in higher cytokine expression levels in cells in which IFRD1 was knocked-down (Chapter 4). Interestingly, after IFNγ stimulation alone cytokine expression levels were also higher in IFRD1 knock-down HPV+ KCs, suggesting that IFRD1 may also affect the transcriptional activity of STAT1 and/or IRF1. If IFRD1 can regulate transcriptional activity of transcription factors other than NFκB, HPV could deregulate a whole network of cellular genes by simply exploiting one cellular protein.

Interestingly, E2 may promote canonical NFκB signaling [11-13]. It may form an E2-NFκB-p300/CBP transcriptional repressor complex on the LCR of the episome and as such regulates episome transcription which is required for the virus to sustain a low profile. However, as luciferase assays show that the E2 protein renders NFκB more active [13], the virus thus may prompt E2-mediated NFκB-induced pro-inflammatory cytokine production and immune cell attraction. This indicates that the virus needs additional mechanisms in order to regulate the episome while keeping pro-inflammatory cytokine expression in check during infection. The combined expression of E2, UCHL1 and IFRD1 during an infection might form a perfect cocktail to allow hrHPV to regulate its episome while suppressing KCs pro-inflammatory cytokine production.

HPV allows signaling to the non-canonical NFκB pathway

IFNγ and TNFα are known to synergistically affect gene expression, and also in KCs pro-inflammatory cytokine expression is synergistically higher than expression induced by IFNγ or TNFα alone (Chapter 4). Still, hrHPV attenuates IFNγ and/or TNFα-induced pro-inflammatory cytokine expression and the attraction of PBMCs to KCs that have been stimulated with the combination of IFNγ and TNFα. Furthermore, exposure of hrHPV-infected KCs to IFNγ and TNFα fails to induce cellular programs associated with a block of proliferation as seen in uninfected KCs (Chapter 5). The IFN pathways seems to be centrally attacked through downregulation of STAT1 levels which is observed in hrHPV episome-baring KCs when compared to uninfected KCs [14-16]. Downregulation of STAT1 results in attenuated ISG expression, albeit that signaling downstream of the IFNAR and IFNγR still functions (Chapter 5 and [15]). Thus, the attenuated type I IFN-induced ISG expression in HPV+ KCs must be due to the basal lowered STAT1 levels. In contrast, in experiments where E6 is overexpressed, E6 was shown to bind TYK2 and to interfere with STAT1 and STAT2 phosphorylation [17], implying that also STAT1 signaling is hampered by E6. If E6 plays a similar role in early infection remains to be determined. Importantly, IFNγ and TNFα stimulation induced processing of the non-canonical NFκB precursor p100 into p52 in hrHPV-infected cells but not uninfected KCs (Tummers, *Unpublished data*), indicating that hrHPV skews the response of KCs upon stimulation with TNFα and IFNγ towards the non-canonical NFκB pathway. Potentially, this is caused by E7 as this oncoprotein was shown to increase SCF-βTrCP protein levels [18] and in this way might accelerate p100 processing [19]. Although unexplored at this point, it is highly likely that this forms another pathway allowing hrHPV-infected cells to resist control of infection by the immune system and the anti-proliferative effects of IFNγ and TNFα (Chapter 5).

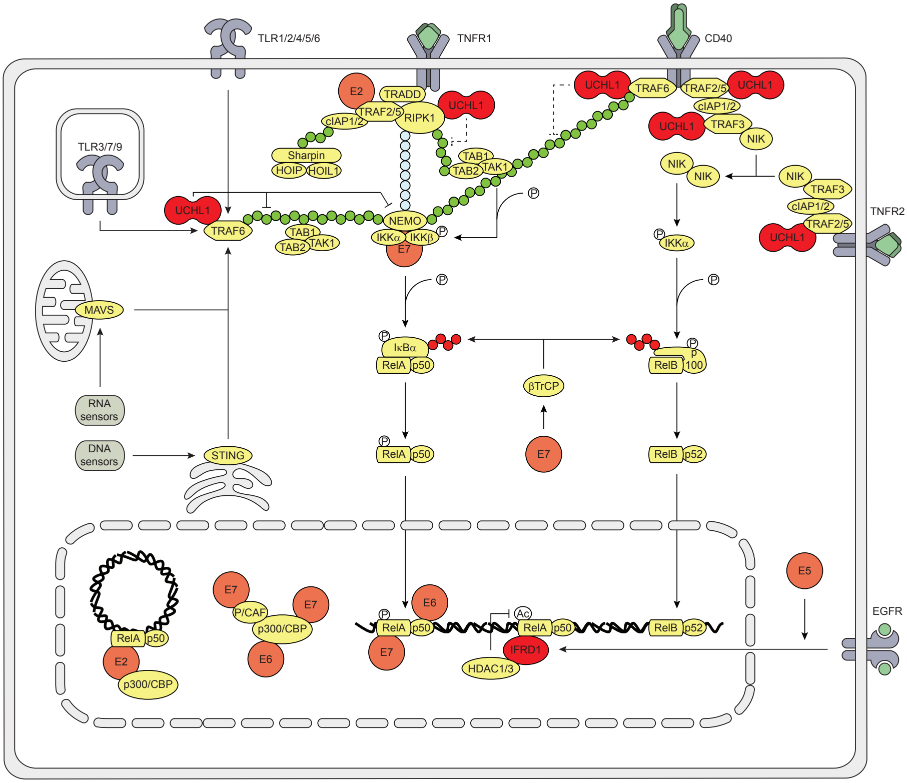
TLR1/2/4/5/6
TNFR1
CD40
TLR3/7/9
E2
TRADD
TRAF2/5
cIAP1/2
RIPK1
UCHL1
Sharpin
HOIP
HOIL1
TAB1
TAB2
TAK1
UCHL1
TRAF6
TRAF2/5
UCHL1
cIAP1/2
UCHL1
TRAF3
NIK
NIK
NIK
NIK
TRAF3
cIAP1/2
TRAF2/5
UCHL1
TNFR2
UCHL1
TRAF6
TAB1
TAB2
TAK1
NEMO
IKKα
IKKβ
E7
P
IKKα
P
P
MAVS
P
IκBα
RelA
p50
P
p100
RelB
βTrCP
RNA sensors
DNA sensors
STING
P
RelA
p50
E7
RelB
p52
E5
E7
P/CAF
E7
p300/CBP
E6
E6
P
RelA
p50
Ac
RelA
p50
RelB
p52
E7
IFRD1
HDAC1/3
RelA
p50
E2
p300/CBP
EGFR

Figure 2: The effects of hrHPV on NFκB signaling

Schematic representation of the effects of hrHPV on NFκB signaling. The canonical NFκB1 pathway is activated by PRRs and CD40 through TRAF6 and TNFR1 through RIP1. Poly-ubiquitination of TRAF6 and RIP1 recruits the TAB1-TAB2-TAK1 and IKK complexes resulting in the phosphorylation of IKKβ by TAK1. IKKβ phosphorylates IκBα, which is then ubiquitinated by SCF-βTrCP and subsequently degraded, and thereby releases the NFκB1 complex to translocate to the nucleus. CD40 and TNFR2 initiate non-canonical NFκB2 signaling by recruitment of TRAF2/5, cIAP1/2 and TRAF3 to the respective receptor, leading to TRAF3 degradation. This *causes NIK to accumulate and activate IKKα to phosphorylate p100. This induces SCF-βTrCP to ubiquitinate p100, leading to the proteosomal processing of p100 into p52, and the subsequent nuclear translocation of NFκB2. In the nucleus NFκB binds to the DNA and is aided by coactivators to initiate gene transcription. HPV utilizes its own encoded E proteins (red) as well as exploits the cellular proteins (red) UCHL1 and IFRD1 to interfere with NFκB1 signaling at multiple positions in the pathway. Green circles indicate K63-linked poly-ubiquitin chains, red circles indicate K48-linked poly-ubiquitin chains, and blue circles indicate linear poly-ubiquitin chains. Dashed lines indicate hypothetical effects.*

Epithelial cells express CD40 on their cell surface [20] and ligation of CD40 induces both canonical and non-canonical NFκB signaling, similar to TNFR1 and 2, respectively [21]. We showed that ligation of CD40 on epithelial cells results in a very coordinated response by KCs, dominated by the expression of genes involved in leukocyte migration, cell-to-cell signaling and interaction, as well as cell death and survival. The presence of HPV does not affect the gene expression profile of CD40 stimulated KCs, but it does attenuate the extent of the response and reduces the attraction of PBMCs (Chapter 3), indicating that the virus also attenuates CD40-induced signaling. Based on our previous studies it is likely that the CD40 – NFκB1 axis of CD40 signaling is affected via the interaction of UCHL1 and TRAF6, the effects of E7 on the IKK complex, and that of IFRD1 on NFκB1 transcriptional activation. Speculatively, at the non-canonical side signaling could be hampered by abrogation of UCHL1-mediated TRAF2 and/or 5- or E7-mediated IKKα functioning. However, UCHL1-mediated TRAF3 hampering could also lead to constitutive NIK accumulation and subsequent pathway activation (Figure 2). It remains to be determined if hrHPV prefers to skew KCs towards non-canonical NFκB activation after CD40 ligation.

NFκB signaling in hrHPV transformed cells

In contrast to hrHPV-infected cells, higher intraepithelial neoplastic lesions and HPV-positive cancers often show overactive canonical NFκB gene expression [22]. Indeed, overexpression experiments showed that E6 and/or E7 can also have pro-NFκB signaling effects and can increase NFκB target gene expression [16]. Mechanistically, E6 targets the NFκB repressor NFX1-91 for degradation [23] and under hypoxic conditions hampers CYLD, a negative regulator of NFκB signaling [24]. E6 also upregulates gene expression of the NFκB signaling components p50, NIK and TRAIP [16]. E7 upregulates SCF-βTrCP protein levels [18], which might lead to accelerated IκBα degradation and p100 processing [19]. The transformed cell may benefit from E6/E7-enhanced NFκB signaling by maintaining a proliferative, anti-apoptotic state, although also pro-inflammatory cytokine expression is increased. Notably, cell type and growth rate are important determinants whether HPV E6 or E6/E7 stimulate or inhibit NFκB activation [25], and since viral gene expression considerably differs between hrHPV-infected KCs and hrHPV-transformed cells, data obtained from viral protein overexpression experiments should be carefully interpreted with respect to what their effects are in infection or cancer.

How HPV regulates cellular gene expression remains unclear

How HPV differentially expresses the genes studied in this thesis is still under investigation, but the episomal nature of the viral genome and it's translation into polycistronic mRNA make it difficult to study the functions of the individual E proteins in the context of a primary infection. We have overexpressed the individual early genes, their combinations and all combined in basal KCs, HaCat cells and primary fibroblasts, but, although the early genes were expressed, we could not detect differential expression of UCHL1, IFRD1 or IFITM1 in any of these overexpression experiments (Tummers, *Unpublished data*). Since plasmid-based overexpression of the early genes does not count for the effects of the episome itself, the presence of the viral episome in regulating cellular gene expression must be important. Transcription of the episome produces a polycistronic mRNA strand that completely disintegrates with current siRNA techniques directed at a single early gene. siRNA directed against E6, E7 (Tummers, *Unpublished data*) or E2 abolishes expression of the other early genes and abrogates the HPV-induced differential expression of UCHL1 (Chapter 2), IFRD1 (Chapter 4), and IFITM1 (Chapter 5), indicating that episome presence is indeed necessary in regulating cellular gene expression. Since single early genes cannot be knocked-down in our model, generating KCs harboring episomes with specific mutations in a gene, rendering the gene functionally inactive without influencing the other genes or polycistronic mRNA strand, could be a way to study specific early genes. This could give important insights into the function of an early gene in the context of early infection, but unfortunately, no such system exists to date.

Genetic predisposition to developing HPV-induced malignancies

Most HPV infections resolve spontaneously, although HPV invests heavily in suppressing host immunity. This indicates that external factors, such as genetic and environmental factors may contribute to the establishment of a persistent infection and progression to cancer. Genetic predisposition to cervical tumors was found [26] and several combinations of single nucleotide polymorphisms (SNPs) were associated with an increased risk to cancer. SNPs in genes of the antigen processing machinery, such as HLA-A, LMP7, TAP2 and ERAP1 [27], and in the FANCA and IRF3 genes [28] were linked to persistent HPV infection and formation of cancer. SNPs in the TLR and NFκB pathways were also studied [29]. Of the thirty-two candidate genes involved in these pathways, including TLR3, NFκB1, NFκB2, RelA, RelB, TRAF3 and TRAF6, only a SNP in the 5' UTR of the lymphotoxin alpha (LTA; TNF superfamily member 1) was significantly associated with increased risks of cervical and vulvar cancers [29]. Based on the interactions between the different proteins in the downstream signaling pathways and their outcomes with respect to activation, splicing, degradation and translocation it might well be that combinations of SNPs, of multiple genes associated with the IRF and NFκB pathways, rather than single SNPs, may confer protection or susceptibility towards persistence of HPV infection.

Final comment

Being a small virus, HPV relies on just 6 encoded early proteins, and some splice variants thereof, to interfere with normal KC physiology. Although the early proteins have a variety of cellular protein targets, it is remarkable that the virus only needs so few encoded genes to persist. Our work showed that HPV, via yet unknown ways, exploits cellular proteins to achieve its goals.

REFERENCES

1. Takami Y, Nakagami H, Morishita R, Katsuya T, Cui TX, Ichikawa T, et al. Ubiquitin carboxyl-terminal hydrolase L1, a novel deubiquitinating enzyme in the vasculature, attenuates NF-kappaB activation. Arterioscler Thromb Vasc Biol 2007,27:2184-2190.
2. Baker SJ, Reddy EP. Modulation of life and death by the TNF receptor superfamily. Oncogene 1998,17:3261-3270.
3. Kalinowski A, Ueki I, Min-Oo G, Ballon-Landa E, Knoff D, Galen B, et al. EGFR activation suppresses respiratory virus-induced IRF1-dependent CXCL10 production. Am J Physiol Lung Cell Mol Physiol 2014,307:L186-196.
4. Mascia F, Mariani V, Girolomoni G, Pastore S. Blockade of the EGF receptor induces a deranged chemokine expression in keratinocytes leading to enhanced skin inflammation. Am J Pathol 2003,163:303-312.
5. Paul T, Schumann C, Rudiger S, Boeck S, Heinemann V, Kachele V, et al. Cytokine regulation by epidermal growth factor receptor inhibitors and epidermal growth factor receptor inhibitor associated skin toxicity in cancer patients. Eur J Cancer 2014,50:1855-1863.
6. Akerman GS, Tolleson WH, Brown KL, Zyzak LL, Mourateva E, Engin TS, et al. Human papillomavirus type 16 E6 and E7 cooperate to increase epidermal growth factor receptor (EGFR) mRNA levels, overcoming mechanisms by which excessive EGFR signaling shortens the life span of normal human keratinocytes. Cancer Res 2001,61:3837-3843.
7. Kim SH, Juhnn YS, Kang S, Park SW, Sung MW, Bang YJ, et al. Human papillomavirus 16 E5 up-regulates the expression of vascular endothelial growth factor through the activation of epidermal growth factor receptor, MEK/ ERK1,2 and PI3K/Akt. Cell Mol Life Sci 2006,63:930-938.
8. Spangle JM, Munger K. The HPV16 E6 oncoprotein causes prolonged receptor protein tyrosine kinase signaling and enhances internalization of phosphorylated receptor species. PLoS Pathog 2013,9:e1003237.
9. Zhang B, Srirangam A, Potter DA, Roman A. HPV16 E5 protein disrupts the c-Cbl-EGFR interaction and EGFR ubiquitination in human foreskin keratinocytes. Oncogene 2005,24:2585-2588.
10. Micheli L, Leonardi L, Conti F, Maresca G, Colazingari S, Mattei E, et al. PC4/Tis7/IFRD1 stimulates skeletal muscle regeneration and is involved in myoblast differentiation as a regulator of MyoD and NF-kappaB. J Biol Chem 2011,286:5691-5707.
11. Lee D, Lee B, Kim J, Kim DW, Choe J. cAMP response element-binding protein-binding protein binds to human papillomavirus E2 protein and activates E2-dependent transcription.

J Biol Chem 2000,275:7045-7051.

12. *Marcello A, Massimi P, Banks L, Giacca M. Adeno-associated virus type 2 rep protein inhibits human papillomavirus type 16 E2 recruitment of the transcriptional coactivator p300. J Virol 2000,74:9090-9098.*
13. *Prabhavathy D, Prabhakar BN, Karunagaran D. HPV16 E2-mediated potentiation of NF-kappaB activation induced by TNF-alpha involves parallel activation of STAT3 with a reduction in E2-induced apoptosis. Mol Cell Biochem 2014,394:77-90.*
14. *Chang YE, Laimins LA. Microarray analysis identifies interferon-inducible genes and Stat-1 as major transcriptional targets of human papillomavirus type 31. J Virol 2000,74:4174-4182.*
15. *Hong S, Mehta KP, Laimins LA. Suppression of STAT-1 expression by human papillomaviruses is necessary for differentiation-dependent genome amplification and plasmid maintenance. J Virol 2011,85:9486-9494.*
16. *Nees M, Geoghegan JM, Hyman T, Frank S, Miller L, Woodworth CD. Papillomavirus type 16 oncogenes downregulate expression of interferon-responsive genes and upregulate proliferation-associated and NF-kappaB-responsive genes in cervical keratinocytes. J Virol 2001,75:4283-4296.*
17. *Li S, Labrecque S, Gauzzi MC, Cuddihy AR, Wong AH, Pellegrini S, et al. The human papilloma virus (HPV)-18 E6 oncoprotein physically associates with Tyk2 and impairs Jak-STAT activation by interferon-alpha. Oncogene 1999,18:5727-5737.*
18. *Spardy N, Covella K, Cha E, Hoskins EE, Wells SI, Duensing A, et al. Human papillomavirus 16 E7 oncoprotein attenuates DNA damage checkpoint control by increasing the proteolytic turnover of claspin. Cancer Res 2009,69:7022-7029.*
19. *Fukushima H, Matsumoto A, Inuzuka H, Zhai B, Lau AW, Wan L, et al. SCF(Fbw7) modulates the NFkB signaling pathway by targeting NFkB2 for ubiquitination and destruction. Cell Rep 2012,1:434-443.*
20. *Galy AH, Spits H. CD40 is functionally expressed on human thymic epithelial cells. J Immunol 1992,149:775-782.*
21. *Elgueta R, Benson MJ, de Vries VC, Wasiuk A, Guo Y, Noelle RJ. Molecular mechanism and function of CD40/CD40L engagement in the immune system. Immunol Rev 2009,229:152-172.*
22. *Branca M, Giorgi C, Ciotti M, Santini D, Di Bonito L, Costa S, et al. Upregulation of nuclear factor-kappaB (NF-kappaB) is related to the grade of cervical intraepithelial neoplasia, but is not an independent predictor of high-risk human papillomavirus or disease outcome in cervical cancer. Diagn Cytopathol 2006,34:555-563.*
23. *Xu M, Katzenellenbogen RA, Grandori C, Galloway DA. NFX1 plays a role in human papillomavirus type 16 E6 activation of NFkappaB activity. J Virol 2010,84:11461-11469.*

24. *An J, Mo D, Liu H, Veena MS, Srivatsan ES, Massoumi R, et al. Inactivation of the CYLD deubiquitinase by HPV E6 mediates hypoxia-induced NF-kappaB activation. Cancer Cell 2008,14:394-407.*
25. *Vandermark ER, Deluca KA, Gardner CR, Marker DF, Schreiner CN, Strickland DA, et al. Human papillomavirus type 16 E6 and E 7 proteins alter NF-kB in cultured cervical epithelial cells and inhibition of NF-kB promotes cell growth and immortalization. Virology 2012,425:53-60.*
26. *Magnusson PK, Lichtenstein P, Gyllensten UB. Heritability of cervical tumours. Int J Cancer 2000,88:698-701.*
27. *Mehta AM, Jordanova ES, van Wezel T, Uh HW, Corver WE, Kwappenberg KM, et al. Genetic variation of antigen processing machinery components and association with cervical carcinoma. Genes Chromosomes Cancer 2007,46:577-586.*
28. *Wang SS, Bratti MC, Rodriguez AC, Herrero R, Burk RD, Porras C, et al. Common variants in immune and DNA repair genes and risk for human papillomavirus persistence and progression to cervical cancer. J Infect Dis 2009,199:20-30.*
29. *Bodelon C, Madeleine MM, Johnson LG, Du Q, Galloway DA, Malkki M, et al. Genetic variation in the TLR and NF-kappaB pathways and cervical and vulvar cancer risk: a population-based case-control study. Int J Cancer 2014,134:437-444.*

7

Samenvatting in het Nederlands

Het humaan papillomavirus (HPV) onderdrukt signalen in cellen om te ontsnappen aan het immuunsysteem.

Humaan papillomavirus (HPV) is een klein DNA virus dat epitheelcellen van mucosa en de huid - keratinocyten - infecteert. Er zijn momenteel ongeveer 200 HPV types bekend. De meeste types zijn ongevaarlijk en veroorzaken bijvoorbeeld wratten op handen, voeten of genitaliën. Sommige types, echter veroorzaken kanker in het hoofd-hals gebied en de genitaliën. Het bekendst is baarmoederhalskanker. Deze laatste types worden de hoog-risico HPVs (hrHPVs) genoemd. Infecties met hrHPV komen over de gehele wereld voor en ongeveer 80% van alle mensen is ooit met een hrHPV geïnfecteerd geraakt. Het is dan ook de meest voorkomende seksueel overdraagbare aandoening. Het virus kan zich lang weren tegen het afweersysteem maar na een periode van een tot twee jaar verdwijnen de meeste infecties spontaan. Bij iets minder dan 1% van de infecties komt het virus niet onder controle van het afweersysteem. Dan ontstaan er afwijkingen aan het epitheel die, wanneer niet tijdig behandeld, kunnen uitmonden in kanker. Wereldwijd zijn de hrHPV typen verantwoordelijk voor ongeveer 530.000 nieuwe kankergevallen en 275.000 doden per jaar.

Het afweersysteem kan virus-geïnfecteerde cellen herkennen en opruimen wanneer het eerst geattendeerd wordt op de aanwezigheid van een infectie. Om het afweersysteem te alarmeren zijn de cellen in het lichaam uitgerust met sensoren - receptoren - die de aanwezigheid van een virus kunnen herkennen. Als een cel geïnfecteerd raakt reageren de receptoren op specifieke structuren van het virus waardoor allerlei signaleringsroutes op gang komen die leiden tot de aanmaak van verschillende eiwitten in de geïnfecteerde cel. Deze eiwitten kunnen de infectie onderdrukken door onder andere a) de cel in een staat van verdediging te brengen, b) de virus productie te voorkomen, en c) afweercellen - lymfocyten - aan te trekken. Wanneer de aangetrokken lymfocyten het virus herkennen reageren ze door eiwitten te produceren die nog meer afweercellen kunnen aantrekken (cytokines) en eiwitten die verschillende uitwerkingen hebben op de geïnfecteerde cel. Zo kunnen eiwitten zoals interferon gamma (IFNγ) en tumor necrosis factor alpha (TNFα) ervoor zorgen dat de geïnfecteerde cel stopt met delen of dat de cel dood gaat, zodat de verspreiding van het virus voorkomen wordt.

Om zich te weren tegen een aanval van het afweersysteem hebben virussen verschillende methodes ontwikkeld die ingrijpen op verschillende fases van de aanval. Door de expressie van de sensoren te onderdrukken, de signaleringsroutes te blokkeren, of de productie van cytokines te onderdrukken proberen virussen te voorkomen dat het afweersysteem reageert. Daarnaast kunnen virussen proberen te voorkomen dat de geïnfecteerde cellen worden herkend door gealarmeerde lymfocyten of dat de geïnfecteerde cel adequaat kan reageren op de door lymfocyten uitgescheiden eiwitten die de cel instrueren om te stoppen met groeien of om dood te gaan. Vanuit eerdere studies weten we dat het afweersysteem pas laat op gang komt tegen HPV en ook dat het virus nog lang resistent is tegen een aanval. Dit duidt erop dat HPV ook methodes heeft om zichzelf in ieder geval een tijdje te beschermen tegen aanvallen van het afweersysteem. Hoe HPV in staat is om het afweersysteem om de tuin te leiden is in dit proefschrift bestudeerd voor de twee meest voorkomende hoog-risico types, HPV16 en 18.

Voorheen was al aangetoond dat bepaalde viruseiwitten van HPV verschillende signaleringsroutes in de keratinocyt onderdrukken of de interactie tussen geïnfecteerde cel en afweercel verhinderen (**hoofdstuk 1**). In dit proefschrift tonen we aan dat hrHPVs ook cellulaire eiwitten uitbuit om te ontsnappen aan het immuunsysteem.

In **hoofdstuk 2** wordt aangetoond dat een infectie met hrHPV leidt tot de verhoogde expressie van het cellulaire eiwit UCHL1. Dit eiwit hindert verdere activering van de IRF3 en NF-κB signaleringsroutes als deze worden aangezet door binding van virale structuren aan de virussensoren TLR3, RIG-I en Mda5. Signalering van deze receptoren naar de kern verloopt onder meer door de ubiquitinering van enkele signaal eiwitten. UCHL1 verhindert de ubiquitinering van de eiwitten TRAF3 en TRAF6 en beïnvloedt de expressie van NEMO. Hierdoor verloopt de signalering minder efficiënt met als resultaat dat de geïnfecteerde keratinocyt minder cytokines uitscheidt die het afweersysteem kunnen alarmeren en activeren.

Hoofdstuk 3 laat zien dat een infectie met een hrHPV leidt tot de verhoogde expressie van het cellulaire eiwit IFRD1. Dit cellulaire eiwit blijkt de activatie van NF-κB te onderdrukken als deze wordt aangezet via de virussensor TLR3, of via de IFNγ en/of TNFα receptoren. IFRD1 vormt een brug tussen het NF-κB complex en een de-acetylase (HDAC3) waardoor de acetylatie van NF-κB, welke belangrijk is voor het functioneren van dit eiwit complex, kan verhinderen. Ook hierdoor verloopt de signalering minder efficiënt waardoor de geïnfecteerde cel minder eiwitten maakt die het afweersysteem kunnen aantrekken en activeren.

Het was eerder bekend dat hrHPV de expressie van de epidermal growth factor receptor (EGFR) verhoogt en EGFR signalering versterkt. Deze signalering verhoogt ook de expressie van IFDR1, waardoor er een link kan worden gemaakt tussen de remming van de aanmaak van afweersysteem aantrekkende eiwitten en de expressie van EGFR. In de kliniek worden momenteel tests gedaan met stoffen die de werking van de EGFR en diens signalering kunnen remmen en met stoffen die de werking van HDAC3 kunnen tegengaan. Als geïnfecteerde keratinocyten behandeld worden met deze stoffen gaan deze meer afweersysteem aantrekkende cytokines produceren. Deze resultaten zijn therapeutisch zeer interessant, maar er is nog veel meer onderzoek nodig om te bepalen of deze stoffen ook daadwerkelijk de afweerreactie tegen HPV infecties en HPV-geïnduceerde kankers stimuleren.

In **hoofdstuk 4** laten we het gen expressie profiel zien van keratinocyten wanneer signalering door de receptor CD40 wordt aangezet. CD40 is een receptor van de keratinocyt dat het molecuul CD154 (CD40L) herkent dat aanwezig is op bepaalde afweercellen. Snel na het activeren van CD40 worden er door de keratinocyt cytokines geproduceerd die ervoor kunnen zorgen dat de afweercellen geactiveerd en naar het geïnfecteerde gebied gerekruteerd worden. In een latere fase van CD40 activatie worden er cellulaire programma's aangezet die ertoe leiden dat de cel stopt met groeien. HrHPV verandert dit gen expressie profiel op zich niet, maar onderdrukt de intensiteit van de expressie. Dit leidt ertoe dat de CD40-geinduceerde aanmaak van cytokines onderdrukt is en dat lokale versterking van de afweerreactie minder goed plaatsvindt.

De eiwitten IFNγ en TNFα worden gemaakt door de lymfocyten van het afweersysteem. Deze cytokines hebben verscheidene effecten op de cellen die daar receptoren voor hebben, zo kunnen zij de mate van celgroei beïnvloeden en de dood van cellen veroorzaken. In **hoofdstuk 5** is de invloed van hrHPV op de reactie van keratinocyten na stimulatie met IFNγ en TNFα bepaald. Niet-geïnfecteerde keratinocyten stopten met groeien. Dit bleek minder het geval te zijn met hrHPV geïnfecteerde cellen, deze groeiden veel gemakkelijker door. HPV onderdrukte onder andere de expressie van de genen IFITM1 en RARRES1 die bij de normale regulatie van celgroei betrokken zijn.

Het is duidelijk dat HPV er veel aan doet om te ontsnappen aan het immuunsysteem. HPV onderdrukt verschillende signaleringsroutes die ervoor zorgen dat de geïnfecteerde cel tegen het virus op kan treden. Met name de activatie van het NF-κB complex blijkt te worden aangepakt op verschillende niveaus in de verschillende routes die allemaal tot NF-κB activatie leiden. Hierdoor verhindert HPV dat de geïnfecteerde keratinocyt eiwitten aanmaakt die het afweersysteem kunnen alarmeren en activeren wanneer de cel het virus herkent. HPV zorgt er ook voor dat de afweercellen die toch worden aangetrokken de geïnfecteerde cellen moeilijk kunnen herkennen. Zelfs als de afweercellen op de geïnfecteerde cel reageren beïnvloedt HPV de reactie van zijn gastheercel door signaleringsroutes te onderdrukken die ervoor zorgen dat de cel stopt met groeien.

In het kort wordt in dit proefschrift aangetoond dat hrHPV cellulaire eiwitten exploiteert om tijdelijk te kunnen ontsnappen aan het immuunsysteem.

ADDENDUM

Frequently used abbreviations

Curriculum Vitae

List of Publications

Acknowledgements

FREQUENTLY USED ABBREVIATIONS

CCL2	Chemokine (c-c motif) ligand 2
CD40	Cluster of differentiation 40
CXCL9	Chemokine (c-x-c motif) ligand 9
E protein	Early protein
EC	Epithelial cell
EGFR	Epidermal growth factor receptor
hrHPV	High-risk Human papillomavirus
IFITM1	Interferon-induced transmembrane protein 1
IFN	Interferon
IFNAR	Interferon-α/β receptor
IFNγR	Interferon-γ receptor
IFRD1	Interferon-related developmental regulator 1
IKK	Inhibitor of nuclear factor kappa-B kinase
IL8	Interleukin 8
IRF	Interferon regulatory factor
ISG	Interferon-stimulated gene
KC	Keratinocyte
MIP3α	Macrophage inflammatory protein 3α
NEMO	NF-kappa-B essential modulator
MHC	Major histocompatibility complex
NFκB	Nuclear factor of kappa-light-chain-enhancer of activated B cells
PRR	Pattern-recognition receptor
RANTES	Regulated on activation, normal T cell expressed and secreted
TLR	Toll-like receptor
TNFα	Tumor necrosis factor α
TNFR	Tumor necrosis factor receptor
TRAF	TNF receptor associated factor
UCHL1	Ubiquitin carboxy-terminal hydrolase L1

CURRICULUM VITAE

Bart Tummers was born on February 23rd 1984 in IJsselstein, The Netherlands. In 2002, he graduated at the Anna van Rijn College, Nieuwegein, The Netherlands, after which he studied Biomedical Sciences at Utrecht University, Utrecht, The Netherlands, between 2002 and 2008. As part of the master program ‘Immunity and Infection’, he studied the pre-fusogenic form of the Severe Acute Respiratory Syndrome Coronavirus (SARS-CoV) spike glycoprotein ectodomain (SED) under the supervision of Dr. Ir. B.J. Bosch in the lab of Prof. Dr. P. Rottier at Utrecht University, Faculty of Veterinary Medicine, Department of Infectious diseases and Immunity, Virology Division. He then worked in the lab of Prof Dr. Müller at the Laboratoire National de Santé - Institute d’Immunologie, Luxembourg, Luxembourg on the expression of modified Infectious Bronchitis Virus (IBV) Spike Glycoprotein domain 1 (S1) and Avian Influenza Virus (AIV) Hemagglutinin 5 Glycoprotein (H5) for anti-S1 and anti-H5 monoclonal antibody production, under the supervision of Dr. M.F. Ducatez and Dr. F.B. Bouche. At the University of Erasmus MC, Rotterdam, The Netherlands, Department of Virology he worked under the supervision of Dr. B.L. Haagmans and Dr. S.L. Smits in the lab of Prof. Dr. A.D.M.E. Osterhaus to set up an *in vitro* and *in vivo* model system for Hepatitis C virus research. For his master thesis he studied the life cycle of the spirochete *Borrelia burgdorferi*, supervised by Prof. Dr. J. van Strijp at Utrecht University, Faculty of Veterinary Medicine, Department of Infectious diseases and Immunology. In 2009 he started to work in the lab of Prof. Dr. S.H. van der Burg at the Leiden University Medical Center (LUMC), department of Clinical Oncology, Leiden, The Netherlands, where he developed a method to isolate, transduce, store and analyze CD8+ T cells for the generation of standard samples that were later distributed within a large network of laboratories involved in studying the immune response in patients with cancer. In 2010 he started his PhD thesis in the same lab, studying the immune evasion strategies of high-risk human papillomaviruses (hrHPV), which has led to this thesis. In June 2015 he started as a post-doc in the lab of Prof. Dr. D.R. Green at the St. Jude Children’s Research Hospital, department of Immunology in Memphis, Tennessee, USA on the molecular mechanisms of apoptosis and necroptosis.

LIST OF PUBLICATIONS

Human papillomavirus targets crossroads in immune signaling
Tummers B, van der Burg SH.
Viruses. 2015 May 21;7(5):2485-506.

The interferon-related developmental regulator (IFRD1) is used by Human papillomavirus (HPV) to suppress NF-kappaB activation
Tummers B, Goedemans R, Pelascini LPL, Jordanova ES, van Esch EMG, Meyers C, Melief CJM, Boer JM, van der Burg SH.
Nat Commun. 2015 Mar 13;6:6537.

CD40-mediated amplification of local immunity by epithelial cells is impaired by HPV.
Tummers B, Goedemans R, Jha V, Meyers C, Melief CJM, van der Burg SH, Boer JM.
J Invest Dermatol. 2014 Dec;134(12):2918-27.

Alterations in classical and nonclassical HLA expression in recurrent and progressive HPV-induced usual vulvar intraepithelial neoplasia and implications for immunotherapy.
van Esch EM, Tummers B, Baartmans V, Osse EM, Ter Haar N, Trietsch MD, Hellebrekers BW, Holleboom CA, Nagel HT, Tan LT, Fleuren GJ, van Poelgeest MI, van der Burg SH, Jordanova ES.
Int J Cancer. 2014 Aug 15;135(4):830-42.

Human papillomavirus (HPV) upregulates the cellular deubiquitinase UCHL1 to suppress the keratinocyte's innate immune response.
Tummers B, Karim R, Meyers C, Biryukov JL, Alam S, Backendorf C, Jha V, Offringa R, van Ommen GJ, Melief CJ, Guardavaccaro D, Boer JM, van der Burg SH.
PLoS Pathog. 2013;9(5):e1003384.

Chemotherapy alters monocyte differentiation to favor generation of cancer-supporting M2 macrophages in the tumor microenvironment.
Dijkgraaf EM, Heusinkveld M, Tummers B, Vogelpoel LT, Goedemans R, Jha V, Nortier JW, Welters MJ, Kroep JR, van der Burg SH.
Cancer Res. 2013 Apr 15;73(8):2480-92.

The development of standard samples with a defined number of antigen-specific T cells to harmonize T cell assays: a proof-of-principle study.
Singh SK, Tummers B, Schumacher TN, Gomez R, Franken KL, Verdegaal EM, Laske K, Gouttefangeas C, Ottensmeier C, Welters MJ, Britten CM, van der Burg SH.
Cancer Immunol Immunother. 2013 Mar;62(3):489-501.

ACKNOWLEDGEMENTS

This thesis could not have been realized without the help of many. I am grateful to anyone who, directly or indirectly, helped me with this thesis.

Sjoerd, heel erg bedankt voor je mentorschap. Je hebt me enorm veel geleerd en daar ben ik je heel dankbaar voor. We hebben een aantal mooie papers gemaakt en daarmee de immuun evasie mechanismen van HPV goed op de kaart gezet. Bedankt voor de congressen in Berlijn, Whistler en Seattle.
Judith, ik heb heel veel van je geleerd. Heel erg bedankt, vooral voor je motivatie en geduld. Het was heel fijn om met je samen te werken.
Kees, bedankt voor de waardevolle discussies elke maandagmorgen, de papers zijn er een stuk beter van geworden.
Lien, zonder jou geen lab Klinische Oncologie. Gelukkig is onze reflectie tijdens mijn solliciteren nooit uitgekomen. Dank je voor alles, in alle talen van de wereld.

Renske and Veena, thank you so much for the countless hours you helped me with the projects. Veena, without you I would still be pipetting all the samples for the microarray and PCRs. You are great, thank you so much. Renske, you just are the best. Zonder jou geen boekje. Heel erg bedankt voor alles wat je gedaan hebt.

Roser and Sofia, thanks for all the great work you have done. The whole of chapter 5 would not exist without you ladies. Roser, muchos gracias! Sofia, grazie mille!

Special thanks to the Clinical Oncology lab; Lien, Sjoerd, Marij, Els, Thorbald, Satwinder, Valeria, Saskia, Sara, Sytse, Elien, Koen, Moniek, Eleni, Wenbo, Edith, Evelyne, Peggy, Rezaul, Margit, Ursula, Claudia, Renske, Zohara, Marjolein, Marten, Bianca, Vanessa, Nikki and Linda. Many thanks for all your help in the lab and ‘gezelligheid’ at the B@Fjes and lab days out.
Thanks to everyone of the Tumor Immunology lab for their collaboration.

Thanks to all the collaborators for their contributions to this work. Claude

Backendorf, Michelle Osse, Katja Jordanova, thanks for all your help. Laetitia Pelascini, thanks for your big influence, input and collaboration to this thesis. Edith en Evelyne, dank voor onze goede samenwerking, we hebben mooie papers gemaakt.
Dr. Craig Meyers, thank you for your collaboration and kind welcome to your lab. Jen, Eric, Rachel, Janice and Samina, you guys are great, thank you so much for your warm welcome during my stay and all the help with the experiments.

Wilco en Renske, ik kan me geen betere paranimfen wensen. Jullie zijn geweldig.

Lieve vriend(innet)jes van Dury Lane, de allerbeste vriendengroep die ik me kan wensen. Dank voor de afgelopen 13 jaar, we weten allemaal dat er nog heel veel jaren gaan volgen.

Mijn proefschrift is beïnvloed door heel veel mensen. Mijn lieve zus Marjolein, Kevin en Max, Hessel, Kirsten, Hessel en Jorick, Marvin, Natasa, Han, Ria, André, Roy, Riet, en op de ereplaats, natuurlijk, Pierre.

To all of you: Heel erg bedankt, Thanks, Gracias, Obrigado, Danke, Grazie, Merci, مرسي, आभारीहुँ ευχαριςτώ.

Pap en mam, dit proefschrift is voor jullie. Dankzij jullie weet ik dat stelling 12 alles zegt.